

Superquantile-Gibbs Relaxation for Minima-selection in Bilevel Optimization

Saeed Masiha¹, Zebang Shen², Negar Kiyavash¹, and Niao He²

¹EPFL School of Management of Technology, Station 5, 1015 Lausanne, Switzerland,
mohammadsaeed.masiha@epfl.ch, negar.kiyavash@epfl.ch

²ETH Department of Computer Science, Universitätstrasse 6, 8092 Zürich, Switzerland,
zebang.shen@inf.ethz.ch, niao.he@inf.ethz.ch

Abstract

Bilevel optimization (BLO) becomes fundamentally more challenging when the lower-level objective admits multiple minimizers. In contrast to the commonly studied unique-minimizer setting, this regime introduces two additional difficulties: (1) evaluating the hyper-objective F_{\max} requires a *minima-selection* step, which, in the worst case, amounts to solving an optimization problem over a *topologically disconnected* set; (2) F_{\max} is in general discontinuous without strong structural assumptions. We show that both issues can be circumvented under a local Polyak–Łojasiewicz (PL) property, denoted by PL° , on the lower-level objective. This condition is strictly weaker than the global PL property assumed in recent BLO studies and covers problems such as hyperparameter tuning in over-parameterized deep learning. Under PL° , we prove that F_{\max} is Lipschitz continuous and that, for all upper-level variables, the corresponding lower-level minimizer sets are *topologically connected* and are provably closed embedded submanifolds, all sharing a *common* intrinsic dimension k . We show that this intrinsic dimension k , rather than the ambient dimension, governs the complexity of BLO: We propose a method that finds an (ϵ, ρ) -Goldstein stationary point of F_{\max} using at most $\tilde{O}(m^{8k+11}\epsilon^{-2}(\epsilon\rho)^{-8k-10})$ queries to the gradient oracle of the lower-level function, where m is the dimension of the upper-level domain. The key ingredient is a *Superquantile-Gibbs relaxation* that yields an approximate function-evaluation oracle for F_{\max} : it turns minima selection into a sampling problem that can be efficiently addressed using standard Langevin dynamics. To the best of our knowledge, this is the first work that rigorously tackles the minima selection step in BLO and explicitly characterizes how the overall complexity of BLO scales with the *intrinsic dimensionality* of the lower-level problem.

Keywords: Bilevel optimization, Nonconvex lower-level problem, Local PL condition, and Nonsmooth optimization.

1 Introduction

We study the pessimistic/optimistic formulation of Bilevel Optimization (BLO), which is a common paradigm in the literature [23, 62, 84, 87, 90], although alternatives to pessimistic/optimistic formulation for BLO also exist (see e.g., [4, 11, 43]). The pessimistic formulation of BLO is defined as follows¹:

$$\min_{\theta \in \Theta \subseteq \mathbb{R}^m} F_{\max}(\theta) := \left\{ \max_{x \in \mathcal{S}(\theta) \subseteq \mathbb{R}^d} f(\theta, x) \right\}, \quad \mathcal{S}(\theta) := \arg \min_{x \in \mathbb{R}^d} g(\theta, x), \quad (1)$$

¹All results extend to the optimistic setting where minimizing is considered instead of maximizing f over x .

where θ and x are the upper- and lower-level variables, f and g are the upper- and lower-level objectives, respectively, and Θ is a *closed compact convex* subset of \mathbb{R}^m . We focus on the setting where the lower-level minima set $\mathcal{S}(\theta)$ is *non-singleton*. We refer to the maximization of f over $x \in \mathcal{S}(\theta)$ as *minima-selection* and call F_{\max} the *hyper-objective*. BLO captures problems with a nested structure, such as hyper-parameter optimization [28], meta-learning [8], and reinforcement learning [39, 61]. In particular, when the lower-level problem pertains to deep learning, the set $\mathcal{S}(\theta)$ is typically nonconvex and non-singleton [27, 31, 48, 55, 58, 69, 75, 80]. Therefore, minima-selection becomes important.

Relaxing strong convexity to the global PL condition Recent works on BLO have studied nonconvex lower-level problems under the *global* Polyak-Łojasiewicz (PL) condition [14, 40, 50, 59, 77, 83]. This condition relaxes the classical strong convexity assumption on g , which implies singleton $\mathcal{S}(\theta)$, to cover nonconvex and potentially non-singleton optimal solution sets. Another motivation for adopting the global PL condition is to guarantee the continuity of the hyper-objective function F_{\max} , which might otherwise become discontinuous and render BLO problems generally intractable [14, 50].

All of the aforementioned work and their results are crucially dependent on the assumption that g is \mathcal{C}^2 and satisfies the global PL condition. Under these conditions, it can be proved that the lower-level solution set $\mathcal{S}(\theta)$ would be limited to either a singleton or an unbounded subset of \mathbb{R}^d [20]. More specifically, Huang [40] assume a nondegenerate Hessian of g at global minimizers, implicitly enforcing uniqueness; Liu et al. [59] explicitly assume $\mathcal{S}(\theta)$ is a singleton; Xiao et al. [83] and Shen et al. [77, Sec. 4] assume additional convexity of the lower-level objective, implying that the minimizer set is a linear subspace; and Kwon et al. [50] require g to be coercive which again yields a singleton solution². The above observations hint at the necessity of a further relaxation to capture richer landscapes.

Our setting: Relaxing the global PL condition to a local PL condition We relax the global PL assumption to the PL° condition, which was recently proposed by [35], to accommodate applications of interest such as those in deep learning. For a fixed θ , a PL° lower-level objective $g(\theta, \cdot)$ admits a provably connected optimal set $\mathcal{S}(\theta)$ and it satisfies the PL inequality *locally* in a neighborhood of $\mathcal{S}(\theta)$. Moreover, the PL° condition ensures that $\mathcal{S}(\theta)$ is a \mathcal{C}^2 embedding submanifold of the ambient space \mathbb{R}^d without boundary [35]. We shall define PL° condition formally in Definition 2.2. This setting is sufficiently rich because the lower-level problem admits bounded *non-singleton* minimizers. Hence, the minima-selection step remains relevant. One such example is when g represents the loss function of some deep learning tasks in the over-parameterized regime, where the local minima are observed to be connected [27, 31, 48, 58, 69]. Another advantage of this setting is that, as we prove in Section 3.1, the hyper-objective under the PL° condition is Lipschitz continuous. However, under the same condition, the hyper-objective function is not necessarily differentiable, and conditions on functions f and g that would ensure the differentiability of the hyper-objective are often restrictive and unrealistic in practice (see the discussion in Section A.2).

Solution concept for nonsmooth nonconvex optimization. Solving BLO problems with a *non-singleton* lower-level solution set $\mathcal{S}(\theta)$ involves two main challenges: 1) As previously emphasized, for a fixed upper-level variable θ , the minima-selection problem requires maximization over a *nonconvex* set. Consequently, exact evaluations of the hyper-objective F_{\max} are generally inaccessible. 2) Even when the minima-selection subproblem can be solved exactly, the resulting hyper-objective F_{\max} may still be *non-differentiable* with respect to the upper-level variable θ . Addressing this issue requires establishing local optimality guarantees for a nonsmooth nonconvex objective, a widely recognized challenge in the literature [44, 46, 47, 78, 93].

²Kwon et al. [50] assume the proximal error bound for g (with $\sigma = 0$), equivalent to the global PL condition for smooth g [14, Prop. C.1].

To address these issues, we introduce the superquantile–Gibbs relaxation to approximate the hyper-objective, providing a practical surrogate for F_{\max} . Using evaluations of this surrogate, we propose a zeroth-order method that seeks a *generalized Goldstein stationary point* of F_{\max} (see Definition 5.4; cf. [64]).

1.1 Finding a Goldstein Stationary Point of the Hyper-objective

As we shall see in Theorem 4.5, under the PL° condition the hyper-objective F_{\max} is Lipschitz continuous. A natural choice for approximate stationarity in this setting is Clarke’s notion of stationarity [18]. However, Zhang et al. [93] showed that, for nonsmooth Lipschitz problems, obtaining an ϵ -Clark stationary point in polynomial time is generally impossible, motivating more nuanced concepts. We therefore adopt the notion of (ϵ, ρ) -Goldstein stationarity [34].

For the domain-constrained objective in (1), akin to [64], we measure stationarity by a *generalized* (ϵ, ρ) -Goldstein criterion which is defined for the gradient mapping³, denoted by (ϵ, ρ, η) -generalized Goldstein stationary point (see Definition 5.4). As F_{\max} may not be differentiable, we propose a zeroth-order (ZO) method to find such a stationary point of F_{\max} .

The major obstacle to applying ZO methods to minimize F_{\max} is that exact function values of this hyper-objective are typically unavailable. To address this, we introduce a tractable surrogate, the superquantile-Gibbs $\tilde{F}_{\text{SQ-G}}(\theta)$, which we define next and show that it approximates F_{\max} well. Consequently, querying $\tilde{F}_{\text{SQ-G}}$ in place of F_{\max} provides the finite-difference gradient estimates for our zeroth-order (ZO) method. We prove that the approximation error incurred by replacing F_{\max} with $\tilde{F}_{\text{SQ-G}}$ does not adversely affect the convergence guarantees of our ZO algorithm for obtaining an (ϵ, ρ, η) -Goldstein stationary point.

1.2 Superquantile-Gibbs Relaxation (SQ-G)

In this part, we introduce the superquantile of the random variable $f(\theta, X)$ where X is sampled according to the the Gibbs measure $\sim \exp(-g(\theta, x)/\lambda)$. Our idea is that as $\lambda \rightarrow 0$, the Gibbs measure concentrates on the feasible domain $\mathcal{S}(\theta)$, and the superquantile at a high confidence level would approach the maximum value of $f(\theta, \cdot)$ on $\mathcal{S}(\theta)$. Formally, we define the Superquantile-Gibbs Relaxation (SQ-G)-loss using the variational formulation of the superquantile by [74]:

$$\begin{aligned} \text{(SQ-G-loss)} \quad \tilde{F}_{\text{SQ-G}}(\theta) &:= \min_{\beta \in \mathbb{R}} \phi_{\lambda, \delta}(\theta, \beta) \\ \text{with } \phi_{\lambda, \delta}(\theta, \beta) &:= \beta + \frac{1}{\delta} \mathbb{E}_{X \sim \mu_\theta^\lambda} [\max\{f(\theta, X) - \beta, 0\}]. \end{aligned} \tag{2}$$

Here $\lambda > 0$ and $\delta > 0$ are parameters controlling the level of SQ-G relaxation, with $(1 - \delta)$ known as the confidence level, and μ_θ^λ denotes the Gibbs measure:

$$\mu_\theta^\lambda(x) := \frac{\exp(-g(\theta, x)/\lambda)}{Z_\lambda(\theta)}, \tag{3}$$

where $Z_\lambda(\theta) := \int_{\mathbb{R}^d} \exp(-g(\theta, z)/\lambda) dz$ is a normalizing factor. A key contribution of this project is that we characterize how λ and δ impact the accuracy with which $\tilde{F}_{\text{SQ-G}}(\theta)$ approximates F_{\max} .

1.3 Our Contributions

Our main contributions are as follows.

³The gradient mapping for $F : \Theta \rightarrow \mathbb{R}$ at a point θ is $\mathcal{G}_\Theta(\theta, \nabla F; \eta) := \eta^{-1}(\theta - \text{Proj}_\Theta(\theta - \eta \nabla F(\theta)))$.

- To allow for lower-level optimal sets with rich structures, we relax the global $\mathbb{P}\mathcal{L}$ condition, commonly imposed on the lower-level objective, to the weaker $\mathbb{P}\mathcal{L}^\circ$ condition from [35]. We show that the $\mathbb{P}\mathcal{L}^\circ$ condition is sufficient to ensure Lipschitz continuity of the hyper-objective function F_{\max} .
- We use the Superquantile–Gibbs relaxation (SQ-G) to approximate F_{\max} . This converts the crucial minima-selection step in BLO, originally a nonconvex optimization over a nonconvex set, into sampling from a Gibbs distribution, which we implement efficiently via Langevin dynamics.
- Building on the manifold structure of the lower-level optimal set, we derive the following results.

Result 1 (Approximation). *Assume that g satisfies the $\mathbb{P}\mathcal{L}^\circ$ condition (to be stated in Assumption 2.6), along with standard regularity conditions such as continuity of the gradient and Hessian for both f and g . As shown in Section 4, this implies the approximation bound $|F_{\max}(\theta) - \tilde{F}_{\text{SQ-G}}(\theta)| = \mathcal{O}\left(\delta^{\frac{1}{k}} + \delta^{-1}\lambda^{1/2}\right)$. Here k is the common⁴ dimension of the embedding submanifolds $\{\mathcal{S}(\theta)\}_{\theta \in \Theta}$.*

Result 2 (Optimization). *Assume that g satisfies $\mathbb{P}\mathcal{L}^\circ$ and the regularity conditions for f and g (to be stated in Assumption 2.8). As shown in Section 5, by using a Projected Stochastic Zeroth-Order method with Minima-Selection (see Algorithm 2) to optimize F_{\max} , we obtain an (ϵ, ρ, η) -generalized Goldstein stationary point of F_{\max} on average using $\tilde{\mathcal{O}}(m^{2k+5}\epsilon^{-2}(\epsilon\rho)^{-2k-4})$ samples from the distribution μ_θ^λ for $k \geq 1$. When the samples of μ_θ^λ are approximated by the Langevin Monte Carlo method, we show in Section 5.3 that the same goal can be achieved with $\tilde{\mathcal{O}}(m^{8k+11}\epsilon^{-2}(\epsilon\rho)^{-8k-10})$ queries to a gradient oracle for g and $\tilde{\mathcal{O}}(m^{2k+5}\epsilon^{-2}(\epsilon\rho)^{-2k-4})$ queries to a value oracle for f .*

The precise statements of these results appear in Theorem 4.5, Theorem 5.5 and Theorem 5.7, respectively.

- We evaluate our approach on both synthetic and real-world benchmarks and demonstrate the effect of minima-selection. As shown in Section 6, our proposed approach outperforms hyper-gradient and penalty-based baselines.

Remark 1.1. *(Exponential dependence on k)* The ϵ^{-k} factor in our results reflects the intrinsic difficulty of the problem. Since evaluating $F_{\max}(\theta) = \max_{y \in \mathcal{S}(\theta)} f(\theta, y)$ is equivalent to solving a nonconvex optimization problem over a nonconvex set, a single ϵ -accurate evaluation of $F_{\max}(\theta)$ yields an $\Omega(\epsilon^{-k})$ complexity lower bound. More specifically, consider the instance where $\mathcal{S}(\theta) = \mathbb{S}^k$ is a hypersphere. Reparameterizing y in polar coordinates yields $F_{\max}(\theta) = \max_{x \in \mathbb{B}_k} f(\theta, y(x))$. Here $\mathbb{B}_k = [0, \pi]^k$ and the point $y(x) \in \mathbb{S}^k$ is given by $y_i(x) = \sin(x_1) \cdots \sin(x_{i-1}) \cos(2x_i)$ for $i \in [k]$ and $y_{k+1}(x) = \sin(x_1) \cdots \sin(x_{k-1}) \sin(2x_k)$. It follows from [67, Section 1.6.2] that the worst-case complexity of finding an ϵ -accurate solution to is $\Omega(\epsilon^{-k})$ for $f(\theta, \cdot) \in \mathcal{C}^1$.

1.4 Related Work

Bilevel optimization has a long history in mathematical programming; see, e.g., the early bibliographic review by [81], the monograph [22], the survey [19], the classical text on mathematical programs with equilibrium constraints (MPECs) by [66], and the recent collection [25]. Classical approaches often reduced bilevel problems to single-level programs, either via value-function reformulations or by replacing the lower-level problem with its Karush–Kuhn–Tucker (KKT) optimality system. A related value-function-based reduction for bilevel programs with nonconvex lower-level objectives yields single-level formulations with nonsmooth inequality constraints, for which smoothing and augmented-Lagrangian type algorithms were developed in, e.g., [56, 84]. The latter route yields MPEC formulations in which complementarity conditions between multipliers and constraint violations appear as explicit equilibrium constraints; see, for example,

⁴In Lemma 3.5, we show that the manifolds $\{\mathcal{S}(\theta)\}_{\theta \in \Theta}$ admit a common dimension k .

[26, 88, 89, 91]. In practice, these complementarity constraints are frequently handled through mixed-integer or so-called big- M linearizations; however, their performance can be sensitive to the choice of constants, with overly small values excluding feasible bilevel solutions and overly large values leading to weak relaxations and numerical instability [45]. Complementing these algorithmic considerations, recent work has also highlighted inherent geometric and computational hardness in bilevel programming, even under smoothness, which motivates the search for additional structural assumptions and tailored relaxations [12].

Gradient-based bilevel methods with strongly convex lower level. Modern large-scale machine-learning applications led to gradient-based methods for bilevel empirical risk minimization and hyperparameter optimization. When the lower-level objective is strongly convex in the inner variable and f, g are smooth, the hyper-objective is differentiable and its gradient can be obtained by implicit differentiation. Representative works in this setting include approximate hyper-gradient methods such as HOAG [70], stochastic bilevel schemes [32, 85], and complexity-refined algorithms for empirical risk minimization [15, 21], as well as more abstract treatments of optimization layers via automatic differentiation [1], amortized implicit differentiation [3], and modular implicit differentiation frameworks [10, 37]. In these approaches, computing exact hyper-gradients typically required Hessian or Hessian-inverse information for the lower-level problem, which could be prohibitive in large neural networks. This motivated a substantial line of *Hessian-free* or fully first-order methods that approximated the hyper-gradient using only first-order information, including BOME [59], Hessian/Jacobian-free stochastic methods with improved sample complexity [86], fully first-order stochastic approximation methods such as F²BO [49], and bilevel stochastic-gradient methods that also accommodate nonlinear lower-level constraints and inexact hyper-gradient computations [33]. A different line of work revisits bilevel learning from a functional viewpoint: Petruionytė et al. [72] treat the lower-level variable as a *prediction function* (rather than a parameter vector) and optimize it over a convex function space. Assuming strong convexity in this functional variable yields a unique lower-level solution and enables implicit differentiation via a functional implicit-function theorem, shifting the strong-convexity requirement from parameters to function space. These developments made bilevel optimization scalable in settings with a unique lower-level solution, so the minima-selection problem that we study did not arise.

Relaxing strong convexity to global PŁ. A complementary line of work relaxed lower-level strong convexity to a global Polyak–Łojasiewicz (PŁ) condition and developed bilevel gradient methods under this assumption [14, 40, 50, 59, 77, 83]. To obtain a smooth and well-behaved hyper-objective, these methods typically combined the global PŁ condition with additional regularity assumptions on the lower-level problem (as discussed earlier), so that minima-selection was effectively avoided. In contrast, our analysis is based on a local PŁ condition and explicitly exploits the geometry of nontrivial minimizer manifolds. In a complementary direction, Chen et al. [13] introduce a *set-smoothness* property of the lower-level solution mapping and show that it yields weak convexity/concavity of the induced optimistic/pessimistic hyper-objectives, enabling the computation of approximate Clarke hyper-stationary points. Their analysis relies on assumptions such as a *uniform* error bound together with smoothness, which imply a global PŁ condition for the lower-level problem. When the lower-level objective is \mathcal{C}^2 in the lower-level variable, this global PŁ property forces $\arg \min_x g(\theta, x)$ to be either a singleton or an unbounded set [20]. As a consequence, these conditions rule out the bounded non-singleton minimizer manifolds that motivate the minima-selection regime studied in our work.

Alternative formulations of BLO. Beyond such regularity-based assumptions (strong convexity or global PŁ), recent works proposed alternative formulations of BLO that target nonconvex lower-level problems. For instance, Bolte et al. [11] worked under a (piecewise) Morse-type parametric qualification, showed that the graphs of lower-level critical points and local minima are generically decomposed into finitely

many smooth manifolds, and used this structure to define branch-wise hyper-objectives and study gradient methods that updated the upper-level variable along individual branches. Arbel and Mairal [4] introduced bilevel games with selection maps, where the selection map chooses a specific lower-level critical point for each upper-level parameter (e.g., the limit of a gradient flow from a given initialization). They showed that popular unrolled/iterative-differentiation bilevel algorithms with a finite inner budget approximate equilibria of these selection-based games up to approximation errors, and they extended implicit differentiation to characterize the selection and proposed a correction that removes the finite-budget error. Jiang et al. [43] further argued that, for general nonconvex lower levels, the classical hyper-objective may be ill-posed when global minimizers are unattainable; they proposed a correspondence-driven hyper-objective that evaluated the upper-level loss at the output of a prescribed lower-level algorithm, applied Gaussian smoothing to this mapping, and developed a projected stochastic gradient method with oracle-complexity guarantees for the smoothed problem. Another recent line develops *Moreau-envelope* single-level reformulations as an alternative to classical value-function and KKT-based complementarity-constrained reductions. Bai et al. [5] derive directional necessary optimality conditions in this framework, Gao et al. [30] propose a difference-of-weakly-convex reformulation with a sequentially convergent algorithm, and Lu [65] builds on these ideas to obtain a two-sided smoothed primal–dual method for general *nonconvex* bilevel problems with KKT-type convergence guarantees. In contrast, our work retains the classical (pessimistic or optimistic) hyper-objective, combines it with a local PL condition to obtain a manifold structure for the lower-level minimizers, and uses a superquantile–Gibbs relaxation to convert the minima-selection into sampling from a Gibbs measure.

Pessimistic bilevel optimization. The approaches discussed above treat lower-level non-uniqueness either by enforcing regularity conditions (strong convexity or global PL) or by embedding explicit selection mechanisms (Morse branches, selection maps, or algorithmic correspondences), and thus remain essentially in an optimistic or selection-based setting. By contrast, the *pessimistic* formulation evaluates each upper-level decision against the worst upper-level value over all lower-level minimizers, which is natural when the follower may act adversarially or unreliably [6]. This risk-averse viewpoint was studied in mathematical programming, including structural and complexity results for general pessimistic models [82], surveys of modelling and solution schemes [60], and necessary optimality conditions based on generalized differentiation and value-function techniques [24]. On the algorithmic side, several works constructed single-level relaxations of the pessimistic problem: Zeng and Ye [92] designed a tight relaxation and a computation scheme for (mainly linear) pessimistic bilevel problems; Benchoouk et al. [7] analyzed a Scholtes-type relaxation of the KKT system; and Antoniou et al. [2] proposed a δ -perturbed formulation that enforced an *approximate* unique follower response and derived error bounds between the perturbed and original pessimistic problems. Pessimistic ideas also appeared in machine learning: Ustun et al. [79] formulated hyperparameter tuning as a pessimistic bilevel problem over a finite set of tasks and highlighted advantages of this formulation over the optimistic counterpart, and Jiang et al. [42] interpreted adversarial training as a bilevel game in which a learned attacker played the role of the follower. All these approaches, however, either (i) resolved non-uniqueness by modifying the lower-level problem (e.g., δ -perturbations, KKT relaxations) or (ii) specialized to finite or discrete follower responses, rarely addressed the continuous pessimistic setting with a non-singleton solution set. In contrast, we work directly with the pessimistic hyper-objective F_{\max} under a local PL condition, model pessimism via a superquantile risk over Gibbs samples on the minimizer manifolds, and obtain complexity results that explicitly depend on the intrinsic dimension k of $\mathcal{S}(\theta)$ rather than on the ambient dimension.

1.5 Organization

The remainder of the paper is organized as follows. Section 2 introduces the PL^o assumption and additional regularity conditions, and discusses their implications for the structure of the solution set as well as for

the convergence of the Gibbs measure to its limit. Building on this, Section 3 develops uniform geometric properties of the minimizer manifolds $\{\mathcal{S}(\theta)\}_{\theta \in \Theta}$, showing in particular that the solution mapping is locally Lipschitz and that these manifolds share a common intrinsic dimension. Section 4 shows that, under our assumptions, the SQ-G relaxation provides a sharp approximation of F_{\max} (see Lemma 4.4). Using this approximation result, in Section 5 we show our main complexity guarantees: Theorem 5.5 and Theorem 5.7 show that the complexity of optimizing F_{\max} via a zeroth-order algorithm (see Algorithm 2) scales with the common intrinsic dimension of the lower-level solution manifolds. Finally, Section 6 presents our numerical results: we first study the dependence on the Riemannian dimension in a synthetic example and then compare our method with several competitive baselines on both a toy problem and a data hyper-cleaning task.

1.6 Notations

Unless stated otherwise, $\|\cdot\|$ denotes the Euclidean (ℓ_2) vector norm and the associated operator norm on matrices and higher-order tensors. For a random variable Z , $\text{supp}(Z)$ denotes its support. For $d \in \mathbb{N}$, $x \in \mathbb{R}^d$, and $r > 0$, we write $\mathbb{B}_d(x; r) := \{y \in \mathbb{R}^d : \|y - x\| \leq r\}$ for the closed d -dimensional Euclidean ball with center x and radius r . For $p \geq 1$ and probability measures μ, ν on \mathbb{R}^d with finite p -th moments, the p -Wasserstein distance is

$$\mathbb{W}_p(\mu, \nu) := \left[\inf_{\pi \in \Pi(\mu, \nu)} \int_{\mathbb{R}^d \times \mathbb{R}^d} \|x - y\|^p d\pi(x, y) \right]^{1/p},$$

where $\Pi(\mu, \nu)$ is the set of all couplings of μ and ν . In particular, \mathbb{W}_1 is the 1-Wasserstein distance. Given a twice differentiable function $f : \mathbb{R}^m \times \mathbb{R}^d \rightarrow \mathbb{R}$, we write $\partial_\theta f(\theta, x)$ and $\partial_x f(\theta, x)$ for the gradients of f with respect to its first and second arguments, respectively. The mixed derivative $\partial_{\theta, x}^2 f(\theta, x) := \partial_\theta(\partial_x f(\theta, x))$ denotes the Jacobian of the vector $\partial_x f(\theta, x)$ with respect to θ , and $\partial_\theta^2 f(\theta, x)$ denotes the Hessian of f with respect to θ . The diameter of a set $\Theta \subset \mathbb{R}^d$, is defined as $\text{diam}(\Theta) := \sup_{\theta_1, \theta_2 \in \Theta} \|\theta_1 - \theta_2\|$. The class of continuous real-valued functions on \mathbb{R}^d is denoted by $\mathcal{C}(\mathbb{R}^d, \mathbb{R})$. We write $f \in \mathcal{C}^k$ if f has continuous derivatives up to order k . For a set $A \subset \mathbb{R}^d$, we denote its closure by \bar{A} . For a scalar random variable Z and $\delta \in (0, 1)$, the $(1 - \delta)$ -quantile is defined as

$$\mathbb{Q}_{1-\delta}(Z) := \inf\{t \in \mathbb{R} : \mathbb{P}[Z > t] \leq \delta\}.$$

For a closed convex set $\Theta \subset \mathbb{R}^m$ and $y \in \mathbb{R}^m$, we denote by $\text{Proj}_\Theta(y) = \arg \min_{z \in \Theta} \|y - z\|$ the (Euclidean) projection of y onto Θ . We use the notation \mathcal{O} to hide constants, and the notation $\tilde{\mathcal{O}}$ to hide both constants and logarithmic factors. We write $a \lesssim b$ to indicate that $a \leq cb$ for some universal positive constant $c > 0$ that is independent of the problem parameters. We write $\mathbb{R}_\alpha(P\|Q)$ for the Rényi divergence of order $\alpha \in (0, \infty) \setminus \{1\}$, defined by

$$\mathbb{R}_\alpha(P\|Q) = \begin{cases} \frac{1}{\alpha - 1} \log \int \left(\frac{dP}{dQ}\right)^\alpha dQ, & P \ll Q, \\ +\infty, & \text{otherwise.} \end{cases}$$

We denote $\text{Law}(X)$ as the probability distribution (or law) of a random variable X .

2 Summary of Assumptions and Preliminaries

In this work, we focus on the setting where the lower-level objective is coercive and satisfies a local Polyak-Łojasiewicz (PL^o) condition for all upper-level variables $\theta \in \Theta$, formally stated as follows.

Definition 2.1. Let \mathcal{M} be the collection of all local minima of a function $g \in \mathcal{C}^1(\mathbb{R}^d, \mathbb{R})$. g is locally $\mathcal{P}\mathcal{L}$ if there exists a constant $\mu > 0$ such that for any connected component $\mathcal{M}' \subseteq \mathcal{M}$, there exists an open neighborhood $\mathcal{N}(\mathcal{M}')$ containing \mathcal{M}' ($\mathcal{N}(\mathcal{M}') \supset \mathcal{M}'$) such that

$$\forall x \in \mathcal{N}(\mathcal{M}'), \quad g(x) - \min_{x' \in \mathcal{N}(\mathcal{M}')} g(x') \leq (2\mu)^{-1} \|\nabla g(x)\|^2. \quad (4)$$

Definition 2.2. A function $g : \mathbb{R}^d \rightarrow \mathbb{R}$ satisfies the $\mathcal{P}\mathcal{L}^\circ$ condition if the following hold.

- g is a \mathcal{C}^2 and locally $\mathcal{P}\mathcal{L}$ function, and g is a \mathcal{C}^4 function in every neighborhood $\mathcal{N}(\mathcal{M}')^5$.
- Let $\mathcal{N}(\mathcal{M}) := \cup_{\mathcal{M}'} \mathcal{N}(\mathcal{M}')$. For any $x \in \mathbb{R}^d \setminus \mathcal{N}(\mathcal{M})$, if $\nabla g(x) = 0$, then $\nabla^2 g(x) \prec 0$.
- The collection of all local minima \mathcal{M} is contained within a compact set.

A fundamental implication of the $\mathcal{P}\mathcal{L}^\circ$ condition is the connectivity of the optimal set.

Proposition 2.3 (Connectivity, Proposition 3 in [35]). For a $\mathcal{P}\mathcal{L}^\circ$ function, its local minima set \mathcal{M} is path-connected.

Consequently, all local minima of a $\mathcal{P}\mathcal{L}^\circ$ function are global minima which are all connected. Further, Rebjock and Boumal [73] proved the local manifold structure of \mathcal{M} . This was later extend to a global version in [35], where they also provide an explicit statement about the boundary.

Remark 2.4 (No-saddle point property). The second condition in Definition 2.2 is used solely to establish the connectedness of the local minima set via the mountain pass theorem (see the proof of Proposition 3 in [35] for details). Our results remain valid if this condition is replaced with the assumption that $\mathcal{S}(\theta)$ is connected. Empirically, such connectedness has been widely observed in over-parameterized deep learning settings; see, e.g., [27, 48, 69].

Proposition 2.5 (Manifold structure, Corollary 1 in [35]). For a $\mathcal{P}\mathcal{L}^\circ$ function, its optimal set \mathcal{M} is a compact \mathcal{C}^2 embedding submanifold of the ambient space \mathbb{R}^d without boundary.

Assumption 2.6. For every $\theta \in \Theta$, the lower-level objective $g(\theta, \cdot)$ satisfies the $\mathcal{P}\mathcal{L}^\circ$ condition.

Following [35], we make the next assumption to exclude the manifolds with ill-conditioned charts. We also use it to establish a nonzero lower bound on the injectivity radius, allowing us to analyze the volume-radius relationship of geodesic balls, which is crucial for our approximation results.

Assumption 2.7 (Second-order fundamental form). For every $\theta \in \Theta$, the manifold $\mathcal{S}(\theta)$ has a well-defined second fundamental form in the sense of Definition A.1 in Section A.1, and its operator norm is uniformly bounded by a constant $C > 0$.

We further need the following regularity conditions, which are standard in the BLO literature.

⁵Gong et al. [35] require $g \in \mathcal{C}^3$. Here we slightly enhance the assumption to \mathcal{C}^4 to enable Proposition 2.11.

Assumption 2.8. *The following statements hold for all $\theta \in \Theta$.*

- f is a C^1 function and $L_{f,1}$ -Lipschitz, and $L_{f,2}$ -smooth w.r.t. (θ, x) . For all $x \in \mathbb{R}^d$, $|f(\theta, x)| \leq C_f \|x\|^{n_f} + D_f$ where $C_f, D_f \geq 0$ are two constants and $n_f \geq 1$ is an integer constant.
- g is a C^2 function and $L_{g,2}$ -smooth w.r.t. θ for every $x \in \mathbb{R}^d$. For all $x \in \mathbb{R}^d$, $\|\partial_\theta g(\theta, x)\| \leq C_g \|x\|^{n_g} + D_g$ where $C_g, D_g \geq 0$ are two constants and $n_g \geq 1$ is an integer constant.
- The Hessian $\partial_x^2 g(\theta, x)$ is continuous w.r.t. (θ, x) .
- Beyond a compact set, $g(\theta, \cdot)$ satisfies the quadratic growth, i.e., $\exists D > 0$ such that $\forall |x| \geq D$, $\mu_{\text{qg}} \cdot \text{dist}^2(x, \mathcal{S}(\theta))/2 \leq g(\theta, x) - \min_{z \in \mathbb{R}^d} g(\theta, z)^a$.

^aW.L.O.G., we assume that D is sufficiently large so that $\mathcal{S}(\theta) \subseteq \mathbb{B}_d(0; D)$ for all $\theta \in \Theta$. This assumption implies the coercivity of function $g(\theta, \cdot)$.

The regularity conditions in Assumption 2.8, such as Lipschitzness and smoothness, are standard in the literature [14, 50]. However, unlike in [50], we do not assume a bounded x -domain in the lower-level problem. Instead, we impose quadratic growth beyond a compact set, ensuring μ_g^λ is well-defined [38]. Additionally, whereas [50] assumes boundedness of f , we relax this to a polynomial bound condition. We also assume a bounded θ -domain and polynomial bound on $\partial_\theta g$, which we plan to further relax in future work.

Example 2.9. *To justify that the assumptions allow for a nontrivial function class, we provide a simple example. Since f only requires regularity conditions, it can be easily constructed, so we focus on g . Consider $g(\theta, x) = \frac{1}{4}(\|x\|^2 - \theta)^2 - \frac{1}{2}\|x\|^2$ for $0 \leq \theta \leq 1$, which satisfies all given assumptions. Here, the lower-level minima set $\mathcal{S}(\theta) = \{x : \|x\| = \theta + 1\}$ is non-singleton and nonconvex.*

Under Assumption 2.8, the mappings $(\theta, x) \mapsto f(\theta, x)$ and $(\theta, x) \mapsto \partial_\theta g(\theta, x)$ are continuous on the compact set $\Theta \times \mathbb{B}_d(0; R)$ with $R > 0$. We define the constants

$$L_{f,0}(R) := \sup_{\theta \in \Theta} \sup_{x \in \mathbb{B}_d(0; R)} |f(\theta, x)|, \quad L_{g,1}(R) := \sup_{\theta \in \Theta} \sup_{x \in \mathbb{B}_d(0; R)} \|\partial_\theta g(\theta, x)\|. \quad (5)$$

By compactness and continuity, these suprema are finite.

2.1 Implications of the \mathbf{PE}° Condition

We review implications of Assumption 2.6, in particular how it helps to quantify the convergence of the Gibbs measures μ_θ^λ to the limiting measure μ_θ^0 under the Wasserstein-1 metric. In this subsection, θ is considered fixed, and hence for ease of the notation, we omit it and simply write μ^λ , and μ^0 .

2.1.1 Implications of the Embedding Submanifold Structure in Proposition 2.5

Following Remark 1 in [35], WLOG and for the ease of notation, we assume that the atlas of the manifold \mathcal{S} consists of a single chart (\mathcal{U}, ϕ) , where $\mathcal{U} = \mathcal{S}$. Let $\Gamma = \phi(\mathcal{U}) \subseteq \mathbb{R}^k$ denote the coordinate domain⁶. The corresponding parametrization (the inverse of the chart) can be represented as $x = \mathcal{S}(u) := [m_1(u), \dots, m_d(u)]^\top$ for all $u \in \Gamma$, where $m_j : \Gamma \rightarrow \mathbb{R}$ for $j \in [d]$ are C^2 coordinate functions.

Tubular Neighborhood. For $x \in \mathcal{S}$, the tangent space at x is denoted by $T_x(\mathcal{S})$. The orthogonal complement of $T_x(\mathcal{S})$ in \mathbb{R}^d is denoted by $T_x(\mathcal{S})^\perp$. The tubular neighborhood $\mathcal{N}(\varepsilon)$ of \mathcal{S} for $\varepsilon > 0$ is defined as: $\mathcal{N}(\varepsilon) := \{x + v : x \in \mathcal{S}, v \in T_x(\mathcal{S})^\perp, \|v\| < \varepsilon\}$. A key property of the C^2 embedded submanifold is as

⁶The standard technique of partition of unity can be used to translate the results to the multi-chart case.

follows⁷ [52, Theorem 6.24]: There exists $\varepsilon_0 > 0$ such that for all $0 < \varepsilon \leq \varepsilon_0$, there is a \mathcal{C}^2 diffeomorphism Φ :

$$\Phi : \mathcal{S} \times \mathbb{B}_{d-k}(0; \varepsilon) \rightarrow \mathcal{N}(\varepsilon), \quad (x, t) \mapsto x + \sum_{j=1}^{d-k} t_j e^{(j)}(x), \quad (6)$$

where $\{e^{(1)}(x), \dots, e^{(d-k)}(x)\}$ forms an orthonormal basis for the normal space $T_x(\mathcal{S})^\perp$. Under the local chart (Γ, ϕ) , any $y \in \mathcal{N}(\varepsilon)$ can be written as $y = x + v$, where x is a point on \mathcal{S} and $v \perp \mathcal{S}$ at x with $\|v\| \leq \varepsilon$. The map $y(u, t) := \Phi(\mathcal{S}(u), t) \rightarrow (x, v)$ is a \mathcal{C}^2 diffeomorphism.

Volume measure. We define the Riemannian (tensor) metric $g_{\mathcal{S}}$ on \mathcal{S} as the pullback metric by including map $i_{\mathcal{S}} : \mathcal{S} \hookrightarrow \mathbb{R}^d$, i.e. $g_{\mathcal{S}} = i_{\mathcal{S}}^*(g_E)$, where g_E is the standard Riemannian metric on \mathbb{R}^d and $i_{\mathcal{S}}^*$ is the pullback map associated with $i_{\mathcal{S}}$. Now we can define the standard volume form $d\mathcal{M}^8$ as $d\mathcal{M}(u) = \sqrt{\det(g_{\mathcal{S}})} du$, $u \in \Gamma$, where $\det(g_{\mathcal{S}})$ is the determinant of $g_{\mathcal{S}}$.

Poincaré constant. A probability measure π over \mathbb{R}^d is said to satisfy the Poincaré inequality with inverse Poincaré constant C_{PI} if for all test functions $\varphi \in \mathbb{H}^1(\mu)$, the following inequality holds:

$$\int \left(\varphi - \int \varphi d\mu \right)^2 d\mu \leq C_{PI} \int \|\nabla \varphi\|^2 d\mu,$$

where $\mathbb{H}^1(\mu)$ denotes the Sobolev space weighted by μ . Importantly, for all $\mathbb{P}\mathbb{L}^\circ$ functions $g : \mathbb{R}^d \rightarrow \mathbb{R}$, the constant C_{PI} for the Gibbs probability measure $\mu^\lambda \propto \exp(-g/\lambda)$ is *independent* of λ for all sufficiently small $\lambda \leq \lambda_0$, where both λ_0 and an upper bound of C_{PI} are explicitly given in [35].

2.1.2 Limiting Measure of Gibbs Measures

To sample approximately from the optimal set \mathcal{S} , we select a temperature parameter λ approaching zero, which causes the Gibbs measure (3) to concentrate on \mathcal{S} . Let $\mu^0 := \lim_{\lambda \rightarrow 0} \mu^\lambda$ denote the weak limit of the Gibbs measures. By combining the manifold characterization of the optimal set for $\mathbb{P}\mathbb{L}^\circ$ functions in [35] with the asymptotic analysis in [41, Theorem 3.1], the following lemma establishes that μ^0 is well-defined, has support restricted to \mathcal{S} , and admits a closed-form density function with respect to the Riemannian volume measure $d\mathcal{M}$ on the manifold.

Proposition 2.10 (Theorem 3.1 in [41]). *Suppose that Assumption 2.6 holds and let k be the dimension of the submanifold \mathcal{S} . Let $\mu^0 := \lim_{\lambda \rightarrow 0} \mu^\lambda$ be the weak limit of the Gibbs measures, then $\text{supp}(\mu^0) = \mathcal{S}$ and*

$$\rho(u) := \frac{d\mu^0}{d\mathcal{M}} = \frac{|\partial_t^2 g(y(u, t))|_{t=0}|^{-\frac{1}{2}}}{\int_{\mathcal{S}} |\partial_t^2 g(y(v, t))|_{t=0}|^{-\frac{1}{2}} d\mathcal{M}(v)}. \quad (7)$$

Here $|\cdot| : \mathbb{R}^{(d-k) \times (d-k)} \rightarrow \mathbb{R}$ denotes the matrix determinant. We write $\mu^0(du) = \rho(u) d\mathcal{M}(u)^9$.

Wasserstein-1 distance between the Gibbs measure and its limit measure. The following proposition from [38, Theorem 3.6] proves the non-asymptotic convergence of μ^λ as $\lambda \rightarrow 0$ to μ^0 (defined above) in the Wasserstein-1 sense¹⁰. Establishing convergence in \mathbb{W}_1 is crucial for our analysis because it directly bounds

⁷For simplicity, we assume a single chart and omit the dependence on the inclusion $i_{\mathcal{S}}$.

⁸Note that $d\mathcal{M}$ stands for $d\mathcal{M}_\theta$ in all the following sections.

⁹Note that μ^0 and ρ stand for μ_θ^0 and ρ_θ in all the following sections.

¹⁰We use the assumption on g in Definition 2.2 to ensure that the conditions in [38, Theorem 3.6] hold. Further discussion on the validity of their conditions can be found in Appendix A.3.

the approximation error between the superquantile-Gibbs surrogate and the superquantile loss taken over the limiting measure μ^0 (to be defined in (11)). This bound is established by exploiting the Lipschitz continuity of the upper-level objective (see Lemma 4.4).

Proposition 2.11 (Theorem 3.6 in [38]). *Under Assumptions 2.6 to 2.8, $\mathbb{W}_1(\mu^\lambda, \mu^0) \leq K_0 \lambda^{\frac{1}{2}}$ where K_0 is λ -independent.*

3 Regularity of the Solution Mapping and Geometric Properties

We first establish that $\mathcal{S}(\theta)$ varies locally Lipschitz in Hausdorff distance under the local $\mathbb{P}\mathbb{L}^\circ$ condition, and consequently that the hyper-objective F_{\max} is Lipschitz continuous (Corollary 3.4). In Section 3.2, we show that the minimizer manifolds $\{\mathcal{S}(\theta)\}_{\theta \in \Theta}$ share a common intrinsic dimension κ (Lemma 3.5), and then show θ -independent geometric bounds such as a uniform diameter, curvature control, and a positive injectivity radius (Proposition 3.6). We also show that the limiting Gibbs density on $\mathcal{S}(\theta)$ is uniformly bounded from below and above (Proposition 3.7). These uniform geometric properties will play a role later in our approximation analysis (Section 4).

3.1 Lipschitz Continuity of the Solution Mapping

In this subsection, our goal (Lemma 3.2) is to show that, under the $\mathbb{P}\mathbb{L}^\circ$ condition, the set-valued mapping $\theta \mapsto \mathcal{S}(\theta)$ is locally Lipschitz with respect to the Hausdorff distance. We then combine this regularity with the Lipschitz continuity of $f(\theta, x)$ to deduce the Lipschitz continuity of F_{\max} (Corollary 3.4). We begin by recalling the notion of Hausdorff distance.

Definition 3.1 (Hausdorff distance). *Let \mathcal{S}_1 and \mathcal{S}_2 be two subsets of \mathbb{R}^d . The Hausdorff distance between \mathcal{S}_1 and \mathcal{S}_2 is defined as*

$$\text{dist}(\mathcal{S}_1, \mathcal{S}_2) := \max \left\{ \sup_{x_1 \in \mathcal{S}_1} \inf_{x_2 \in \mathcal{S}_2} \|x_1 - x_2\|, \sup_{x_2 \in \mathcal{S}_2} \inf_{x_1 \in \mathcal{S}_1} \|x_1 - x_2\| \right\}.$$

Since the $\mathbb{P}\mathbb{L}^\circ$ condition provides only a *local* $\mathbb{P}\mathbb{L}$ inequality in a neighborhood of the minimizer set $\mathcal{S}(\theta)$, Lipschitz stability of the solution mapping does not follow from standard global error-bound arguments. By contrast, under a *global* $\mathbb{P}\mathbb{L}$ condition for $g(\theta, \cdot)$, one obtains a global error bound and then deduces Lipschitz continuity of $\theta \mapsto \mathcal{S}(\theta)$ directly from the smoothness of g on θ (see, e.g., [14, 50]). In our local setting, the obstruction is geometric: a local error bound alone still allows the minimizer set to have multiple disconnected components, and minimizers could jump from one component to another under arbitrarily small changes in θ , precluding any Hausdorff Lipschitz control. This is why we need that $\mathcal{S}(\theta)$ is connected under our assumptions (see Proposition 2.3) to prove a quantitative stability result showing that minimizers cannot jump and must move continuously under small perturbations of θ . The next lemma makes this precise.

Lemma 3.2. *Under Assumption 2.6 and Assumption 2.8, the minimizer mapping $\theta \mapsto \mathcal{S}(\theta)$ is locally Lipschitz continuous in the Hausdorff distance sense: there exists $\gamma > 0$ such that for every θ_1 and θ_2 with $\|\theta_1 - \theta_2\| \leq \gamma$, we have*

$$\text{dist}(\mathcal{S}(\theta_1), \mathcal{S}(\theta_2)) \leq \frac{L_{g,2}}{\mu} \|\theta_1 - \theta_2\|.$$

Proof. The proof has two steps. First, the local $\mathbb{P}\mathbb{L}$ condition and \mathcal{C}^2 regularity imply that there exists a neighborhood $\mathcal{U}(\theta_1)$ of the minimizer manifold $\mathcal{S}(\theta_1)$ such that inside $\mathcal{U}(\theta_1)$, the distance to $\mathcal{S}(\theta_1)$ is controlled by $\|\partial_x g(\theta_1, \cdot)\|$. Second, we show that for small perturbations θ_2 of θ_1 , every minimizer $x_2 \in \mathcal{S}(\theta_2)$

lies in $\mathcal{U}(\theta_1)$, by comparing $g(\theta_1, x_2)$ and $g(\theta_1, x_1)$ for $x_1 \in \mathcal{S}(\theta_1)$ using Lipschitz continuity in θ . Once $x_2 \in \mathcal{U}(\theta_1)$, the error bound and $L_{g,2}$ -smoothness in θ give

$$\text{dist}(x_2, \mathcal{S}(\theta_1)) \lesssim \|\partial_x g(\theta_1, x_2)\| \lesssim L_{g,2} \|\theta_1 - \theta_2\|,$$

and taking the supremum over $x_2 \in \mathcal{S}(\theta_2)$ yields the desired local Lipschitz bound in Hausdorff distance.

Step 1: local error bound around $\mathcal{S}(\theta)$. Fix $\theta \in \Theta$. By Proposition 2.3, Assumption 2.6 implies that every local minimizer of $g(\theta, \cdot)$ is in fact global, so the local PL inequality in Assumption 2.6 holds in a neighborhood of the global minimizer set $\mathcal{S}(\theta)$. In particular, there exists an open neighborhood $\mathcal{N}(\mathcal{S}(\theta))$ of $\mathcal{S}(\theta)$ such that

$$g(\theta, x) - \min_{z \in \mathbb{R}^d} g(\theta, z) \leq \frac{1}{2\mu} \|\partial_x g(\theta, x)\|^2 \quad \forall x \in \mathcal{N}(\mathcal{S}(\theta)). \quad (8)$$

By the local PL condition and \mathcal{C}^2 regularity, $g(\theta, \cdot)$ satisfies a local *error bound* in a smaller neighborhood of $\mathcal{S}(\theta)$ [73, Propositions 2.2 & 2.8]: there exists an open set $\mathcal{U}(\theta) \subseteq \mathcal{N}(\mathcal{S}(\theta))$ with $\mathcal{S}(\theta) \subset \mathcal{U}(\theta)$ such that

$$\text{dist}(x, \mathcal{S}(\theta)) \leq \mu^{-1} \|\partial_x g(\theta, x)\| \quad \forall x \in \mathcal{U}(\theta). \quad (9)$$

Moreover, since $\mathcal{S}(\theta)$ is compact and $\mathcal{U}(\theta)$ is open, we can find $\tilde{\epsilon} > 0$ such that the $\tilde{\epsilon}$ -sub-level set of $g(\theta, \cdot)$ lies inside $\mathcal{U}(\theta)$:

Lemma 3.3. *Under the local error bound for $g(\theta, \cdot)$ with $\mathcal{U}(\theta)$ being as above, there exists $\tilde{\epsilon} > 0$ such that*

$$\left\{ x \in \mathbb{R}^d : g(\theta, x) - \min_{z \in \mathbb{R}^d} g(\theta, z) \leq \tilde{\epsilon} \right\} \subset \mathcal{U}(\theta).$$

The proof of Lemma 3.3 is given in Appendix B.1. Intuitively, since $\mathcal{U}(\theta)$ is an open neighborhood of $\mathcal{S}(\theta)$ and $g(\theta, \cdot)$ is continuous, a small enough sub-level set around $\mathcal{S}(\theta)$ must be contained in $\mathcal{U}(\theta)$.

Step 2: stability of $\mathcal{S}(\theta)$ under small perturbations of θ . Let $\mathcal{U}(\theta_1)$ and $\tilde{\epsilon} > 0$ be as above. By Assumption 2.8 and using Equation (5), g is $L_{g,1}(\mathbb{D})$ -Lipschitz in θ on a compact domain $\mathbb{B}_d(0; \mathbb{D})$ in x , so for any $x \in \mathbb{R}^d$ and any $\theta_1, \theta_2 \in \Theta$,

$$|g(\theta_1, x) - g(\theta_2, x)| \leq L_{g,1}(\mathbb{D}) \|\theta_1 - \theta_2\|.$$

Let $x_1 \in \mathcal{S}(\theta_1)$ and $x_2 \in \mathcal{S}(\theta_2)$, where θ_2 will be taken close to θ_1 . Using optimality of x_1 for $g(\theta_1, \cdot)$ and of x_2 for $g(\theta_2, \cdot)$, we have

$$\begin{aligned} 0 &\leq g(\theta_1, x_2) - g(\theta_1, x_1) \\ &= [g(\theta_1, x_2) - g(\theta_2, x_2)] + [g(\theta_2, x_2) - g(\theta_2, x_1)] + [g(\theta_2, x_1) - g(\theta_1, x_1)] \\ &\leq |g(\theta_1, x_2) - g(\theta_2, x_2)| + 0 + |g(\theta_2, x_1) - g(\theta_1, x_1)| \\ &\leq 2L_{g,1}(\mathbb{D}) \|\theta_1 - \theta_2\|. \end{aligned} \quad (10)$$

Hence, if we choose $\gamma \leq \tilde{\epsilon}/(2L_{g,1}(2\mathbb{D}))$ and $\|\theta_1 - \theta_2\| \leq \gamma$, then (10) implies

$$g(\theta_1, x_2) - \min_z g(\theta_1, z) = g(\theta_1, x_2) - g(\theta_1, x_1) \leq \tilde{\epsilon},$$

so x_2 belongs to the sub-level set in Lemma 3.3. Therefore $x_2 \in \mathcal{U}(\theta_1)$ whenever $\|\theta_1 - \theta_2\| \leq \gamma$. Then the error bound (9) for $g(\theta_1, \cdot)$ yields

$$\text{dist}(x_2, \mathcal{S}(\theta_1)) \leq \mu^{-1} \|\partial_x g(\theta_1, x_2)\|.$$

Because x_2 is a minimizer for $g(\theta_2, \cdot)$, we have $\partial_x g(\theta_2, x_2) = 0$, hence

$$\|\partial_x g(\theta_1, x_2)\| = \|\partial_x g(\theta_1, x_2) - \partial_x g(\theta_2, x_2)\| \leq L_{g,2} \|\theta_1 - \theta_2\|,$$

where we used the $L_{g,2}$ -smoothness of g with respect to θ . Combining the two last inequalities results in

$$\text{dist}(x_2, \mathcal{S}(\theta_1)) \leq \frac{L_{g,2}}{\mu} \|\theta_1 - \theta_2\|.$$

By symmetry (interchanging the roles of θ_1 and θ_2 and repeating the same argument) and recalling the definition of the Hausdorff distance in Definition 3.1, we get

$$\text{dist}(\mathcal{S}(\theta_1), \mathcal{S}(\theta_2)) \leq \frac{L_{g,2}}{\mu} \|\theta_1 - \theta_2\| \quad \text{whenever} \quad \|\theta_1 - \theta_2\| \leq \gamma.$$

□

Having established the local Lipschitz continuity of $\mathcal{S}(\theta)$ in Lemma 3.2, we now turn to the regularity of the hyper-objective F_{\max} . The following corollary follows by combining the local Lipschitz continuity of $\theta \mapsto \mathcal{S}(\theta)$ with the Lipschitz continuity of $f(\theta, x)$ ¹¹; see, e.g., [14, Theorem 3.1].

Corollary 3.4. *Under Assumptions 2.6 and 2.8, $F_{\max}(\theta)$ is $(L_{f,1} + L_{f,1}L_{g,2}/\mu)$ -Lipschitz continuous.*

For completeness, we provide the proof in Section B.

3.2 Common Dimension and Geometric Properties of $\{\mathcal{S}(\theta)\}_{\theta \in \Theta}$

For each $\theta \in \Theta$, the local PL condition implies that on $\mathcal{S}(\theta)$ the Hessian $\partial_x^2 g(\theta, x)$ is positive definite in the normal directions and degenerate in the tangent directions [73, Proposition 2.7]. In particular, its rank $\mathfrak{r}(\theta)$ is constant over $x \in \mathcal{S}(\theta)$, and the dimension of the minimizer manifold can be written as $\dim \mathcal{S}(\theta) = \mathfrak{k}(\theta) = d - \mathfrak{r}(\theta)$. Moreover, the solution mapping $\theta \mapsto \mathcal{S}(\theta)$ is continuous (Lemma 3.2), and $\partial_x^2 g(\theta, x)$ is continuous in (θ, x) . Thus, when θ is perturbed slightly, points in $\mathcal{S}(\theta)$ move continuously and the corresponding Hessians remain close, so no eigenvalue can cross zero and the rank $\mathfrak{r}(\theta)$ cannot change. Hence $\mathfrak{r}(\theta)$, and therefore $\mathfrak{k}(\theta)$, is locally constant in θ and we obtain a single intrinsic dimension shared by all manifolds $\{\mathcal{S}(\theta)\}_{\theta \in \Theta}$. We summarize this in the following lemma.

Lemma 3.5. *Under Assumptions 2.6 to 2.8, the manifolds $\{\mathcal{S}(\theta)\}_{\theta \in \Theta}$ admit a common dimension \mathfrak{k} .*

The proof is given in Section B.3. Lemma 3.5 allows us to work with a single geometric parameter \mathfrak{k} in all later bounds, rather than letting the dimension depend on θ . In particular, when we study the Gibbs relaxation and the superquantile approximation of F_{\max} , the scaling with accuracy is expressed in terms of this common dimension \mathfrak{k} (see Theorem 4.5). Throughout the paper, we consider $\mathfrak{k} \geq 1$, since when $\mathfrak{k} = 0$, $\mathcal{S}(\theta)$ is a singleton and minima-selection is redundant. Next, we collect basic geometric properties of $\{\mathcal{S}(\theta)\}_{\theta \in \Theta}$ that will be used in our approximation analysis (see Section 4). The proofs are based on the uniform compactness of the manifolds.

Proposition 3.6. *Under compactness of Θ and Assumptions 2.6 and 2.7, the following holds for all $\theta \in \Theta$.*

- *There exists a constant D independent of θ , such that $\text{diam}(\mathcal{S}(\theta)) \leq D$.*
- *The absolute value of sectional curvature¹² of $\mathcal{S}(\theta)$ is bounded by some constant $C_0 > 0$.*
- *There is a constant $r_0 > 0$ such that the injectivity radius¹³ $\text{inj}(p) \geq r_0$ for all $p \in \mathcal{S}(\theta)$.*

¹¹A standard chaining argument shows that if $|F_{\max}(\theta_1) - F_{\max}(\theta_2)| \leq L\|\theta_1 - \theta_2\|$ whenever $\|\theta_1 - \theta_2\| \leq \gamma$, then the same constant works uniformly on Θ .

¹²Refer to Definition A.3 for the definition of sectional curvature.

¹³Refer to Definition A.2 for the definition of injectivity radius.

The proof is given in Section B.4. Finally, we show a uniform bound on the limiting density ρ_θ defined in eq. (7).

Proposition 3.7. *Under Assumptions 2.6 and 2.8, there exists a constant $\kappa > 0$ such that $\kappa \leq \rho_\theta(x) \leq 1/\kappa$ for all $x \in \mathcal{S}(\theta)$ and $\theta \in \Theta$.*

The proof is given in Section B.5. This result ensures that integration with respect to the limiting Gibbs measure is uniformly comparable to integration with respect to the volume measure on $\mathcal{S}(\theta)$, which is crucial for our approximation analysis in the next section.

Remark 3.8. *(On the size of the constant κ) We chose $\kappa = \mathbf{b} \cdot (\mu/M_g)^{\frac{d-k}{2}}$ in the proof of Proposition 3.7, where $\mu > 0$ is a uniform lower bound on the nonzero normal eigenvalues of $\partial_x^2 g(\theta, x)$, $M_g > 0$ is a uniform upper bound on $\|\partial_x^2 g(\theta, x)\|$ over $\mathcal{S}(\theta)$, and the constant $\mathbf{b} > 0$ comes from the volume bounds on $\mathcal{S}(\theta)$ in Lemma B.5 in Section B.5. In the worst case, the ratio μ/M_g can be very small, so κ may be exponentially small. In contrast, in an idealized case where in normal coordinates $g(\theta, \cdot)$ behaves like a pure squared distance to $\mathcal{S}(\theta)$, we have $\mu = M_g$, so $\kappa = \mathbf{b}$.*

4 Approximation Guarantees with SQ-G Relaxation

In this section, we show that the superquantile-Gibbs relaxation $\tilde{F}_{\text{SQ-G}}$, defined in Equation (2), provides a valid approximation to F_{max} under Assumptions 2.6 to 2.8, given suitable choices of the parameters δ and λ . Our approximation result justifies using $\tilde{F}_{\text{SQ-G}}$ as a surrogate for F_{max} when applying zeroth-order methods to optimize the latter. We establish the result through the following steps:

1. The superquantile loss (SQ-loss), defined as

$$\tilde{F}_{\text{SQ}}(\theta) := \min_{\beta} \left\{ \beta + \frac{1}{\delta} \mathbb{E}_{X \sim \mu_\theta^0} [\max\{f(\theta, X) - \beta, 0\}] \right\}, \quad (11)$$

closely approximates the hyper-objective $F_{\text{max}}(\theta)$ point-wisely.

2. The difference between \tilde{F}_{SQ} and $\tilde{F}_{\text{SQ-G}}$ is bounded by the Wasserstein-1 distance between μ_θ^λ and μ_θ^0 : $|\tilde{F}_{\text{SQ}}(\theta) - \tilde{F}_{\text{SQ-G}}(\theta)| \leq \mathcal{O}(\delta^{-1} \mathbb{W}_1(\mu_\theta^\lambda, \mu_\theta^0))$.

Below we formally present these results.

4.1 Approximation of F_{max} with \tilde{F}_{SQ}

Recall that the $(1 - \delta)$ -superquantile of the random variable $Y = f(\theta, X)$ with $X \sim \mu_\theta^0$ is the average of the values of Y that lie above its $(1 - \delta)$ -quantile threshold. Our goal is to show that, for small δ , the superquantile $\tilde{F}_{\text{SQ}}(\theta)$ provides a good approximation of $F_{\text{max}}(\theta)$. To build intuition, fix θ and suppose that the function $x \mapsto f(\theta, x)$ attains its maximum over $\mathcal{S}(\theta)$ at a unique point $x^*(\theta) \in \mathcal{S}(\theta)$. Consider the high-value set $\mathfrak{X}_\delta(\theta) := \{x \in \mathcal{S}(\theta) : f(\theta, x) \text{ is above the } (1 - \delta)\text{-quantile threshold}\}$. This set forms a neighborhood of $x^*(\theta)$. Since $x^*(\theta) \in \mathfrak{X}_\delta(\theta)$ and f is Lipschitz, the approximation error $|\tilde{F}_{\text{SQ}}(\theta) - F_{\text{max}}(\theta)|$ is controlled by how far one can move away from $x^*(\theta)$ while staying in $\mathfrak{X}_\delta(\theta)$. Denoting by r the minimal geodesic distance from $x^*(\theta)$ to the boundary of $\mathfrak{X}_\delta(\theta)$, the Lipschitz continuity of f then bounds the error in terms of r .

Thus, to bound the approximation error, it suffices to bound r . To bound this radius r given our control over the probability mass δ , we proceed in two steps: 1) *Probability to Volume*: We first translate probability mass δ into Riemannian volume. This is possible because the density of the limiting measure μ_θ^0 is strictly lower-bounded (see Proposition 3.7), ensuring that a small probability mass implies a small geometric volume. 2) *Volume to Radius*: We then translate Riemannian volume into the radius r . By establishing that the

Riemannian volume scales similarly to Euclidean volume ($\propto r^k$), we deduce that the radius shrinks at the rate $r \lesssim \delta^{1/k}$.

Classical results such as [36] give a pointwise asymptotic expansion of the volume of a small geodesic ball, showing that $\mathcal{M}(B_g(p; r))/r^k \rightarrow c(p)$ as $r \rightarrow 0$ with a coefficient depending on the local curvature at p . For our purposes, this is not sufficient: we will see that in the proof of Theorem 4.2 we need a *uniform*, non-asymptotic lower bound that holds simultaneously for all centers $p \in \mathcal{S}(\theta)$ and all radii $0 < r \leq r_1$, with r_1 depending only on the global bounds on sectional curvature and injectivity radius from Proposition 3.7. Lemma 4.1 provides exactly this quantitative version by turning the asymptotic comparison into an explicit estimate with controlled radius and constants.

Lemma 4.1. *Under Assumptions 2.6 and 2.7, there exist constants $c_H, c_L > 0$, and $c_1 > 0$ such that for every $\theta \in \Theta$, for any $p \in \mathcal{S}(\theta)$, and any radius r satisfying $0 < r < \min\{r_0, c_1/\sqrt{2C_0}\}$, the Riemannian volume of the geodesic ball $\mathbb{B}_g(p; r)$ satisfies*

$$c_L \cdot \text{Leb}_k(\mathbb{B}_k(p; r)) \leq \mathcal{M}(\mathbb{B}_g(p; r)) \leq c_H \cdot \text{Leb}_k(\mathbb{B}_k(p; r)),$$

where r_0 and C_0 are defined in Proposition 3.6, $\text{Leb}_k(\mathbb{B}_k(p; r))$ is the standard k -dimensional Lebesgue volume of a ball of radius r in \mathbb{R}^k , and \mathcal{M} is the Riemannian volume measure on $(\mathcal{S}(\theta), g)$.

The proof of Lemma 4.1 is given in Section C.1. Based on Lemma 4.1, the Riemannian volume of a geodesic ball with radius r , $\mathcal{M}(\mathbb{B}_g(p; r))$, scales as r^k . At a high level, the lemma relies on two geometric ingredients: (i) The injectivity radius bound $r_0 > 0$ guarantees that, around every $p \in \mathcal{S}$, we can introduce normal coordinates on the whole geodesic ball $\mathbb{B}_g(p; r)$ for all $r \leq r_0$. (ii) The curvature bound $|\text{Sec}| \leq C_0$ then implies that, in these normal coordinates and for radii r of order $1/\sqrt{C_0}$, at a given point $v \in \mathbb{B}_g(p; r)$, the matrix $(g_{ij}(v))_{i,j=1}^k$ representing the Riemannian metric remains uniformly close to the Euclidean metric $(\delta_{ij}(v))_{i,j=1}^k$ ¹⁴. Consequently, the Riemannian volume element $\sqrt{\det(g_S(v))} dv$ is uniformly comparable from below and above to the Euclidean volume element dv on such balls. Integrating this comparison over $\mathbb{B}_k(0; r)$ yields the stated bounds on the Riemannian volume $\mathcal{M}(\mathbb{B}_g(p; r))$. We now state the following key result.

Theorem 4.2 (\tilde{F}_{SQ} approximates F_{\max}). *Recall $\tilde{F}_{SQ}(\theta) := \min_{\beta} \phi_{0,\delta}(\theta, \beta)$. Under Assumptions 2.6 to 2.8, for every $\theta \in \Theta$ and for*

$$0 < \delta \leq c_L \cdot C_k \cdot \kappa \cdot \left(4^{-1} \min\{c_1/\sqrt{2C_0}, r_0\}\right)^k,$$

we have

$$|F_{\max}(\theta) - \tilde{F}_{SQ}(\theta)| \leq \frac{4L_{f,1}\delta^{\frac{1}{k}}}{(\kappa \cdot c_L \cdot C_k)^{\frac{1}{k}}},$$

where c_L and c_1 are defined in Lemma 4.1, κ in Proposition 3.7, k is the dimension of $\mathcal{S}(\theta)$, $C_k = \pi^{k/2}/\Gamma(k/2 + 1)$, and r_0, C_0 are from Proposition 3.6.

Proof. Let $Z := f(\theta, X)$ where $X \sim \mu_g^0(\theta)$. Since Z takes values in $\{f(\theta, x) : x \in \mathcal{S}(\theta)\}$, we have the elementary bounds

$$\max_{x \in \mathcal{S}(\theta)} f(\theta, x) \geq \tilde{F}_{SQ}(\theta) \geq Q_{1-\delta}(Z),$$

hence

$$|F_{\max}(\theta) - \tilde{F}_{SQ}(\theta)| = F_{\max}(\theta) - \tilde{F}_{SQ}(\theta)$$

¹⁴Here δ_{ij} denotes the Kronecker delta: $\delta_{ij} = 1$ if $i = j$ and $\delta_{ij} = 0$ otherwise.

$$\leq F_{\max}(\theta) - \mathbf{Q}_{1-\delta}(f(\theta, X)). \quad (12)$$

Thus it remains to bound $F_{\max}(\theta) - \mathbf{Q}_{1-\delta}(f(\theta, X))$.

We fix θ and drop it from the notation. Write $\mathcal{S} = \mathcal{S}(\theta)$, $f = f(\theta, \cdot)$, $f^* = \max_{x \in \mathcal{S}} f(x)$, $\mathcal{S}_f = \arg \max f$ (nonempty by compactness), and draw $Y \sim \mu^0$ as in Proposition 2.10. Denote by $\text{dist}_{\mathbf{g}}$ the geodesic distance on \mathcal{S} , and write $\mathbb{B}_{\mathbf{g}}(x; r) := \{u \in \mathcal{S} : \text{dist}_{\mathbf{g}}(u, x) < r\}$ for the geodesic ball (refer to (35) in Section A.1). While \mathcal{S}_f may generally consist of multiple connected components, we assume without loss of generality that it is connected, as the extension of our analysis below to the general case is straightforward.

Proof outline. (i) Let $\varepsilon := f^* - \mathbf{Q}_{1-\delta}(f(Y))$ and $A_\varepsilon := \{u \in \mathcal{S} : f(u) \geq f^* - \varepsilon\}$. Set $r := \text{dist}_{\mathbf{g}}(\overline{\mathcal{S} \setminus A_\varepsilon}, \mathcal{S}_f)$. A minimizing geodesic between these sets has a midpoint x with a geodesic ball $\mathbb{B}_{\mathbf{g}}(x; r/4) \subset A_\varepsilon \setminus \mathcal{S}_f$. (ii) By Proposition 3.7, $\mu^0(\cdot)$ is comparable to $\mathcal{M}(\cdot)$; since $\mu^0(A_\varepsilon) = \delta$, we get $\mathcal{M}(\mathbb{B}_{\mathbf{g}}(x; r/4)) \lesssim \delta$. Under Proposition 3.6 and by Lemma 4.1, $\mathcal{M}(\mathbb{B}_{\mathbf{g}}(x; r/4)) \gtrsim (r/4)^k$. Hence $r \lesssim \delta^{1/k}$ (for small δ). (iii) Lipschitzness of f yields $f^* - \mathbf{Q}_{1-\delta}(f(Y)) \leq L_{f,1} r$. Combining with $r \lesssim \delta^{1/k}$ and the reduction in (12) gives the claimed rate.

(i) Near-optimal set contains a geodesic ball. For any set $A \subseteq \mathcal{S}$, we write \overline{A} for the closure of A in \mathcal{S} , i.e., with respect to the topology induced by the Riemannian metric on \mathcal{S} . We then define the geodesic set-set distance using the closure

$$r := \text{dist}_{\mathbf{g}}(\overline{\mathcal{S} \setminus A_\varepsilon}, \mathcal{S}_f) = \min_{z \in \overline{\mathcal{S} \setminus A_\varepsilon}} \min_{y \in \mathcal{S}_f} \text{dist}_{\mathbf{g}}(z, y).$$

Since $\overline{\mathcal{S} \setminus A_\varepsilon}$ and \mathcal{S}_f are compact, minimizers $z \in \overline{\mathcal{S} \setminus A_\varepsilon}$ and $y \in \mathcal{S}_f$ exist with $\text{dist}_{\mathbf{g}}(z, y) = r$. Let γ be a minimizing geodesic from y to z and set the geodesic midpoint $x := \gamma(r/2)$. We claim

$$\mathbb{B}_{\mathbf{g}}(x; r/4) \subset A_\varepsilon \setminus \mathcal{S}_f.$$

Indeed, for any $w \in \mathbb{B}_{\mathbf{g}}(x; r/4)$, using that the map $x \mapsto \text{dist}_{\mathbf{g}}(x, \mathcal{S}_f)$ is 1-Lipschitz¹⁵ we have

$$\text{dist}_{\mathbf{g}}(w, \mathcal{S}_f) \geq \text{dist}_{\mathbf{g}}(x, \mathcal{S}_f) - \text{dist}_{\mathbf{g}}(w, x) \geq r/2 - r/4 = r/4 > 0,$$

so $w \notin \mathcal{S}_f$; and

$$\text{dist}_{\mathbf{g}}(w, \mathcal{S}_f) \leq \text{dist}_{\mathbf{g}}(w, x) + \text{dist}_{\mathbf{g}}(x, \mathcal{S}_f) \leq r/4 + r/2 = 3r/4 < r.$$

Because $r = \min_{u \in \overline{\mathcal{S} \setminus A_\varepsilon}} \text{dist}_{\mathbf{g}}(u, \mathcal{S}_f)$, the inequality $\text{dist}_{\mathbf{g}}(w, \mathcal{S}_f) < r$ implies $w \notin \overline{\mathcal{S} \setminus A_\varepsilon}$, hence $w \in A_\varepsilon$.

(ii) From probability mass to a bound on r . By Proposition 3.7, the density ρ of μ^0 w.r.t. the Riemannian volume \mathcal{M} satisfies $\kappa \leq \rho \leq \kappa^{-1}$ on \mathcal{S} , hence for any Borel $A \subset \mathcal{S}$,

$$\kappa \mathcal{M}(A) \leq \mu^0(A) \leq \kappa^{-1} \mathcal{M}(A).$$

Using $\mathbb{B}_{\mathbf{g}}(x; r/4) \subset A_\varepsilon$ and $\mu^0(A_\varepsilon) = \delta$, we obtain

$$\mathcal{M}(\mathbb{B}_{\mathbf{g}}(x; r/4)) \leq \mathcal{M}(A_\varepsilon) \leq \kappa^{-1} \mu^0(A_\varepsilon) = \kappa^{-1} \delta.$$

¹⁵For any $a \in \mathcal{S}_f$, the triangle inequality gives $\text{dist}_{\mathbf{g}}(w, a) \leq \text{dist}_{\mathbf{g}}(w, x) + \text{dist}_{\mathbf{g}}(x, a)$. Taking $\inf_{a \in \mathcal{S}_f}$ yields $\text{dist}_{\mathbf{g}}(w, \mathcal{S}_f) \leq \text{dist}_{\mathbf{g}}(w, x) + \text{dist}_{\mathbf{g}}(x, \mathcal{S}_f)$. Swapping w and x gives the reverse inequality, hence $|\text{dist}_{\mathbf{g}}(w, \mathcal{S}_f) - \text{dist}_{\mathbf{g}}(x, \mathcal{S}_f)| \leq \text{dist}_{\mathbf{g}}(w, x)$.

On the other hand, the injectivity–radius and curvature bounds in Proposition 3.6 allow us to apply Lemma 4.1. Hence, for $r \leq \min\{r_0, 1/\sqrt{2K}\}$, we have

$$cC_k (r/4)^k = c\text{Leb}_k(\mathbb{B}_k(0; r/4)) \leq \mathcal{M}(\mathbb{B}_g(x; r/4)),$$

where $C_k = \pi^{k/2}/\Gamma(k/2 + 1)$. Combining the last two inequalities yields

$$cC_k (r/4)^k \leq \kappa^{-1}\delta \implies r \leq 4\left(\delta \kappa^{-1}[cC_k]^{-1}\right)^{\frac{1}{k}}, \quad (13)$$

provided $\delta \leq cC_k \kappa [4^{-1} \min\{r_0, 1/\sqrt{2C_0}\}]^k$ so that the small–radius condition of Lemma 4.1 holds.

(iii) Lipschitz control of the value gap. Since f is $L_{f,1}$ -Lipschitz (in the ambient norm) and $\text{dist}_g \geq \|\cdot\|^{16}$,

$$\begin{aligned} f^* - \mathcal{Q}_{1-\delta}(f(Y)) &= \varepsilon \leq f^* - f(z) \leq L_{f,1} \|y - z\| \leq L_{f,1} \text{dist}_g(y, z) \\ &= L_{f,1} r. \end{aligned} \quad (14)$$

Together with the bound on r in (13), we conclude

$$f^* - \mathcal{Q}_{1-\delta}(f(Y)) \leq 4L_{f,1} \left(\delta \kappa^{-1}[cC_k]^{-1}\right)^{\frac{1}{k}},$$

which completes the proof. \square

Remark 4.3. (Sharpness of the $\delta^{1/k}$) The $\delta^{1/k}$ dependence in Theorem 4.2 is dictated by the k -dimensional volume growth of small balls on $\mathcal{S}(\theta)$ and cannot, in general, be improved. Indeed, fix θ and a point $x^*(\theta) \in \mathcal{S}(\theta)$, and consider the toy function $f(\theta, x) := -\text{dist}_g(x, x^*(\theta))$. Clearly, $F_{\max}(\theta) = 0$. For $r > 0$, the sublevel set $A_r(\theta) = \{x \in \mathcal{S}(\theta) : -f(\theta, x) \leq r\}$ is exactly the geodesic ball $B_g(x^*(\theta); r)$. Let us pick $r = -\mathcal{Q}_{1-\delta}(f(\theta, Y))$ where $Y \sim \mu_\theta^0$ and δ sufficiently small as stated in Theorem 4.2. By Proposition 3.7 and Lemma 4.1, we have

$$\begin{aligned} \delta &= \mu_0(A_r(\theta)) = \mu_0(\mathbb{B}_g(x^*(\theta); r)) \leq \kappa^{-1} \cdot \mathcal{M}(\mathbb{B}_g(x^*(\theta); r)) \\ &\leq \kappa^{-1} \cdot c_H \cdot \text{Leb}_k(\mathbb{B}_g(x^*(\theta); r)) \lesssim r^k. \end{aligned} \quad (15)$$

Then $\delta^{1/k} \lesssim r = F_{\max}(\theta) - \mathcal{Q}_{1-\delta}(f(\theta, Y))$. Thus one cannot, in general, replace the factor $\delta^{1/k}$ in Theorem 4.2 by a smaller power of δ .

4.2 Approximation of SQ-Loss with SQ-G-Loss

The variational formulations $\phi_{0,\delta}$ and $\phi_{\lambda,\delta}$ involve expectations of $\xi(x) := \max\{f(\theta, x) - \beta, 0\}$ over μ_θ^0 and μ_θ^λ , respectively. Using this expectation structure, we bound the difference between $\tilde{F}_{\text{SQ}}(\theta)$ and $\tilde{F}_{\text{SQ-G}}(\theta)$ by the Wasserstein-1 distance between μ_θ^λ and μ_θ^0 : We use the Kantorovich–Rubinstein duality for the Wasserstein-1 distance with $\xi(x)$ as a test function.

Lemma 4.4. Under Assumption 2.8, for every $\theta \in \Theta$, we have,

$$|\tilde{F}_{\text{SQ-G}}(\theta) - \tilde{F}_{\text{SQ}}(\theta)| \leq \frac{L_{f,1}}{\delta} \cdot \mathbb{W}_1(\mu_\theta^\lambda, \mu_\theta^0). \quad (16)$$

¹⁶Here we use the fact that the geodesic distance $\text{dist}_g(x, y)$ is at least as large as the Euclidean distance $\|x - y\|$ in the ambient space.

The proof of Lemma 4.4 is given in Section C.2. As a consequence of Theorem 4.2, Lemma 4.4, and Proposition 2.11, we have that $\tilde{F}_{\text{SQ-G}}(\theta)$ approximates $F_{\text{max}}(\theta)$ by choosing δ and λ properly.

Theorem 4.5. *Under Assumptions 2.6 to 2.8, for $\delta < c \cdot C_k \cdot \kappa \cdot (4^{-1} \min\{1/\sqrt{2C_0}, r_0\})^k$, we have*

$$\left| F_{\text{max}}(\theta) - \tilde{F}_{\text{SQ-G}}(\theta) \right| \leq \frac{4L_{f,1}\delta^{\frac{1}{k}}}{(\kappa \cdot c \cdot C_k)^{\frac{1}{k}}} + \frac{L_{f,1}}{\delta} \cdot K_0\lambda^{\frac{1}{2}}. \quad (17)$$

The bound in (17) makes the role of the manifold dimension k explicit: the bias term scales as $\delta^{1/k}$, so larger k requires smaller δ to reach the same accuracy. This bound also yields a simple rule for choosing the parameters to reach any target accuracy: pick $\delta = \epsilon_v^k$ and $\lambda = \epsilon_v^{2(k+1)}$, where $0 < \epsilon_v < (c \cdot C_k \cdot \kappa)^{\frac{1}{k}} \cdot 4^{-1} \min\{c_1/\sqrt{2C_0}, r_0\}$, then

$$\left| F_{\text{max}}(\theta) - \tilde{F}_{\text{SQ-G}}(\theta) \right| = \mathcal{O}(\epsilon_v).$$

This provides a clear, dimension-aware recipe for setting (δ, λ) that we use in Section 5.

5 Oracle Complexity of Optimizing F_{max}

In this section, we develop a zeroth-order algorithm to find a Goldstein stationary point of the hyper-objective F_{max} . Zeroth-order methods require pointwise evaluations of the objective, but direct evaluation of F_{max} is intractable because it involves an inner maximization over the lower-level solution set. To obtain a tractable objective oracle, we replace F_{max} by its Gibbs–superquantile surrogate $\tilde{F}_{\text{SQ-G}}$ defined in (2), which can be estimated from Gibbs samples. As shown in Theorem 4.5, suitable choices of λ and δ ensure that $\tilde{F}_{\text{SQ-G}}$ uniformly approximates F_{max} . We then query $\tilde{F}_{\text{SQ-G}}$ at multiple points to construct a finite-difference estimator of a proxy gradient of F_{max} , and use this estimator within a zeroth-order scheme to obtain a Goldstein stationary point of the original hyper-objective.

To evaluate $\tilde{F}_{\text{SQ-G}}(\theta)$, we use its variational representation in (2), which involves solving the inner minimization problem $\min_{\beta \in \mathbb{R}} \phi_{\lambda,\delta}(\theta, \beta)$. Since $\phi_{\lambda,\delta}(\theta, \cdot)$ is convex but possibly nonsmooth, a natural choice is to apply the subgradient method¹⁷. To ensure convergence, the nonsmooth optimization must be restricted to a *bounded* interval. In Lemma 5.1, we show that the optimal set $\arg \min_{\beta} \phi_{\lambda,\delta}(\theta, \beta)$ lies within $[-B, B]$, so that

$$\tilde{F}_{\text{SQ-G}}(\theta) = \min_{\beta \in [-B, B]} \phi_{\lambda,\delta}(\theta, \beta).$$

Given that (i) $\phi_{\lambda,\delta}(\theta, \cdot)$ is convex and Lipschitz continuous, (ii) the feasible set is bounded, and (iii) the stochastic subgradient $\tilde{\partial}_{\beta} \phi_{\lambda,\delta}(\theta, \beta; X)$ satisfies $|\tilde{\partial}_{\beta} \phi_{\lambda,\delta}(\theta, \beta; X)| \leq \sigma := 1 + \delta^{-1}$, we invoke the classical convergence guarantees for convex Lipschitz objectives [51, Proposition 2]. Accordingly, the output $\hat{\beta}$ of projected stochastic gradient descent (PSGD) (see Algorithm 1) satisfies

$$\phi_{\lambda,\delta}(\theta, \hat{\beta}) - \min_{\beta} \phi_{\lambda,\delta}(\theta, \beta) \leq \hat{\epsilon}, \quad \text{with probability at least } 1 - \Delta, \quad (18)$$

after at most $\mathcal{O}(B^2\sigma^2\hat{\epsilon}^{-2}\log^2(\Delta^{-1}))$ iterations.

Building on the above discussion, we now use the PSGD output to construct a tractable zeroth-order oracle for F_{max} . For any query θ , we evaluate the scalar quantity $\phi_{\lambda,\delta}(\theta, \hat{\beta})$, where $\hat{\beta}$ is the approximate minimizer returned by PSGD, and regard this as a noisy evaluation of $\tilde{F}_{\text{SQ-G}}(\theta)$ and hence of $F_{\text{max}}(\theta)$. Querying this oracle at carefully chosen perturbations of θ yields a multi-point finite-difference estimator of a proxy gradient, which drives the projected zeroth-order scheme in Algorithm 2.

¹⁷Because the problem is one-dimensional, the bisection method is also applicable, provided the domain is bounded.

Below, we analyze in detail the convergence of Algorithm 1 (inner minimization of the Gibbs–superquantile) and Algorithm 2 (outer minimization of the hyper-objective).

5.1 Inner Minimization of Gibbs-superquantile

In this subsection, we first show that all global minimizers of $\phi_{\lambda,\delta}(\theta, \cdot)$ lie in a common bounded interval. This boundedness allows us to run PSGD on a compact domain and invoke standard convergence guarantees. We then use this result to justify treating the noisy values $\phi_{\lambda,\delta}(\theta, \hat{\beta})$, where $\hat{\beta}$ is the PSGD output, as approximate evaluations of $F_{\max}(\theta)$.

We first briefly introduce the PSGD (Algorithm 1) to solve $\min_{\beta \in [-B, B]} \phi_{\lambda,\delta}(\theta, \beta)$. Specifically, for a given $\theta \in \Theta$, we have

$$\beta^{l+1} \leftarrow \text{Proj}_{[-B, B]}(\beta^l - \eta_l \tilde{\partial}_\beta \phi_{\lambda,\delta}(\theta, \beta^l; \tilde{X}^{(l)})), \quad (19)$$

where $\tilde{\partial}_\beta \phi_{\lambda,\delta}(\theta, \beta; \tilde{X}^{(l)})$ represents a sub-gradient of the noisy sample of $\phi_{\lambda,\delta}(\theta, \beta)$ as follows:

$$\phi_{\lambda,\delta}(\theta, \beta; \tilde{X}^{(l)}) := \beta + \frac{1}{\delta} \max\{f(\theta, \tilde{X}^{(l)}) - \beta, 0\}, \quad (20)$$

and $\{\tilde{X}^{(l)}\}_{l=0}^{L-1}$ are independent and identically distributed (i.i.d.) samples drawn from μ_θ^λ and B is a positive constant. A natural choice for the PSGD output at a fixed θ is the empirical average $L^{-1} \sum_{i=1}^L \beta^i$.

We next show in Lemma 5.1 that the minimizers $\beta^*(\theta) \in \arg \min_\beta \phi_{\lambda,\delta}(\theta, \beta)$ are uniformly bounded. For the upper bound on $\beta^*(\theta)$, recall the definition of $\tilde{F}_{\text{SQ}}(\theta)$ in (11); then

$$\begin{aligned} \beta^*(\theta) &\leq \beta^*(\theta) + \frac{1}{\delta} \mathbb{E}_{X \sim \mu_\theta^\lambda}[\max\{f(\theta, X) - \beta^*(\theta), 0\}] = \phi_{\lambda,\delta}(\theta, \beta^*(\theta)) \\ &= \tilde{F}_{\text{SQ-G}}(\theta) \leq \tilde{F}_{\text{SQ}}(\theta) + |\tilde{F}_{\text{SQ-G}}(\theta) - \tilde{F}_{\text{SQ}}(\theta)| \\ &\leq \tilde{F}_{\text{SQ}}(\theta) + \frac{L_{f,1}}{\delta} K_0 \lambda^{1/2} \end{aligned} \quad (21)$$

$$\leq L_{f,0}(\text{D}) + \frac{L_{f,1}}{\delta} K_0 \lambda^{1/2}, \quad (22)$$

where (21) applies Proposition 2.11 to Lemma 4.4, and (22) uses

$$\tilde{F}_{\text{SQ}}(\theta) \leq \max_{x \in \mathcal{S}(\theta)} f(\theta, x) \leq \max_{x \in \mathbb{B}_d(0; \text{D})} f(\theta, x) \leq L_{f,0}(\text{D}),$$

with $L_{f,0}(\cdot)$ defined in (5) and D large enough that $\mathcal{S}(\theta) \subseteq \mathbb{B}_d(0; \text{D})$ (see Proposition 3.6).

A key part of the proof is a uniform lower bound on $\beta^*(\theta)$: since $\beta^*(\theta)$ is a $(1 - \delta)$ -quantile, we have $\mathbb{P}\{f(\theta, X) \leq \beta^*(\theta)\} \geq 1 - \delta$ for $X \sim \mu_\theta^\lambda$. We then prove a tail bound for the Gibbs measure by using the quadratic growth of g beyond $\mathbb{B}_d(0; \text{D})$ in Assumption 2.8, which ensures $\mu_\theta^\lambda(B(0; 2\text{D})) \geq \delta_0$. Combining both and taking $\delta < \delta_0$, it yields

$$\mu_\theta^\lambda(\{x : f(\theta, x) \leq \beta^*(\theta)\} \cap B(0; 2\text{D})) \geq \delta_0 - \delta > 0,$$

so there exists $x_0 \in B(0; 2\text{D})$ with $f(\theta, x_0) \leq \beta^*(\theta)$. Since $|f(\theta, x)| \leq L_{f,0}(2\text{D})$ on $B(0; 2\text{D})$, we conclude $\beta^*(\theta) \geq -L_{f,0}(2\text{D})$. Together with (22), this shows $\beta^*(\theta) \in [-B, B]$ for a suitable $B < \infty$. Now we state the result in the following lemma. The complete proof is deferred to Section D.1.

Lemma 5.1. *Suppose that Assumption 2.8 holds and the condition $\delta \leq 1/2$ hold. For any minimizer $\beta^*(\theta) \in \arg \min_\beta \phi_{\lambda,\delta}(\theta, \beta)$, we have*

$$|\beta^*(\theta)| \leq B := \max \left\{ L_{f,0}(2\text{D}), L_{f,0}(\text{D}) + \frac{L_{f,1}}{\delta} \cdot K_0 \lambda^{\frac{1}{2}} \right\}. \quad (23)$$

Algorithm 1 PSGD($\theta, \beta_0; (\lambda, \delta)$)

Input: $\theta, \beta_0, \lambda, \delta$, and L

- 1: $l = 0$
 - 2: **while** $\lambda > 0$ and $l \leq L$ **do**
 - 3: $\beta^{l+1} = \text{Proj}_{[-B, B]}(\beta^l - \eta_l \tilde{\partial}_\beta \phi_{\lambda, \delta}(\theta, \beta^l; \tilde{X}^{(l)}))$
 $[\{\tilde{X}^{(l)}\}_{l=0}^{L-1}$ are i.i.d samples of μ_θ^λ .]
 - 4: $l = l + 1$
 - 5: **end while**
 - 6: $\hat{\beta} = \frac{1}{L} \sum_{i=1}^L \beta^i$
-

Combining the existing convergence analysis of PSGD with Lemma 5.1, we can apply the guarantee in (18) to the PSGD output $\hat{\beta}$. We then define the following function as an accessible approximation of $\phi_{\lambda, \delta}(\theta, \hat{\beta})$:

$$\tilde{\psi}(\theta) := \left\{ \phi_{\lambda, \delta}(\theta, \hat{\beta}; \hat{X}_I) = \hat{\beta} + \frac{1}{\delta|I|} \sum_{i \in I} \max\{f(\theta, \hat{X}^{(i)}) - \hat{\beta}, 0\} \right\}. \quad (24)$$

Here $\hat{X}_I = \{\hat{X}^{(i)}\}_{i \in I}$ denote M i.i.d. samples from the sampling oracle of μ_θ^λ .

The next lemma shows that the quantity $\tilde{\psi}(\theta)$ defined in (24) closely approximates $\tilde{F}_{\text{SQ-G}}(\theta)$. The proof is deferred to Section D.2. Before stating it, we briefly explain the role of the high-probability guarantee in (18). The convergence analysis of the outer zeroth-order algorithm is often based on an L^2 -type control of the oracle error, i.e., $\mathbb{E}[|\tilde{\psi}(\theta) - F_{\max}(\theta)|^2 \mid \theta]$, rather than just on its expectation. An in-expectation convergence result for PSGD would only control the mean optimality gap and does not, in general, translate into a sufficiently tight second-moment bound. In contrast, the high-probability estimate in (18) provides a tail bound on the PSGD optimization error; by choosing the target accuracy $\hat{\epsilon}$ and the failure probability Δ appropriately, this tail bound can be converted into the required L^2 control on the oracle error used in Lemma 5.2.

Lemma 5.2. *Suppose that Assumption 2.8 holds. Given $\theta \in \Theta$, by using Algorithm 1 (PSGD($\theta, \beta_0; (\lambda, \delta)$)), with the number of iterations $L = \mathcal{O}(k^2 B^2 \epsilon_v^{-2-2k} \log^2(\epsilon_v^{-1}))$, and $|I| \geq 4\tilde{C}_f \epsilon_v^{-2-2k}$, we obtain*

$$\mathbb{E}[|\tilde{\psi}(\theta) - \tilde{F}_{\text{SQ-G}}(\theta)|^2 \mid \theta] \leq \epsilon_v^2. \quad (25)$$

Here B is defined in Lemma 5.1 and \tilde{C}_f is a constant.

We now simply show that $\tilde{\psi}(\theta)$ provides a good approximation to $F_{\max}(\theta)$. Applying Lemma 5.2 together with Theorem 4.5 yields

$$\begin{aligned} \mathbb{E}[|\tilde{\psi}(\theta) - F_{\max}(\theta)|^2 \mid \theta] &\leq \mathbb{E}[|\tilde{\psi}(\theta) - \tilde{F}_{\text{SQ-G}}(\theta)|^2 \mid \theta] + |\tilde{F}_{\text{SQ-G}}(\theta) - F_{\max}(\theta)|^2 \\ &\leq \mathbb{E}[|\phi_{\lambda, \delta}(\theta, \hat{\beta}; \hat{X}_I) - \tilde{F}_{\text{SQ-G}}(\theta)|^2 \mid \theta] + \mathcal{O}(\delta^{2/k} + \lambda\delta^{-2}) \\ &= \mathcal{O}(\epsilon_v^2), \end{aligned} \quad (26)$$

where, in the final bound, we choose $\delta = \epsilon_v^k$ and $\lambda = \epsilon_v^{2(k+1)}$. The Equation (26) will serve as a key ingredient in our later convergence analysis.

Algorithm 2 Projected Stochastic Zeroth-order with Minima-selection (PSZO-MinSel)

Initialization: $\beta_0, \theta_0, \lambda, \delta < 1/2$, and integers M, N .

- 1: **for** $n = 0$ to $N - 1$ **do**
 - 2: Query M i.i.d. samples from the sampling oracle of $\mu_{\theta_n}^\lambda$, denoted by $\hat{X}_I = \{\hat{X}^{(i)}\}_{i \in I}$.
 - 3: Sample $\{u_{n,t}\}_{t=1}^{b_u}$ independently and uniformly from a unit sphere.
 - 4: $\beta_{n,t}^+ = \text{PSGD}(\theta_n + \rho u_{n,t}, \beta_0; (\lambda, \delta)), \forall t \in [1 : b_u]$.
 - 5: $\beta_{n,t}^- = \text{PSGD}(\theta_n - \rho u_{n,t}, \beta_0; (\lambda, \delta)), \forall t \in [1 : b_u]$.
 - 6: $\tilde{\psi}(\theta_n + \rho u_{n,t}) = \phi_{\lambda, \delta}(\theta_n + \rho u_{n,t}, \beta_{n,t}^+; \hat{X}_I)$.
 - 7: $\tilde{\psi}(\theta_n - \rho u_{n,t}) = \phi_{\lambda, \delta}(\theta_n - \rho u_{n,t}, \beta_{n,t}^-; \hat{X}_I)$.
 - 8: $\tilde{\mathbf{g}}_\rho(\theta_n) = \frac{m}{2\rho} \cdot \frac{1}{b_u} \sum_{t=1}^{b_u} [\tilde{\psi}(\theta_n + \rho u_{n,t}) - \tilde{\psi}(\theta_n - \rho u_{n,t})] u_{n,t}$
 - 9: $\theta_{n+1} = \text{Proj}_\Theta(\theta_n - \tilde{\eta}_n \tilde{\mathbf{g}}_\rho(\theta_n))$
 - 10: **end for**
-

5.2 Projected Zeroth-order Algorithm with Minima-Selection

In this subsection, we analyze the projected stochastic zeroth-order method with minima-selection (PSZO-MinSel) introduced in Algorithm 2. Our goal is to quantify how many oracle calls are needed for PSZO-MinSel to reach an approximate Goldstein stationary point of F_{\max} . In Algorithm 2, we use the stochastic zeroth-order update

$$\theta_{n+1} \leftarrow \text{Proj}_\Theta(\theta_n - \tilde{\eta}_n \tilde{\mathbf{g}}_\rho(\theta_n)),$$

where $\tilde{\mathbf{g}}_\rho(\theta_n) := b_u^{-1} \sum_{t=1}^{b_u} \tilde{\mathbf{g}}_\rho(\theta_n, u_{n,t})$, and $\tilde{\mathbf{g}}_\rho(\theta_n, u_{n,t}) := \frac{m}{2\rho} [\tilde{\psi}(\theta_n + \rho u_{n,t}) - \tilde{\psi}(\theta_n - \rho u_{n,t})] u_{n,t}$. Here $\tilde{\psi}$ is defined in (24), and $\{u_{n,t}\}_{t=1}^{b_u}$ are i.i.d. draws from the uniform distribution on the unit sphere \mathbb{S}^{m-1} . The complete procedure is summarized in Algorithm 2. Concretely, lines 4–5 invoke PSGD to approximate the minimisers of the perturbed sub-problems $\min_\beta \phi_{\lambda, \delta}(\theta_n + \rho u, \beta)$ and $\min_\beta \phi_{\lambda, \delta}(\theta_n - \rho u, \beta)$ ¹⁸. These two inner solutions are combined in line 8 to form the standard two-point stochastic gradient estimator of $\tilde{F}_{\text{SQ-G}}$, which then drives the projected descent update for θ in line 9.

To state our main result, we first recall the definitions of the Goldstein ρ -subdifferential set and the generalized Goldstein stationary point, as these will be used to formulate the convergence result in Goldstein stationary sense.

Definition 5.3 ([34]). Denote $\mathbb{B}_m(\theta; \rho) = \{v \in \mathbb{R}^m : \|v - \theta\| \leq \rho\}$. Given a Lipschitz function $f : \mathbb{R}^m \rightarrow \mathbb{R}$, a point $\theta \in \mathbb{R}^m$ and $\rho \geq 0$, the Goldstein ρ -subdifferential of f at θ is defined as

$$\partial_\rho f(\theta) := \text{conv} \left(\bigcup_{v \in \mathbb{B}_d(\theta; \rho)} \partial f(v) \right).$$

Definition 5.4 ([64]). We say the point $\theta \in \Theta$ is a (ϵ, ρ, η) -generalized Goldstein stationary point (GGSP) of the problem (1) if it satisfies

$$\min_{g \in \partial_\rho f(x)} \|\mathcal{G}_\Theta(x, g; \eta)\| \leq \epsilon.$$

Here the gradient mapping for a vector $g \in \partial_\rho f(x)$ at a point θ is $\mathcal{G}_\Theta(\theta, g; \nu) := \nu^{-1}(\theta - \text{Proj}_\Theta(\theta - \nu g))$.

¹⁸If $\tilde{\psi}$ is defined only on Θ , then the perturbed evaluations $\tilde{\psi}(\theta_n \pm \rho u_{n,t})$ can be ill-posed when $\theta_n \pm \rho u_{n,t} \notin \Theta$. A standard workaround is to use the interiorized feasible set $\Theta_\rho := \{\theta \in \Theta : \theta + \rho \mathbb{B}_m(0; 1) \subseteq \Theta\}$ and replace θ_n in the oracle queries by $\bar{\theta}_n := \text{Proj}_{\Theta_\rho}(\theta_n)$, so that $\bar{\theta}_n \pm \rho u_{n,t} \in \Theta$.

Our main result in this section is summarized in the following theorem; we show that Algorithm 2 converges to a generalized Goldstein stationary point of F_{\max} . More specifically, using the error bound in (26), we show that the error incurred by approximating F_{\max} with $\tilde{\psi}$ in Algorithm 2 can be efficiently controlled. The proof of Theorem 5.5 is deferred to Section D.3.

Theorem 5.5. *Let $\{\theta_i\}_{i=1}^N$ be the sequence generated by Algorithm 2. Under Assumptions 2.6 to 2.8, we obtain*

$$\min_{i \in [1:N]} \mathbb{E} \left[\min_{g \in \partial_\rho F_{\max}(\theta_i)} \|\mathcal{G}_\Theta(\theta_i, g; \eta)\| \right] = \mathcal{O}(\epsilon), \quad (27)$$

with $N \geq \mathcal{O}(m\epsilon^{-2}\rho^{-2})$, $b_u \geq \mathcal{O}(m^2\epsilon^{-2})$, $|I| \geq \tilde{C}_f m^{2k+2}(\rho\epsilon)^{-2k-2}$, $\eta \leq \mathcal{O}(m^{-1/2}\rho)$, and

$$L \geq \mathcal{O} \left(\frac{k^2 m^{2k+2} B^2}{(\rho\epsilon)^{2k+2}} \cdot \log^2(m(\rho\epsilon)^{-1}) \right).$$

Based on Theorem 5.5, to obtain (27), the total number of samples from $\{\mu_{\theta_i}^\lambda\}_{i=1}^N$ can be computed as follows:

$$N \times (b_u L + b_u |I|) = \mathcal{O} \left(\frac{m^{5+2k} \cdot (k^2 B^2 + \tilde{C}_f) \cdot \log^2(m\epsilon^{-1}\rho^{-1})}{\epsilon^{2k+6} \rho^{2k+4}} \right). \quad (28)$$

5.3 Gradient Oracle Complexity under LMC-based Implementation

In the previous subsections, we analyze the sampling oracle complexity to identify an (ϵ, ρ, η) -GGSP. For a more concrete complexity result, we analyze the lower-level gradient oracle complexity when using Langevin Monte Carlo (LMC) to implement the Gibbs sampling oracle: To sample from the Gibbs measure in Equation (3), a common choice is the Langevin dynamics

$$dX(t) = -\partial_x g(\theta, X(t))dt + \sqrt{2\lambda}dW(t), \quad (29)$$

where $W(t)$ denotes a d -dimensional Brownian motion. Note that the Gibbs measure in Equation (3) is the unique invariant distribution of the above dynamics under mild conditions [17]. In practice, one uses the Euler-Maruyama discretization of the above dynamics, which is also known as the unadjusted LMC method:

$$\hat{X}^{k+1} = \hat{X}^k - h_k \partial_x g(\theta, \hat{X}^k) + \sqrt{2\lambda h_k} \xi_k, \quad (30)$$

where $\{\xi_k\}_{k=0}^\infty$ is a sequence of i.i.d. standard Gaussian random vectors in \mathbb{R}^d and $\{h_k\}_{k=0}^\infty$ is a sequence of step-sizes. We denote by $\hat{\mu}_n$ the law of the n -th iterate, i.e., $\text{Law}(\hat{X}^n) := \hat{\mu}_n$.

Our idea is to replace the ideal Gibbs oracle in Algorithms 1 and 2 by the output of LMC algorithm. While the analyses of this more concrete implementation closely follow the ones in the previous two subsections, we further need to ensure the following two points hold:

- For a sufficiently large n , $\hat{\mu}_n$ is close to μ_θ^λ in Wasserstein-1 distance;
- Conditioned on the first point, replacing Gibbs samples with LMC samples introduces only a controlled bias in the Gibbs–superquantile estimator.

To fulfill the first point, we first use a general inequality relating \mathbb{W}_1 , \mathbb{W}_2 , and the Rényi divergence. By [63, Theorem 1.1],

$$\mathbb{W}_1(\hat{\mu}_n, \mu_\theta^\lambda) \leq \mathbb{W}_2(\hat{\mu}_n, \mu_\theta^\lambda) \leq 2 C_{\text{PI}}^{1/2} (e^{\mathbb{R}_2(\hat{\mu}_n, \mu_\theta^\lambda)} - 1)^{1/2},$$

where \mathbb{R}_2 is the order-2 Rényi divergence and C_{PI} is the Poincaré constant of μ_θ^λ . To bound $\mathbb{R}_2(\hat{\mu}_n, \mu_\theta^\lambda)$ for the LMC iterates, we invoke the following result.

Proposition 5.6. [16, Theorem 6.2.9] *Consider the LMC iteration*

$$X^{k+1} = X^k - h\nabla G(X^k) + \sqrt{2h}\xi_k.$$

Assume that ∇G is $L_{G,2}$ -Lipschitz and $\pi \propto \exp(-G)$ satisfies a C_{PI} -Poincaré inequality. Then for a sufficiently small target accuracy ε and an appropriate choice of h , we obtain $\mathbb{R}_2(\hat{\mu}_n \parallel \pi) \leq \varepsilon^2$, with

$$n = \Theta \left(\frac{C_{PI}^2 L_{G,2}^2 d}{\varepsilon^2} \left(\mathbb{R}_3(\hat{\mu}_0 \parallel \pi)^2 + \log^2 \frac{1}{\varepsilon} \right) \right) \quad \textit{iterations},$$

where \mathbb{R}_3 denotes the order-3 Rényi divergence.

For the update (30), we pick $G(x) := g(\theta, x)/\lambda$ and $h_k = h/\lambda$. Then one has $\mathbb{R}_2(\hat{\mu}_n, \mu_\theta^\lambda) \leq \varepsilon^2$ with $n = \tilde{\mathcal{O}}(dC_{PI}^2\lambda^{-2}\varepsilon^{-2})$. Combining this with the preceding Wasserstein bound shows that $\mathbb{W}_1(\hat{\mu}_n, \mu_\theta^\lambda) \leq 2C_{PI}^{\frac{1}{2}}C^{\frac{1}{2}}\varepsilon$, where $C = 2(e^{1/2} - 1)$. Moreover, as discussed in the end of Section 2.1.1, the inverse Poincaré constant C_{PI} in our context is $\mathcal{O}(1)$, independent of λ [35].

To establish the second point, we show in Section E that the additional bias resulting from replacing the ideal Gibbs oracle in Algorithms 1 and 2 by the output of an n -step LMC run is bounded by $\delta^{-1}\mathbb{W}_1(\hat{\mu}_n, \mu_\theta^\lambda)$. We then choose n large enough so that this LMC-induced error is at most a constant multiple of the accuracy ϵ_v used in Lemma 5.2. With this choice, the total oracle error remains of the same order as in the ideal Gibbs-sampling analysis, so the convergence guarantee of Theorem 5.5 carries over to the LMC-based implementation with only constant-factor changes. This yields a concrete lower-level gradient oracle complexity, summarized in the following theorem.

Theorem 5.7. *Let $\{\theta_i\}_{i=1}^N$ be the sequence generated by Algorithm 4 (refer to Section E.2). Under Assumptions 2.6 to 2.8, we obtain*

$$\min_{i \in [1:N]} \mathbb{E} \left[\min_{g \in \partial_\rho F_{\max}(\theta_i)} \|\mathcal{G}_\Theta(\theta_i, g; \eta)\| \right] = \mathcal{O}(\epsilon), \quad (31)$$

with $N \geq \mathcal{O}(m\epsilon^{-2}\rho^{-2})$, $b_u \geq \mathcal{O}(m^2\epsilon^{-2})$, $|I| \geq \tilde{C}_f m^{2k+2}(\rho\epsilon)^{-2k-2}$, $\eta \leq \mathcal{O}(m^{-1/2}\rho)$,

$$L = \mathcal{O} \left(\frac{k^2 m^{2k+2} B^2}{(\rho\epsilon)^{2k+2}} \log^2(m\epsilon^{-1}\rho^{-1}) \right),$$

and the number of LMC steps $n = \tilde{\mathcal{O}}(dm^{6+6k}(\epsilon\rho)^{-6-6k})$. Moreover, the total number queries to the lower-level gradient oracle and the upper-level function oracle are

$$N \times n \times (b_u L + b_u |I|) = \mathcal{O} \left(\frac{d m^{11+8k} [k^2 B^2 + \tilde{C}_f] \log^2(m\epsilon^{-1}\rho^{-1})}{\epsilon^{8k+12} \rho^{8k+10}} \right),$$

$$N \times b_u \times |I| = \mathcal{O} \left(\frac{m^{2k+5}}{\rho^{2k+4} \epsilon^{2k+6}} \right),$$

respectively.

The LMC layer only changes the cost of each oracle call. The theorem above shows that Algorithm 2 preserves its intrinsic-dimension complexity guarantees when the ideal Gibbs oracle is replaced by an LMC-based implementation, while making explicit the additional polynomial dependence on the ambient dimension d and the factors m^k and $(\rho\epsilon)^{-k}$.

6 Experiments

Before detailing the experiments, we outline our adaptation of Algorithm 2 to the *optimistic* formulation (see footnote 1), the standard in hyperparameter optimization. We will compare this optimistic variant against existing baselines in both synthetic and data hyper-cleaning setups. To approximate $F_{\min}(\theta) := \min_{x \in \mathcal{S}(\theta)} f(\theta, x)$, we use the lower-tail superquantile

$$\tilde{F}_{\text{LSQ}}(\theta) := \max_{\beta} \left\{ \beta - \delta^{-1} \mathbb{E}[\max\{\beta - f(\theta, X), 0\}] \right\}.$$

In our implementation of Algorithm 2, we replace $\phi_{\lambda, \delta}(\theta, \beta)$ with the surrogate

$$\psi_{\lambda, \delta}(\theta, \beta) := \beta - \delta^{-1} \mathbb{E}_{\mu_{\delta}^{\lambda}(\theta)}[\max\{\beta - f(\theta, X), 0\}].$$

Additionally, in Algorithm 1 we change the projected gradient *descent* step in line 2 to a projected gradient *ascent* step.

Compute budget and reporting protocol. Our method is zeroth-order and each outer update invokes a Gibbs–superquantile oracle implemented via PSGD and (parallel-chain) Langevin Monte Carlo, so the wall-clock cost per outer iteration can be higher than that of gradient-based baselines. Accordingly, in the main text we report *iteration-based* results to illustrate algorithmic behavior and minima-selection effects, and in Appendix F we additionally provide *compute-matched* comparisons under a fixed wall-clock time budget (including per-iteration timings for all methods).

Experiments are run on a single machine with CPU: Apple M1 Pro (10 cores), RAM: 16 GB with no discrete GPU. Code to reproduce all experiments is released at GitHub. Toy-example methods are implemented in JAX, while data hyper-cleaning methods are implemented in PyTorch.

6.1 Toy Example

Optimistic formulation: We evaluate our algorithm along with three more algorithms in the literature on the optimistic BLO problem as follows

$$\min_{\theta \in [-\pi, \pi]} \min_{x \in \mathcal{S}(\theta)} f(\theta, x),$$

where $f(\theta, x) = 2\|x\| + \langle x, u(\theta) \rangle$ and

$$g_k(\theta, x) = \frac{1}{4} \left(\sum_{i=1}^{k+1} x_i^2 - \theta^2 \right)^2 - \frac{1}{2} \|x\|^2. \quad (32)$$

and $u(\theta) = [\cos \theta, \sin \theta, 0, \dots, 0]^\top \in \mathbb{R}^d$. The solution set is the k -dimensional sphere of radius $\sqrt{1 + \theta^2}$ embedded in \mathbb{R}^d along the first $k + 1$ coordinates:

$$\mathcal{S}(\theta) = \left\{ x \in \mathbb{R}^d : \sum_{i=1}^{k+1} x_i^2 = 1 + \theta^2, x_{k+2} = \dots = x_d = 0 \right\}.$$

So the induced hyper-objective

$$F_{\min}(\theta) = \sqrt{1 + \theta^2}$$

has the unique global minimizer $\theta^* = 0$.

Throughout the experiments, we compare the following algorithms:

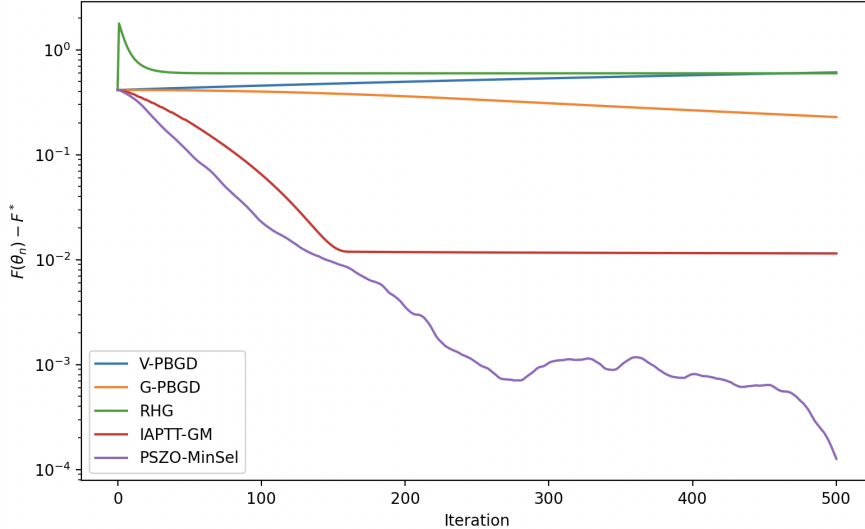


Figure 1: Comparison of $F(\theta_n) - F^*$ versus iteration for $d = 2$. Our algorithm converges faster with the chosen hyperparameters $\delta = 0.1$ and $\lambda = 0.01$ in optimistic formulation, while V-PBGD, G-PBGD, RHG, and IAPTT-GM obtain higher values.

d	V-PBGD	G-PBGD	RHG	IAPTT-GM	PSZO-MinSel
2	0.297	0.160	0.304	0.152	0.009 ± 0.001
5	0.273	0.160	0.302	0.151	0.015 ± 0.012
10	0.169	0.153	0.303	0.152	0.023 ± 0.017
20	0.113	0.174	0.302	0.154	0.043 ± 0.025

Table 1: Best-so-far absolute error $|\hat{\theta}_N - \theta^*|$ after $N = 500$ outer iterations, where $\hat{\theta}_N$ is the selected iterate defined by the best objective value along the trajectory. PSZO-MinSel reports mean \pm 95% CI over 10 runs.

- **PSZO-MinSel (Algorithm 2)** adapted to $\min_{x \in \mathcal{S}(\theta)} f(\theta, x)$ instead of pessimistic formulation.
- **V-PBGD** [77]: joint gradient descent on the penalized objective $\Phi(\theta, x) = f(\theta, x) + \gamma(g(\theta, x) - g^*(\theta))$,
- **G-PBGD** [77]: joint gradient descent on the penalized objective $\Phi(\theta, x) = f(\theta, x) + \frac{\gamma}{2} \|\nabla_x g(\theta, x)\|^2$,
- **RHG** [29]: truncated reverse-mode hypergradient with re-initialization of θ every outer step,
- **IAPTT-GM** [62]: unroll T inner steps $x_{k+1} = x_k - \beta \nabla_x g(\theta, x_k)$ from $x_0 = z$, pick the pessimistic truncation $k_* = \arg \max_k F(\theta, x_k)$, and update θ, z by gradient descent on the truncated objective $F(\theta, x_{k_*})$.

In this part, all methods are implemented in JAX with identical initialization $\theta_0 = 1.0$, $x_0 \sim \mathcal{N}(0, I_d)$, and random seed.

Figure 1 plots $F(\theta_n) - F^*$ over iterations for $d = 2$. The zeroth-order method rapidly converges toward zero, while the other methods tend to plateau or oscillate around suboptimal objective values, primarily due to the absence of a minima-selection phase.

6.1.1 Dimension Sweep and Minima-selection

In this experiment, we examine the setting where the intrinsic dimension scales with the ambient dimension, specifically setting $k = d - 1$. This simplifies the lower-level objective to $g(\theta, x) = \frac{1}{4}(\|x\|^2 - \theta^2)^2 - \frac{1}{2}\|x\|^2$.

d	V-PBGD	G-PBGD	RHG	IAPTT-GM	PSZO-MinSel
5	0.495	0.313	0.302	0.119	0.015 ± 0.014
10	0.499	0.313	0.316	0.114	0.018 ± 0.012
20	0.511	0.315	0.307	0.121	0.018 ± 0.011
30	0.532	0.313	0.311	0.121	0.02 ± 0.02

Table 2: Best-so-far absolute error $|\hat{\theta}_N - \theta^*|$ after $N = 500$ outer iterations, with a fixed intrinsic dimension $k = 1$.

Table 1 reports the best-so-far absolute error $|\hat{\theta}_N - \theta^*|$ after $N = 500$ outer iterations across varying dimensions d , where $\hat{\theta}_N$ denotes the selected iterate with the smallest achieved hyper-objective value along the run. Despite this scaling, our algorithm consistently outperforms the three baseline methods, achieving a significantly closer approximation to the global minimizer $\theta^* = 0$. For robustness, we report the mean and confidence intervals over 10 independent runs for our randomized method, compared to single runs for the deterministic baselines. Baselines are deterministic given initialization; repeated runs match up to numerical tolerance.

6.1.2 Constant Manifold Dimension

We next investigate the distinction between intrinsic and ambient dimensionality by fixing the manifold dimension at $k = 1$ while varying the ambient dimension d , using the corresponding instance of $g_k(\theta, x)$ as the lower-level objective. To align the implementation with our theoretical bounds, we chose the number of Langevin Monte Carlo (LMC) iterations and the batch size M to closely approximate the target Gibbs distribution. As demonstrated in Table 2, the best-so-far error of Algorithm 2 remains nearly constant as d increases, confirming that the complexity is almost independent of the ambient dimension.

This outcome, when combined with the finding that error increases with k , validates our central theoretical prediction that the final optimization error is governed solely by the intrinsic dimensionality of the solution set.

Pessimistic formulation. To show that our method is able to handle both the optimistic and pessimistic settings, we solve the previous synthetic problem also in the latter setup. To our knowledge, existing hypergradient and penalty-based methods do not model the minimizer-selection step. They either (i) assume the lower-level solution set is a singleton or (ii) return points satisfying KKT conditions, without guaranteeing that these correspond to a selected minimizer of the original bilevel objective. Thus, the connection between their outputs and the true BLO solution is unclear. We also observe that their algorithms are *identical* under the optimistic and pessimistic formulations; when the lower-level solution is non-unique, comparing them in both settings is hence not meaningful. Because these methods are designed for the optimistic case, we benchmark against them only in the optimistic setting. For the pessimistic formulation, we report results only for our method.

We now study the following pessimistic toy problem

$$\min_{\theta \in [-\pi, \pi]} \max_{x \in \mathcal{S}(\theta)} f(\theta, x), \quad (33)$$

with f and g_k identical to the previous setup. The induced hyper-objective $F_{\max}(\theta) = 3\sqrt{1 + \theta^2}$ admits the unique global minimizer $\theta^* = 0$.

We also repeat the experiment under a fixed manifold dimension k , using the function instance in (32) as the lower-level objective. In Table 3 we replicate the last set of experiments exclusively for Algorithm 2 in

d	LL: $g_{d-1}(\theta, x)$ (32)	LL: $g_1(\theta, x)$ (32)
5	0.011 ± 0.010	0.021 ± 0.011
10	0.025 ± 0.020	0.023 ± 0.024
20	0.030 ± 0.025	0.026 ± 0.023
30	0.045 ± 0.029	0.027 ± 0.021

Table 3: Best-so-far absolute error $|\hat{\theta}_N - \theta^*|$ after $N = 500$ outer iterations, evaluated using Algorithm 2 in the pessimistic setting. The first column corresponds to (33) with lower-level g_{d-1} from (32); the second uses the same problem with lower-level g_1 from (32).

the pessimistic setting. In both choices of the lower-level function, we observe a clear dependence on the manifold dimension of the solution set.

6.2 Data Hyper-cleaning

In this section, we evaluate our method on the data hyper-cleaning benchmark [29, 76], a canonical BLO task widely used in the machine learning community. Given a set of corrupted¹⁹ training samples $\mathcal{D}_{\text{tr}} = \{(d_i^{\text{tr}}, \ell_i^{\text{tr}})\}_{i=1}^N$, a *small* clean validation set $\mathcal{D}_{\text{val}} = \{(d_i^{\text{val}}, \ell_i^{\text{val}})\}_{i=1}^M$, and a clean test set, the goal is to learn a data cleaner that down-weights mislabeled training points so as to improve generalization on unseen data. Let θ denote the data-cleaner parameters (producing per-example weights) and x the model parameters. We use a sigmoid parameterization for the weights, $\omega_i(\theta) = (1 + \exp(-\theta_i))^{-1}$, ($i = 1, \dots, N$), and constrain $\|\theta\| \leq B$ to avoid exploding weights. The task is cast as the optimistic bilevel problem in the following:

$$\begin{aligned} \min_{\theta, x} \quad & -\frac{1}{M} \sum_{i=1}^M \log P(\ell_i^{\text{val}} | d_i^{\text{val}}; x) \\ \text{s.t.} \quad & \|\theta\| \leq B, \quad x \in \arg \min_{x' \in \mathbb{R}^{d_y}} \left[-\frac{1}{N} \sum_{i=1}^N \omega_i(\theta) \log P(\ell_i^{\text{tr}} | d_i^{\text{tr}}; x') + \frac{\eta}{2} \|x'\|^2 \right]. \end{aligned} \quad (34)$$

Setup. We use MNIST with $N = 5,000$ training, $M = 100$ validation, and 10,000 test examples, and uniformly corrupt a fraction $p \in \{0.4, 0.6, 0.8\}$ of the training labels. In practice, the corrupted/imprecise data are widely available, but clean/precise data are scarce. Thus we intentionally adopt a very small validation set. Much of the literature uses roughly equal training/validation splits, in which case the effect of the corruption rate in the uncleaned training data during training is often not apparent. We compare our zeroth-order method (Algorithm 2) against V-PBGD and G-PBGD [77], RHG [29], and IAPTT-GM [62], using both a linear model and a two-layer MLP which are standard Neural network models in data hyper-cleaning tasks.

Results. Table 4 reports solution quality (test accuracy and F1 score²⁰, averaged over 10 runs with 95% confidence intervals). Our zeroth-order method (see Algorithm 2) adapted to the optimistic formulation attains higher accuracy and F1-score in three different pollute rates ($p = 40\%, 60\%, 80\%$). Our method’s high performance stems from the *minima-selection* step: by choosing the iterate with the lowest validation loss

¹⁹A sample is *clean* if its label equals the true class; otherwise it is *corrupted*. In MNIST, we corrupt by flipping the label of a fraction p of training points uniformly to a different (incorrect) class. p is the pollute-rate.

²⁰F1-score is defined as follows: We take *clean* samples as the positive class and *corrupted* samples as the negative class. Each sample i is assigned a score $s_i = \sigma(\theta_i)$. We predict “clean” for the top $(1 - p)$ -fraction by s_i . We compute Precision = $\frac{\text{TP}}{\text{TP} + \text{FP}}$, Recall = $\frac{\text{TP}}{\text{TP} + \text{FN}}$, where TP, FP, and FN denote true positives, false positives, and false negatives, respectively. The F1 score is the harmonic mean of Precision and Recall, $\text{F1} = \frac{2 \text{Precision} \cdot \text{Recall}}{\text{Precision} + \text{Recall}}$. Note that this F1 measures the *cleaner’s* quality, not the classifier’s accuracy.

along the trajectory, it produces higher-quality cleaner parameters θ , yields better model parameters x , and ultimately improves generalization on the held-out test set. Appendix F additionally reports compute-matched comparisons under a fixed wall-clock time budget.

Table 4: Data hyper-cleaning on MNIST across three noise phases (pollute rate $p \in \{40, 60, 80\}\%$): test accuracy (%) and F1 score (%) over 10 runs ($\pm 95\%$ CI). F1 reflects data-cleaner quality.

p	Method	Linear model		2-layer MLP	
		Test acc.	F1	Test acc.	F1
40	RHG	55.64 \pm 0.45	36.5 \pm 0.4	54.64 \pm 0.29	36.4 \pm 0.2
	IAPTT-GM	60.4 \pm 0.22	54.3 \pm 0.4	59.37 \pm 0.25	52.5 \pm 0.4
	G-PBGD	73.89 \pm 0.13	65.9 \pm 0.3	72.54 \pm 0.32	65.8 \pm 0.3
	V-PBGD	65.34 \pm 0.33	59.2 \pm 0.2	64.77 \pm 0.2	57.2 \pm 0.2
	PSZO-MinSel	82.85 \pm 0.32	72.1 \pm 0.4	85.31 \pm 0.24	73.2 \pm 0.5
60	RHG	51.24 \pm 0.19	29.8 \pm 0.1	52.94 \pm 0.42	28.5 \pm 0.5
	IAPTT-GM	59.52 \pm 0.38	43.2 \pm 0.5	58.72 \pm 0.35	44.2 \pm 0.3
	G-PBGD	64.56 \pm 0.52	50.2 \pm 0.5	62.65 \pm 0.42	51.7 \pm 0.4
	V-PBGD	63.14 \pm 0.43	48.7 \pm 0.5	62.63 \pm 0.53	50.4 \pm 0.4
	PSZO-MinSel	79.50 \pm 0.18	55.2 \pm 0.1	80.70 \pm 0.28	55.9 \pm 0.2
80	RHG	48.14 \pm 0.22	21.5 \pm 0.2	50.32 \pm 0.34	21.9 \pm 0.3
	IAPTT-GM	56.94 \pm 0.44	27.5 \pm 0.3	58.24 \pm 0.36	26.1 \pm 0.3
	G-PBGD	46.84 \pm 0.32	28.9 \pm 0.3	47.70 \pm 0.44	27.3 \pm 0.3
	V-PBGD	61.23 \pm 0.32	33.5 \pm 0.3	60.42 \pm 0.42	34.9 \pm 0.4
	PSZO-MinSel	69.45 \pm 0.45	35.2 \pm 0.4	70.27 \pm 0.48	44.1 \pm 0.3

7 Conclusion and Future Work

This paper studies minima-selection in bilevel optimization and proposes a method that is both theoretically grounded and implementable. Under the PE° condition, exploiting the manifold structure of the lower-level solution set, allows to introduce a dimension-aware viewpoint: the difficulty of BLO with minima-selection is governed by the intrinsic dimension of the minimizer manifold, rather than the ambient dimension of the lower-level variable. The proposed superquantile–Gibbs (SQ–G) relaxation turns minima-selection into a sampling-based procedure with an explicit selection rule. Overall, the results suggest that minima-selection can be handled in a structured way by combining geometric information (the minimizer manifold), stochastic approximation (Gibbs measures), and risk-type criteria (superquantiles).

Looking ahead, several directions appear particularly promising. On the algorithmic side, a natural next step is to move from zeroth-order schemes to *hyper-gradient methods*, in which one first selects a point on the minimizer manifold (using ideas similar to the Gibbs-based selection studied here) to maximize²¹ the upper-level objective, and then differentiates through this choice via implicit differentiation. In parallel, it is important to improve the efficiency of the Gibbs sampling oracle. Our current framework relies on a standard Langevin Monte Carlo implementation; geometry-aware Langevin samplers tailored to the identified manifold structure could sharpen the dependence on both the intrinsic dimension k and the ambient dimension d . Such developments would make the proposed PSZO-MinSel algorithm more practical for large-scale applications.

²¹For the optimistic formulation, one can also minimize the upper-level function over the lower-level solution manifold.

A Definitions and Technical Lemmas

This appendix collects the background components used throughout the paper. We first fix notation and recall a few basic Riemannian notions for the minimizer manifold (distance, second fundamental form, injectivity radius, and curvature) that are repeatedly used in Section 3. We then briefly summarize standard differentiability results for bilevel hyper-objectives. Finally, we verify that our assumptions imply the technical conditions required to apply [38, Theorem 3.6] in the discussion of Gibbs-measure convergence.

Additional Notations. We use the notation $(\cdot)_+$ to denote the positive part of a scalar or vector, defined as $(\cdot)_+ := \max\{\cdot, 0\}$.

A.1 Riemannian Notions

In this subsection we fix notation for basic Riemannian objects and record definitions that will be used repeatedly in later proofs. Any compact manifold \mathcal{S} of class \mathcal{C}^3 (indeed \mathcal{C}^1) without boundary admits a Riemannian metric²². Given a Riemannian metric g on \mathcal{S} , define

$$\text{dist}_g(p, q) := \inf\{\ell(\Gamma) : \Gamma \text{ is a piecewise smooth path in } \mathcal{S} \text{ between } p \text{ and } q.\}. \quad (35)$$

By compactness of \mathcal{S} , there exists at least one minimizing path Γ^* .

Definition A.1 (Second fundamental form). *Let $\mathcal{S} \subset \mathbb{R}^d$ be a \mathcal{C}^2 embedded submanifold endowed with the Riemannian metric induced by the Euclidean inner product. For each $x \in \mathcal{S}$, let $T_x\mathcal{S}$ and $T_x\mathcal{S}^\perp$ denote the tangent space and its orthogonal complement, respectively. The second fundamental form of \mathcal{S} at x is the bilinear map*

$$\mathbb{I}_{\mathcal{S}}(x) : T_x\mathcal{S} \times T_x\mathcal{S} \rightarrow T_x\mathcal{S}^\perp, \quad \mathbb{I}_{\mathcal{S}}(x)[u, v] := (\nabla_u^{\mathbb{R}^d} v)^\perp,$$

where $\nabla^{\mathbb{R}^d}$ is the Euclidean (Levi-Civita) connection, i.e., the usual directional derivative on \mathbb{R}^d : for a smooth vector field v defined near x , $\nabla_u^{\mathbb{R}^d} v = Dv(x)[u]$, and $(\cdot)^\perp$ denotes orthogonal projection onto $T_x\mathcal{S}^\perp$.

We measure its size by the operator norm

$$\|\mathbb{I}_{\mathcal{S}}(x)\|_{\text{op}} := \sup\{\|\mathbb{I}_{\mathcal{S}}(x)[u, u]\| : u \in T_x\mathcal{S}, \|u\| = 1\},$$

where $\|\cdot\|_{\text{op}}$ denotes the operator norm induced by the Euclidean norm $\|\cdot\|$. This quantity coincides with the maximal normal curvature of \mathcal{S} at x . In particular, if γ is a unit-speed geodesic in \mathcal{S} , then

$$\|\ddot{\gamma}(t)\| = \|\mathbb{I}_{\mathcal{S}}(\gamma(t))[\dot{\gamma}(t), \dot{\gamma}(t)]\| \leq \|\mathbb{I}_{\mathcal{S}}(\gamma(t))\|_{\text{op}}.$$

Assumption 2.7 requires that, for each $\theta \in \Theta$, the second fundamental form $\mathbb{I}_{\mathcal{S}(\theta)}$ is uniformly bounded in this sense, with a constant $C > 0$ independent of θ . For further background, see also [35, Appendix D].

Definition A.2 (Injectivity radius). *Injectivity radius at a point $p \in \mathcal{S}$ is defined as*

$$\text{inj}(p) = \sup\{r > 0 \mid \exp_p : \mathbb{B}_{d-k}(p; r) \subset T_p\mathcal{S} \rightarrow \mathbb{B}_g(p; r) \subset \mathcal{S} \text{ is a diffeomorphism}\},$$

where $\mathbb{B}_{d-k}(p; r) \subset T_p\mathcal{S}$ is the open ball of radius r in the tangent space at p , \exp_p is the Riemannian exponential map at p , $\mathbb{B}_g(p; r) \subset \mathcal{S}$ is the geodesic ball of radius r in \mathcal{S} . Equivalently, $\text{inj}(p)$ is the distance from p to the first place where the exponential map fails to be one-to-one. The injectivity radius of the whole manifold is the infimum of the pointwise injectivity radii:

$$\text{inj}(\mathcal{S}) = \inf_{p \in \mathcal{S}} \text{inj}(p).$$

²²A fundamental theorem in differential geometry states that every paracompact manifold M of class \mathcal{C}^k with $k \geq 1$ can be endowed with a Riemannian metric.

In words, $\text{inj}(\mathcal{S})$ is the largest radius r such that every point in \mathcal{S} has a geodesic ball of radius r on which the exponential map at that point is a diffeomorphism.

Definition A.3 (Sectional Curvature). *In a Riemannian manifold $(\mathcal{S}, \mathbf{g})$, the sectional curvature measures how curved the manifold is in each two-dimensional “slice” (or “plane”) of the tangent space at a point. Concretely 1) Pick a point $p \in \mathcal{S}$. 2) Pick a 2-dimensional subspace $A_p \subset T_p\mathcal{S}$. (In other words, A_p is a plane in the tangent space at p .) The sectional curvature $K(p, A_p)$ is defined using the Riemann curvature tensor²³ R . If X and Y are any two linearly independent vectors spanning A_p , then*

$$K(p, A_p) = \frac{\mathbf{g}(R(X, Y)Y, X)}{\mathbf{g}(X, X)\mathbf{g}(Y, Y) - \mathbf{g}(X, Y)^2}.$$

Equivalently, if you choose an orthonormal basis $\{e_1, e_2\}$ of A_p with respect to \mathbf{g} (so $\mathbf{g}(e_i, e_j) = \delta_{ij}$), then the denominator becomes 1, and one obtains the simpler formula

$$K(p, A_p) = \mathbf{g}(R(e_1, e_2)e_2, e_1).$$

A.2 Differentiability of Hyper-objective

The authors of [14, 50] reformulate BLO via the classical value-function approach and assume that a PŁ-type condition (or an error bound) holds for the penalized objective $\sigma f + g$, uniformly over $\sigma \in [0, \sigma_0]$ where $\sigma_0 > 0$ is a constant. More precisely, Kwon et al. [50] impose a proximal error bound for $\sigma f + g$, whereas Chen et al. [14] assume a global PŁ condition for $\sigma f + g$; Chen et al. [14, Proposition C.1] show these two assumptions are equivalent.

Under this global regularity, both works establish a Danskin-type result implying that the hyper-objective F_{\max} is differentiable. However, their conclusion also entails that every choice $x \in \mathcal{S}(\theta)$ yields the same hyper-gradient $\nabla F_{\max}(\theta)$, so minima-selection becomes redundant. Finally, requiring a uniform PŁ condition (or error bound) for $\sigma f + g$ is quite stringent and may fail even when f and g individually satisfy PŁ-type properties.

A.3 Discussion on The Validity of Assumptions in [38, Theorem 3.6]

The assumptions required by [38, Theorem 3.6] follow from our standing conditions. First, their *positive definiteness* requirement for $g(\theta, \cdot)$ holds because the PŁ° condition implies that $g(\theta, \cdot)$ is locally Morse–Bott [73, Section 2.3], and hence the Hessian of g is positive definite in directions normal to the minimizer manifold $\mathcal{S}(\theta)$. Second, their *tail condition* [38, Assumption 3.1] is ensured by our coercivity assumption on g .

Finally, Propositions 2.3 and 2.5 verify the geometric conditions in [38, Assumption 2.2] (smooth, boundaryless, and connected minimizer manifolds). It is worth noting that the orientability of the manifold is not necessary in our setting. We define the volume measure \mathcal{M} in a coordinate-free manner based on the Riemannian metric $g_{\mathcal{S}}$. Orientability, a stronger condition, ensures the existence of a global top-form rather than just a density, which is not required in our framework.

B Proofs of Results in Section 3

This appendix contains deferred proofs for results in Section 3 concerning the structure and regularity of the minimizer sets $\{\mathcal{S}(\theta)\}_{\theta \in \Theta}$.

²³In a Riemannian manifold $(\mathcal{S}, \mathbf{g})$ with Levi-Civita connection ∇ , the Riemann curvature tensor is a $(1, 3)$ -tensor R that measures how much the covariant derivative ∇ fails to commute.

B.1 Proof of Lemma 3.3

Proof. Consider the decreasing sublevel sets $E_\varepsilon := \{x : g(x) - g_\star \leq \varepsilon\}$; if none is contained in $\mathcal{U}(\theta)$, compactness yields a limit point in $\mathcal{S}(\theta) \cap (\mathbb{R}^d \setminus \mathcal{U}(\theta))$, a contradiction.

We provide a detailed proof here. Fix θ and write $g(x) := g(\theta, x)$, $g_\star := \min_z g(z)$, and $\mathcal{S} := \arg \min_z g(z)$. Let $\mathcal{U} = \mathcal{U}(\theta)$ be the neighborhood in (9). Consider the nested sublevel sets

$$E_j := \{x : g(x) \leq g_\star + 1/j\}, \quad j \in \mathbb{N}.$$

By continuity of g , each E_j is closed and $E_{j+1} \subseteq E_j$, and clearly $\bigcap_{j \geq 1} E_j = \mathcal{S}$.

By coercivity of g (from Assumption 2.8), E_1 is compact, hence the family $\{E_j\}$ is a nested sequence of nonempty compact sets. If the claim were false, then for every j we could pick $x_j \in E_j \setminus \mathcal{U}$. By compactness of E_1 , there exists a subsequence $x_{j_k} \rightarrow \bar{x} \in E_1$. Since the sets are nested, $\bar{x} \in E_\ell$ for every fixed ℓ , so $\bar{x} \in \bigcap_\ell E_\ell = \mathcal{S}$. On the other hand, $\mathbb{R}^d \setminus \mathcal{U}$ is closed, hence $\bar{x} \notin \mathcal{U}$, contradicting $\mathcal{S} \subset \mathcal{U}$.

Therefore, there exists j_0 such that $E_{j_0} \subset \mathcal{U}$. Setting $\tilde{\varepsilon} := 1/j_0$ yields $\{x : g(x) - g_\star \leq \tilde{\varepsilon}\} \subset \mathcal{U}$, as claimed. \square

B.2 Proof of Corollary 3.4

The following lemma formalizes a simple but useful observation: if a map is L_G -Lipschitz on every pair of points that are sufficiently close (i.e., within a fixed radius r), then the same Lipschitz constant extends globally. This will be used in the proof of Corollary 3.4.

Lemma B.1. *For a given $r > 0$, if $G : \mathbb{R}^{d_1} \rightarrow \mathbb{R}^{d_2}$ is a functional that satisfies $\|G(x) - G(y)\| \leq L_G \|x - y\|$ for $x, y \in \mathbb{R}^{d_1}$ with $\|x - y\| \leq r$, then G satisfies L_G -Lipschitzness over \mathbb{R}^{d_1} .*

Proof. We aim to show that $\|G(x) - G(y)\| \leq L_G \|x - y\|$ for all $x, y \in \mathbb{R}^{d_1}$. If $\|x - y\| \leq r$, our proof is complete. Assume $\|x - y\| = R$ where $R > r$. Define $z_t = (1 - t) \cdot x + t \cdot y$ for $t \in [0, 1]$. Let $w_k := z_{k/(2R/r)}$ for $k = [1 : 2R/r]$. Notice that $\|w_k - w_{k-1}\| = \|x - y\|/2R/r \leq r/2$. Then

$$\begin{aligned} \|G(x) - G(y)\| &= \left\| \sum_{k=1}^{2R/r} G(w_k) - G(w_{k-1}) \right\| \leq \sum_{k=1}^{2R/r} \|G(w_k) - G(w_{k-1})\| \\ &\leq L_G \sum_{k=1}^{2R/r} \|z_k - z_{k-1}\| = L_G \sum_{k=1}^{2R/r} \frac{k}{2R/r} \cdot \|x - y\| = L_G \|x - y\|. \end{aligned} \quad (36)$$

\square

For completeness, we provide a proof of Corollary 3.4:

Proof. For any $\theta_1, \theta_2 \in \Theta$ satisfying $\|\theta_1 - \theta_2\| \leq \delta$ with $\delta \leq \tilde{\varepsilon}/(2L_{g,1}(D))$ (where $\tilde{\varepsilon}$ is defined in Lemma 3.3), we obtain the bound:

$$\text{dist}(\mathcal{S}(\theta_1), \mathcal{S}(\theta_2)) \leq \frac{L_{g,2}}{\mu} \|\theta_1 - \theta_2\|.$$

Selecting $x_1 \in \arg \max_{x \in \mathcal{S}(\theta_1)} f(\theta_1, x)$ and $x_2 \in \arg \min_{y \in \mathcal{S}(\theta_2)} \text{dist}(y, x_1)$, we derive

$$\begin{aligned} F_{\max}(\theta_1) - F_{\max}(\theta_2) &= f(\theta_1, x_1) - F_{\max}(\theta_2) \leq f(\theta_1, x_1) - f(\theta_2, x_2) \\ &\leq |f(\theta_1, x_1) - f(\theta_2, x_1)| + |f(\theta_2, x_1) - f(\theta_2, x_2)| \\ &\stackrel{(a)}{\leq} L_{f,1} \|\theta_1 - \theta_2\| + L_{f,1} \|x_1 - x_2\| \end{aligned}$$

$$\begin{aligned}
&\stackrel{(b)}{\leq} L_{f,1}\|\theta_1 - \theta_2\| + L_{f,1}\text{dist}(\mathcal{S}(\theta_1), \mathcal{S}(\theta_2)) \\
&\stackrel{(c)}{\leq} L_{f,1}\|\theta_1 - \theta_2\| + L_{f,1} \cdot \frac{L_{g,2}}{\mu} \cdot \|\theta_1 - \theta_2\|.
\end{aligned} \tag{37}$$

Step (a) follows from $L_{f,1}$ -Lipschitzness of f . Step (b) follows from

$$\|x_1 - x_2\| = \text{dist}(x_1, \mathcal{S}(\theta_2)) \leq \max_{x \in \mathcal{S}(\theta_1)} \text{dist}(x, \mathcal{S}(\theta_2)) \leq \text{dist}(\mathcal{S}(\theta_1), \mathcal{S}(\theta_2)).$$

Step (c) follows from Lemma 3.2 under the condition $\delta \leq \tilde{\epsilon}/(2L_{g,1}(D))$.

A similar argument shows that $F_{\max}(\theta_2) - F_{\max}(\theta_1) \leq (L_{f,1} + L_{f,1} \cdot \frac{L_{g,2}}{\mu})\|\theta_1 - \theta_2\|$. Thus, for all $\theta_1, \theta_2 \in \Theta$ with $\|\theta_1 - \theta_2\| \leq \delta$,

$$|F_{\max}(\theta_1) - F_{\max}(\theta_2)| \leq \left(L_{f,1} + L_{f,1} \frac{L_{g,2}}{\mu} \right) \cdot \|\theta_1 - \theta_2\|.$$

In other words, F_{\max} is *locally* Lipschitz on Θ with the same Lipschitz constant and a radius δ that do not depend on the base point θ . As explained in Lemma B.1, such a uniform local Lipschitz property on Θ implies that F_{\max} is globally (uniformly) Lipschitz on Θ with the same constant, which proves the claim. \square

B.3 Proof of Lemma 3.5

This subsection proves that all minimizer manifolds $\mathcal{S}(\theta)$ share a common intrinsic dimension. The key step is to show that the Hessian rank (equivalently, the normal-space dimension) cannot change under small perturbations of θ , and hence is constant on Θ . We provide the proof of Lemma 3.5 in the following.

Proof. Fix $\theta \in \Theta$. By [73, Corollary 2.13] and the path-connectedness of $\mathcal{S}(\theta)$, the rank of $\partial_x^2 g(\theta, x)$ is constant over $\mathcal{S}(\theta)$. Denote it by

$$r(\theta) := \text{rank}(\partial_x^2 g(\theta, x)), \quad x \in \mathcal{S}(\theta),$$

then the dimension of $\mathcal{S}(\theta)$ is $k(\theta) = d - r(\theta)$.

We show that $r(\theta)$ is constant on Θ by contradiction. Suppose not. Then there exist $\theta_n \rightarrow \bar{\theta}$ with $r(\theta_n) \neq r(\bar{\theta})$. Pick $x_n \in \mathcal{S}(\theta_n)$. By the Lipschitz continuity of the solution mapping (Lemma 3.2), there exists $\bar{x} \in \mathcal{S}(\bar{\theta})$ such that $\|x_n - \bar{x}\| \rightarrow 0$. Since $\partial_x^2 g$ is continuous in (θ, x) (Assumption 2.8),

$$\|\partial_x^2 g(\theta_n, x_n) - \partial_x^2 g(\bar{\theta}, \bar{x})\| \rightarrow 0.$$

Moreover, PE° implies a local Morse–Bott structure for $g(\theta, \cdot)$ [73, Corollary 2.13], hence the nonzero eigenvalues of $\partial_x^2 g(\bar{\theta}, x)$ are bounded away from 0 uniformly for x near $\mathcal{S}(\bar{\theta})$. Therefore, for n large enough, the perturbation above cannot change the number of nonzero eigenvalues, and thus

$$\text{rank}(\partial_x^2 g(\theta_n, x_n)) = \text{rank}(\partial_x^2 g(\bar{\theta}, \bar{x})) = r(\bar{\theta}).$$

Since the rank is constant on each $\mathcal{S}(\theta_n)$, the left-hand side equals $r(\theta_n)$, contradicting $r(\theta_n) \neq r(\bar{\theta})$. Hence $r(\theta)$ is constant on Θ , and so is $k(\theta) = d - r(\theta)$. \square

B.4 Proof of Proposition 3.6

Using the Lipschitz continuity of the solution mapping established in Lemma 3.2, we first show that the family of sets $\{\mathcal{S}(\theta)\}_{\theta \in \Theta}$ is uniformly bounded.²⁴ This lemma will be used in the proof of Property 2 in Proposition 3.6 and in the proof of Proposition 3.7.

Lemma B.2. *A collection of sets $\{\mathcal{A}(\theta)\}_{\theta \in \Theta}$ is uniformly bounded if $\mathcal{A}(\theta)$ is a compact and non-empty set for every $\theta \in \Theta$, Θ is a compact set, and $\mathcal{A}(\theta)$ is continuous in Hausdorff distance.*

Proof. We aim to show that $\sup_{\theta \in \Theta} \sup_{x \in \mathcal{A}(\theta)} \|x\|$ is finite. Let define $M(\theta) := \sup_{x \in \mathcal{A}(\theta)} \|x\|$. Since $\mathcal{A}(\theta)$ is compact and non-empty, $M(\theta)$ is finite for each $\theta \in \Theta$. We will show that $M(\theta)$ is continuous and since Θ is compact, $M(\theta)$ attains its maximum value on Θ .

The mapping $\theta \mapsto \mathcal{A}(\theta)$ is continuous in the Hausdorff metric. Hence given $\|\theta_1 - \theta_2\| \leq \delta$, for any $x \in \mathcal{A}(\theta_2)$, there exists $y \in \mathcal{A}(\theta_1)$ such that $\|x - y\| < \epsilon$. Then

$$\|x\| = \|y + (x - y)\| \leq \|y\| + \|x - y\| < \|y\| + \epsilon.$$

Taking the supremum over all $y \in \mathcal{A}(\theta_1)$:

$$\|x\| < M(\theta_1) + \epsilon.$$

Since this holds for all $x \in \mathcal{A}(\theta_2)$, we have:

$$M(\theta_2) = \sup_{x \in \mathcal{A}(\theta_2)} \|x\| \leq M(\theta_1) + \epsilon.$$

By similar argument, $M(\theta_1) \leq M(\theta_2) + \epsilon$. Then

$$|M(\theta_2) - M(\theta_1)| \leq \epsilon.$$

□

We then provide a proof for Proposition 3.6 in the following:

Proof. Property 1. Since we know that $g(\theta, \cdot)$ is coercive, it follows that for each $\theta \in \Theta$, the diameter of $\mathcal{S}(\theta)$ is finite. We aim to prove that $\sup_{\theta \in \Theta} \text{diam}(\mathcal{S}(\theta))$ is also bounded. Given Assumption 2.6, from Lemma 3.2, we deduce that $\mathcal{S}(\theta)$ is continuous with respect to θ in the Hausdorff distance. Using this property, we will further establish that the diameter of $\mathcal{S}(\theta)$ is a continuous function of θ . We aim to show that for every $\epsilon > 0$, there exists $\delta \in \mathbb{R}_+^m$ such that $|\text{diam}(\mathcal{S}(\theta + \delta)) - \text{diam}(\mathcal{S}(\theta))| \leq \epsilon$.

For a given pair $(x, y) \in \mathcal{S}(\theta) \times \mathcal{S}(\theta)$, we define their projections onto $\mathcal{S}(\theta + \delta)$ as (\tilde{x}, \tilde{y}) , where \tilde{x} is a projection of x onto $\mathcal{S}(\theta + \delta)$ and \tilde{y} is a projection of y onto $\mathcal{S}(\theta + \delta)$. The difference in diameters between $\mathcal{S}(\theta)$ and $\mathcal{S}(\theta + \delta)$ can be expressed as:

$$\begin{aligned} \text{diam}(\mathcal{S}(\theta)) - \text{diam}(\mathcal{S}(\theta + \delta)) &= \sup_{x, y \in \mathcal{S}(\theta)} \|x - y\| - \sup_{x', y' \in \mathcal{S}(\theta + \delta)} \|x' - y'\| \\ &\stackrel{(a)}{\leq} \sup_{x, y \in \mathcal{S}(\theta)} \{\|x - y\| - \|\tilde{x} - \tilde{y}\|\} \\ &\stackrel{(b)}{\leq} \sup_{x, y \in \mathcal{S}(\theta)} \{\|x - \tilde{x}\| + \|\tilde{y} - y\|\} \end{aligned}$$

²⁴A collection of sets $\{\mathcal{B}(\theta)\}_{\theta \in \Theta}$ is uniformly bounded if there exists a ball $\mathbb{B}_d(0; R) \subset \mathbb{R}^d$ such that $\mathcal{B}(\theta) \subset \mathbb{B}_d(0; R)$ for all $\theta \in \Theta$.

$$\leq \sup_{x,y \in \mathcal{S}(\theta)} \text{dist}(\mathcal{S}(\theta), \mathcal{S}(\theta + \delta)) \leq \epsilon, \quad (38)$$

where (a) comes from $(\tilde{x}, \tilde{y}) \in \mathcal{S}(\theta + \delta) \times \mathcal{S}(\theta + \delta)$. (b) follows by $\|x - y\| - \|\tilde{x} - \tilde{y}\| \leq \|x - y - \tilde{x} + \tilde{y}\| \leq \|x - \tilde{x}\| + \|\tilde{y} - y\|$. The last inequality holds based on the continuity of the solution sets in Hausdorff distance with respect to θ , i.e., there exist $\delta \in \mathbb{R}_+^m$ such that $\text{dist}(\mathcal{S}(\theta + \delta), \mathcal{S}(\theta)) \leq \epsilon$.

Similarly, for the reverse case, we have

$$\text{diam}(\mathcal{S}(\theta + \delta)) - \text{diam}(\mathcal{S}(\theta)) \leq \epsilon$$

Therefore, for every $\epsilon > 0$ there exists $\delta \in \mathbb{R}_+^m$ such that

$$|\text{diam}(\mathcal{S}(\theta + \delta)) - \text{diam}(\mathcal{S}(\theta))| \leq \epsilon.$$

According to Weierstrass's extreme value theorem, for the continuous function $\text{diam}(\mathcal{S}(\theta))$, there exists a $\theta_0 \in \Theta$ such that $\text{diam}(\mathcal{S}(\theta_0))$ equals the supremum of $\text{diam}(\mathcal{S}(\theta))$ over all $\theta \in \Theta$. We denote $\text{diam}(\mathcal{S}(\theta_0))$ by D .

Property 2. We will show that there exists a constant $C_0 > 0$ such that $|\text{Sec}(\mathcal{S}(\theta))| \leq C_0$ for all $\theta \in \Theta$. In general, for every $\theta \in \Theta$, the sectional curvature of a compact manifold is bounded both above and below as stated in the following result.

Lemma B.3 ([9], Section 9.3). *If \mathcal{M} is a compact Riemannian manifold, then there exist $k, K \in \mathbb{R}$ such that for any plane section A_p at any point $p \in \mathcal{M}$, $k \leq K(A_p) \leq K$.*

For any fixed $\theta \in \Theta$, the manifold $\mathcal{S}(\theta)$ is a compact, boundaryless C^2 submanifold (by Proposition 2.5). As a consequence of general Riemannian geometry (see Lemma B.3), the sectional curvature $\text{Sec}(\mathcal{S}(\theta))$ is bounded on $\mathcal{S}(\theta)$. The sectional curvature $K_{\mathcal{S}(\theta)}(x, A_x)$ is a continuous function of both the position $x \in \mathcal{S}(\theta)$ and the upper-level parameter $\theta \in \Theta$. This continuity holds because the manifold metrics, coordinate functions, and tangent spaces depend continuously and smoothly on θ (stemming from the regularity assumptions on g in Definition 2.2).

Since the parameter domain Θ is compact, the entire collection of manifolds $\{\mathcal{S}(\theta)\}_{\theta \in \Theta}$ is uniformly bounded (Lemma B.2) and varies continuously, implying that the space of all possible geometric configurations (i.e., all points x and all planes A_x) forms a compact set in the corresponding product space $\Theta \times \mathcal{S}(\theta)$. By the Weierstrass Extreme Value Theorem, a continuous function on a compact set attains its maximum. Therefore, the absolute value of the sectional curvature attains a global maximum, C_0 , establishing the uniform bound $|\text{Sec}(\mathcal{S}(\theta))| \leq C_0$ for every $\theta \in \Theta$.

Property 3. Given the boundaryless and compactness properties of \mathcal{S} as well as the C^2 property (see Proposition 2.3), we can apply the following result to establish Property 3.

Proposition B.4 ([71], Lemma 6.4.7). *Let \mathcal{S} be a compact, boundaryless Riemannian manifold of dimension k with a C^2 metric. Then if $\text{Sec}(\mathcal{S}) \leq C_0$ for $C_0 > 0$,*

$$\text{inj}(\mathcal{S}) \geq \min \left\{ \frac{\pi}{C_0}, \frac{1}{2} \ell(\mathcal{S}) \right\},$$

where $\ell(\mathcal{S})$ is the infimum of lengths of closed geodesics in \mathcal{S} .

In order to give a lower bound on $\ell(\mathcal{S})$, we know that for any unit-speed closed geodesic $\gamma \in \mathcal{S}$, the extrinsic curvature of γ is given by $|g(\dot{\gamma}, \dot{\gamma})| \leq C$ where C is the uniform bound on second fundamental form in Assumption 2.7, then

$$\ell(\gamma) \geq \frac{2\pi}{C}.$$

Thus $\ell(\mathcal{S}) \geq \frac{2\pi}{C}$.

From Property 2, we have $|\text{Sec}(\mathcal{S}(\theta))| \leq C_0$ for every $\theta \in \Theta$. Additionally, since C uniformly bounds the second fundamental form of $\{\mathcal{S}(\theta)\}_{\theta \in \Theta}$, the injectivity radius satisfies $\text{inj}(\mathcal{S}(\theta)) \geq \min\left\{\frac{\pi}{C_0}, \frac{\pi}{C}\right\}$. \square

B.5 Proof of Proposition 3.7

To establish the uniform bounds on the limiting density ρ_θ in (7), it is necessary to control the θ -dependent normalizing factor, which involves the Riemannian volume $\mathcal{M}(\mathcal{S}(\theta))$. We therefore first show that the volumes of the minimizer manifolds are uniformly bounded away from 0 and ∞ over $\theta \in \Theta$.

Lemma B.5. *Under Assumption 2.6, there exists a constant $0 < b < 1$ such that*

$$b \leq \mathcal{M}(\mathcal{S}(\theta)) \leq b^{-1}, \quad \forall \theta \in \Theta,$$

where \mathcal{M} denotes the Riemannian volume measure on $(\mathcal{S}(\theta), g)$.

Proof. For each fixed θ , $\mathcal{S}(\theta)$ is a compact k -dimensional Riemannian manifold, hence $0 < \mathcal{M}(\mathcal{S}(\theta)) < \infty$ by the standard coordinate formula for the Riemannian volume element; see [53, Section ‘‘Riemannian volume’’].

It remains to make the bounds uniform over Θ . Define $V(\theta) := \mathcal{M}(\mathcal{S}(\theta))$. By Lemma B.2, the family $\{\mathcal{S}(\theta)\}_{\theta \in \Theta}$ is uniformly bounded, i.e., there exists $D < \infty$ such that $\mathcal{S}(\theta) \subset \mathbb{B}_d(0; D)$ for all $\theta \in \Theta$. Since $\theta \mapsto \mathcal{S}(\theta)$ is continuous in Hausdorff distance and the manifolds are \mathcal{C}^1 (indeed \mathcal{C}^2) with the induced metric varying continuously in (θ, x) on $\Theta \times \mathbb{B}_d(0; D)$, the volume functional $V(\theta)$ depends continuously on θ .

Because Θ is compact and $V(\theta) > 0$ for all θ , the extreme value theorem yields

$$0 < V_{\min} := \min_{\theta \in \Theta} V(\theta) \quad \text{and} \quad V_{\max} := \max_{\theta \in \Theta} V(\theta) < \infty.$$

Setting $b := \min\{V_{\min}, V_{\max}^{-1}\}$ gives $b \leq V(\theta) \leq b^{-1}$ for all $\theta \in \Theta$. \square

Now we provide the proof of Proposition 3.7:

Proof. To establish the boundedness of the density ρ_θ , it suffices to show that $|\partial_r^2 g(\theta, y(u, r))|$ is bounded. Since the $\mathbb{P}\mathbb{L}^\circ$ condition ensures that $g(\theta, \cdot)$ is locally Morse-Bott (see [73, Section 2.3]), we have $\partial_r^2 g(\theta, y(u, r))|_{r=0} \succeq \mu \cdot I_{(d-k) \times (d-k)}$.

Note that $y(u, r)$ is linear in r and we have

$$\partial_r g(\theta, y(u, r)) = \partial_r y(u, r) \partial_x g(\theta, y(u, r)) = \mathbf{N} \partial_x g(\theta, y(u, r)),$$

where $\mathbf{N} := [v_{k+1}(u), \dots, v_d(u)]^T$. Then

$$\partial_r^2 g(\theta, y(u, r)) = \mathbf{N} \partial_x^2 g(\theta, y(u, r)) \mathbf{N}^T.$$

When $r = 0$, $y(u, r) = u$, then for every $u \in \mathcal{S}(\theta)$, $\partial_r^2 g(\theta, y(u, r))|_{r=0} = \mathbf{N} \partial_x^2 g(\theta, u) \mathbf{N}^T$.

From Assumption 2.8, $\partial_x^2 g(\theta, x)$ is continuous with respect to (θ, x) . Since Θ is a compact set, the collection $\{\mathcal{S}(\theta)\}_{\theta \in \Theta}$ is uniformly bounded (see Lemma B.2). By Weierstrass’s extreme value theorem, $\|\partial_x^2 g(\theta, u)\|$ achieves its supremum at some $(\theta_0, u_0) \in \Theta \times \mathcal{S}(\theta_0)$, denoted by $\|\partial_x^2 g(\theta_0, u_0)\| = M_g$. Then $\partial_r^2 g(\theta, y(u, r))|_{r=0} \preceq M_g I_{(d-k) \times (d-k)}$

Now, recall the definition of the density $\rho_\theta(u)$:

$$\rho_\theta(u) = \frac{d\mu_\theta^0}{d\mathcal{M}_\theta} = \frac{|\partial_r^2 g(\theta, y(u, r))|_{r=0}|^{-\frac{1}{2}}}{\int_{\mathcal{S}(\theta)} |\partial_r^2 g(\theta, y(v, r))|_{r=0}|^{-\frac{1}{2}} d\mathcal{M}_\theta(v)}.$$

Using the lower and upper bounds on $\partial_r^2 g(\theta, y(u, r))|_{r=0}$, we obtain:

$$\frac{M_g^{-\frac{d-k}{2}}}{\mu^{-\frac{d-k}{2}} \mathcal{M}_\theta(\mathcal{S}(\theta))} \leq |\rho_\theta(u)| \leq \frac{\mu^{-\frac{d-k}{2}}}{M_g^{-\frac{d-k}{2}} \mathcal{M}_\theta(\mathcal{S}(\theta))}.$$

From Lemma B.5, we have $b \leq \mathcal{M}_\theta(\mathcal{S}(\theta)) \leq b^{-1}$. Finally, we define $\kappa := b \cdot \left(\frac{\mu}{M_g}\right)^{\frac{d-k}{2}}$. \square

C Proofs of Results in Section 4

This appendix provides proofs for the geometric and measure-approximation results in Section 3. We first establish a uniform comparison between the volume of small geodesic balls on $\mathcal{S}(\theta)$ and Euclidean balls, and then use Wasserstein stability to control the superquantile functional under perturbations of the underlying measure.

C.1 Proof of Lemma 4.1

We begin by showing that, for a k -dimensional (\mathcal{C}^2) embedded Riemannian manifold, the Riemannian volume of a sufficiently small geodesic ball is comparable to the k -dimensional Lebesgue measure of an Euclidean ball of the same radius. We already used this result to prove Theorem 4.2.

Proof. Let (\mathcal{S}, g) be a k -dimensional compact Riemannian manifold. By compactness, \mathcal{S} is geodesically complete. Assume:

1. $\text{inj}(\mathcal{S}) \geq r_0 > 0$ (uniform lower bound on the injectivity radius),
2. $|\text{Sec}(x)| \leq C_0$ for all $x \in \mathcal{S}$ (uniform bound on sectional curvature).

Step 1: Expressing the volume of a geodesic ball in normal coordinates. For a Riemannian manifold (\mathcal{S}, g) , the volume measure \mathcal{M} is locally given by the *Riemannian volume form*. In a coordinate chart $\{x^i\}$, one has

$$d\mathcal{M}(x) = \sqrt{\det(g_{ij}(x))} dx^1 \cdots dx^k,$$

so that, for any measurable U ,

$$\int_U f(x) d\mathcal{M}(x) = \int_U f(x) \sqrt{\det(g_{ij}(x))} dx^1 \cdots dx^k,$$

where $g_{ij}(x)$ is the coordinate matrix of the metric g .

Fix a point $p \in \mathcal{S}$ and $0 < r < r_0$. By [71, Theorem 5.4.2], the exponential map

$$\exp_p : \mathbb{B}_k(0; r) \subset T_p \mathcal{S} \rightarrow \mathbb{B}_g(p; r) \subset \mathcal{S}$$

is a diffeomorphism, where we identify $T_p \mathcal{S} \cong \mathbb{R}^k$ via an orthonormal basis and $\mathbb{B}_k(0; r)$ is the Euclidean ball of radius r .

Using \exp_p as a change of variables, we write the volume of the geodesic ball as

$$\mathcal{M}(\mathbb{B}_g(p; r)) = \int_{\mathbb{B}_g(p; r)} d\mathcal{M}(x) = \int_{\mathbb{B}_k(0; r)} (\exp_p^* d\mathcal{M})(v), \quad (39)$$

where $v = (v^1, \dots, v^k)$ are coordinates on $T_p \mathcal{S} \cong \mathbb{R}^k$ and dv is the standard Lebesgue measure on \mathbb{R}^k .

In *normal coordinates* at p , the exponential map \exp_p is precisely the coordinate map, so $\exp_p^* d\mathcal{M}$ has the expression

$$(\exp_p^* d\mathcal{M})(v) = \sqrt{\det(\mathbf{g}_{ij}(v))} dv^1 \cdots dv^k,$$

where $\mathbf{g}_{ij}(v)$ is the metric tensor in these normal coordinates. Thus (39) becomes

$$\mathcal{M}(\mathbb{B}_{\mathbf{g}}(p; r)) = \int_{\mathbb{B}_k(0; r)} \sqrt{\det(\mathbf{g}_{ij}(v))} dv. \quad (40)$$

Step 2: Quadratic control of the metric in normal coordinates, uniformly in p . In a normal coordinate neighborhood of p , the metric admits the expansion (see, e.g., [71, Section 5.4])

$$\mathbf{g}_{ij}(v) = \delta_{ij} - \frac{1}{3} R_{ikjl}(p) v^k v^l + \mathcal{O}(\|v\|^3), \quad (41)$$

where $R_{ikjl}(p)$ are the components of the Riemann curvature tensor at p , and δ_{ij} is the Kronecker delta.

The sectional curvature bound $|\text{Sec}| \leq C_0$ implies that the curvature tensor is uniformly bounded on \mathcal{S} : there exists a constant $\tilde{C} > 0$, depending only on C_0 and k , such that

$$|R_{ikjl}(x)| \leq \tilde{C} \quad \text{for all } x \in \mathcal{S} \text{ and all indices } i, k, j, l.$$

(For example, this follows from norm equivalence on the finite-dimensional space of algebraic curvature tensors.) After possibly increasing the constant, we may (and do) assume $\tilde{C} = C_0$ for notational simplicity, so that $|R_{ikjl}(x)| \leq C_0$ for all $x \in \mathcal{S}$.

Since \mathcal{S} is compact, higher-order derivatives of the metric are also bounded, and the $\mathcal{O}(\|v\|^3)$ term in (41) can be dominated uniformly in p . Hence there exist constants $r_1 \in (0, r_0]$ and $C > 0$, depending only on (k, C_0, r_0) , such that for all $p \in \mathcal{S}$ and all $\|v\| \leq r_1$,

$$|\mathbf{g}_{ij}(v) - \delta_{ij}| \leq C C_0 \|v\|^2 \quad \text{for all } i, j. \quad (42)$$

Let $\|\cdot\|_{\text{op}}$ denote the operator norm on matrices with respect to the Euclidean norm. Using the elementary bound $\|\mathbf{g}(v) - I\|_{\text{op}} \leq k \max_{i,j} |\mathbf{g}_{ij}(v) - \delta_{ij}|$, we obtain from (42) that

$$\|\mathbf{g}(v) - I\|_{\text{op}} \leq C' C_0 \|v\|^2, \quad \|v\| \leq r_1, \quad (43)$$

for some constant $C' > 0$ depending only on (k, C_0, r_0) .

Step 3: Explicit small-radius condition in terms of r_0 and C_0 . Define

$$r_* := \min\left\{r_1, \frac{1}{2\sqrt{C' C_0}}\right\}.$$

Then for every v with $\|v\| \leq r_*$, (43) yields $\|\mathbf{g}(v) - I\|_{\text{op}} \leq C' C_0 r_*^2 \leq 1/4$. Thus all eigenvalues of the symmetric matrix $\mathbf{g}(v)$ lie in the interval $[3/4, 5/4]$. In particular,

$$\frac{3}{4} I \preceq \mathbf{g}(v) \preceq \frac{5}{4} I \implies \left(\frac{3}{4}\right)^{k/2} \leq \sqrt{\det(\mathbf{g}_{ij}(v))} \leq \left(\frac{5}{4}\right)^{k/2}, \quad \text{for all } \|v\| \leq r_*. \quad (44)$$

Observe that r_* depends only on (k, C_0, r_0) . In particular, there exists a numerical constant $c_k > 0$, such that

$$r_* \geq \min\left\{r_0, \frac{c_k}{\sqrt{C_0}}\right\}.$$

Thus, up to adjusting the constant, we may think of the admissible radius as

$$0 < r \leq \min\left\{r_0, \frac{c_k}{\sqrt{C_0}}\right\},$$

which makes the dependence on the injectivity radius and sectional curvature bound explicit.

Step 4: Volume comparison. Combining (40) and (44), for any $0 < r \leq r_*$ we get

$$\begin{aligned} \left(\frac{3}{4}\right)^{k/2} \text{Leb}_k(\mathbb{B}_k(p; r)) &\leq \mathcal{M}(\mathbb{B}_g(p; r)) \\ &= \int_{\mathbb{B}_k(0; r)} \sqrt{\det(\mathbf{g}_{ij}(v))} \, dv \leq \left(\frac{5}{4}\right)^{k/2} \text{Leb}_k(\mathbb{B}_k(p; r)). \end{aligned}$$

where Leb_k denotes Lebesgue measure on \mathbb{R}^k . This is the desired comparison, with constants $c_L := (3/4)^{k/2}$ and $c_H := (5/4)^{k/2}$ valid for all radii

$$0 < r \leq r_* \quad \text{and hence for all } 0 < r \leq \min\left\{r_0, \frac{c_k}{\sqrt{C_0}}\right\}.$$

□

C.2 Proof of Lemma 4.4

We next provide the proof of Lemma 4.4 which is essential for our approximation result in Theorem 4.5.

Proof. Recall

$$\phi_{\lambda, \delta}(\theta, \beta) = \beta + \frac{1}{\delta} \mathbb{E}_{X \sim \mu_\theta^\lambda}[(f(\theta, X) - \beta)_+].$$

By Assumption 2.8, $f(\theta, \cdot)$ is $L_{f,1}$ -Lipschitz. Since $t \mapsto (t - \beta)_+$ is 1-Lipschitz, the map

$$G_\beta(x) := (f(\theta, x) - \beta)_+$$

is $L_{f,1}$ -Lipschitz in x . Hence, by the Kantorovich–Rubinstein duality for \mathbb{W}_1 ,

$$|\phi_{\lambda, \delta}(\theta, \beta) - \phi_{0, \delta}(\theta, \beta)| = \frac{1}{\delta} \left| \mathbb{E}_{\mu_\theta^\lambda}[G_\beta(X)] - \mathbb{E}_{\mu_\theta^0}[G_\beta(X)] \right| \leq \frac{L_{f,1}}{\delta} \mathbb{W}_1(\mu_\theta^\lambda, \mu_\theta^0). \quad (45)$$

Finally, to prove the statement of Lemma 4.4, we have

$$\begin{aligned} \min_{\beta'} \phi_{0, \delta}(\theta, \beta') &\leq \phi_{0, \delta}(\theta, \beta) \\ &\leq \phi_{\lambda, \delta}(\theta, \beta) + |\phi_{0, \delta}(\theta, \beta) - \phi_{\lambda, \delta}(\theta, \beta)| \\ &\stackrel{(a)}{\leq} \phi_{\lambda, \delta}(\theta, \beta) + \frac{L_{f,1}}{\delta} \cdot \mathbb{W}_1(\mu_g^\lambda(\theta), \mu_g^0(\theta)), \end{aligned} \quad (46)$$

where (a) follows from (45). Then, taking the minimum over β at the r.h.s. of (46), we get $\min_{\beta'} \phi_{0, \delta}(\theta, \beta') - \min_{\beta} \phi_{\lambda, \delta}(\theta, \beta) \leq \frac{L_{f,1}}{\delta} (\mu_g^\lambda(\theta), \mu_g^0(\theta))$. Interchanging $\min_{\beta} \phi_{\lambda, \delta}(\theta, \beta)$ and $\min_{\beta'} \phi_{0, \delta}(\theta, \beta')$, one obtains

$$\left| \min_{\beta} \phi_{\lambda, \delta}(\theta, \beta) - \min_{\beta'} \phi_{0, \delta}(\theta, \beta') \right| \leq L_{f,1} \delta^{-1} \mathbb{W}_1(\mu_g^\lambda(\theta), \mu_g^0(\theta)). \quad (47)$$

□

D Proofs of Results in Section 5

This appendix collects technical results for the oracle analysis in Section 5. We begin by deriving moment and tail bounds for the Gibbs measure; these bounds are then used to prove Lemma 5.1. Next, we establish accuracy guarantees for the PSGD-based inner estimator. Finally, we present the complete proof of Theorem 5.5, separating the standard zeroth-order argument from our new control of the minima-selection error.

D.1 Proof of Lemma 5.1

We start by presenting the following technical lemma, which is an essential prerequisite for the proof of Lemma 5.1. It establishes a technical result ensuring the finiteness of the moments of the Gibbs measure μ_θ^λ .

Lemma D.1. *Under Assumption 2.6, for*

$$\lambda \leq \min \left\{ \frac{(2\pi)^{d/2} M_g^{-\frac{d}{2}}}{2c}, \frac{2D^2}{n+d} \right\},$$

we have for every $n \in \mathbb{N} \cup \{0\}$

$$\mathbb{E}_{X \sim \mu_\theta^\lambda} [\|X\|^n \cdot \mathbf{1}[X \notin \mathbb{B}_d(0; 2D)]] \leq W_n \cdot \lambda^{-\frac{d}{2}+1} e^{-\frac{D^2}{\lambda}}.$$

Here,

$$W_n := M_g^{\frac{d}{2}} \cdot 2^{-d/2+2} \pi^{d/2+n-1} \cdot 2\mu_{\text{qg}}^{-1} \cdot \max\{(d+n)/2, 1\} \cdot D^{d+n-1}$$

with M_g is defined in Proposition 3.7 and $c > 0$ is a constant.

Proof. Assume without loss of generality that g does not depend on θ , $\min_x g(x) = 0$, and $0 \in \mathcal{S} = \arg \min_x g(x)$. We first note that by switching to spherical coordinates, one obtains for any $n \geq 0$ the bound

$$\begin{aligned} & \int_{x: \|x\| > R} \|x\|^n e^{-c\|x\|^2} dx = \\ & \int_0^\pi \cdots \int_0^\pi \int_0^{2\pi} \int_{r>R} e^{-cr^2} r^{d+n-1} \sin^{d-2}(\phi_1) \sin^{d-3}(\phi_2) \cdots \sin(\phi_{d-2}) dr d\phi_1 \cdots d\phi_{d-1} \\ & \leq \int_0^\pi \cdots \int_0^\pi \int_0^{2\pi} \int_{r>R} e^{-cr^2} r^{d+n-1} dr d\phi_1 \cdots d\phi_{d-1} \\ & \leq 2\pi^{d-1} \int_R^{+\infty} e^{-cr^2} r^{d+n-1} dr \leq 2\pi^{d+n-1} c^{-\frac{d+n}{2}} \cdot \Gamma\left(\frac{d+n}{2}, cR^2\right), \end{aligned} \quad (48)$$

where in the last inequality we use the definition of the upper incomplete Gamma function, i.e., $\Gamma(s, x) := \int_x^{+\infty} t^{s-1} e^{-t} dt$. By Gautschi's inequality²⁵, for $cR^2 > (d+n)/2$ and $d+n \geq 2$,

$$\begin{aligned} & \int_{x: \|x\| > R} \|x\|^n e^{-c\|x\|^2} dx \leq 2\pi^{d+n-1} \cdot c^{-\frac{d+n}{2}} \max\{(d+n)/2, 1\} (cR^2)^{\frac{d+n}{2}-1} e^{-cR^2} \\ & \leq 2\pi^{d+n-1} \cdot c^{-1} \max\{(d+n)/2, 1\} R^{d+n-2} e^{-cR^2}. \end{aligned} \quad (49)$$

Since

$$\mathbb{E}_{X \sim \mu_\theta^\lambda} [\|X\|^n \cdot \mathbf{1}[X \notin \mathbb{B}_d(0; 2D)]] = \frac{1}{Z_\lambda} \int_{\|x\| \geq 2D} \|x\|^n e^{-g(x)/\lambda} dx,$$

²⁵By Gautschi-type's inequality, $\Gamma(x, s) \leq sx^{s-1} e^{-x}$ for $x > s$ and $s \geq 1$. Note that for $s = 1$, $\Gamma(s, x) = e^{-x}$.

and noting that, if $\mathcal{S} \subseteq \mathbb{B}_d(0; D)$, then for $x \notin \mathbb{B}_d(0; 2D)$ we have

$$\|x\| - D \leq \text{dist}(x, \mathcal{S}),$$

the quadratic growth of g outside $\mathbb{B}_d(0; 2D)$ implies

$$\frac{\mu_{\text{qg}}}{2} (\|x\| - D)^2 \leq g(x), \quad \forall \|x\| \geq 2D. \quad (50)$$

Hence,

$$\mathbb{E}_{X \sim \mu_\theta^\lambda} [\|X\|^n \cdot \mathbf{1}[X \notin \mathbb{B}_d(0; 2D)]] \leq \frac{1}{Z_\lambda} \int_{\|x\| \geq 2D} \|x\|^n e^{-\frac{\mu_{\text{qg}}(\|x\| - D)^2}{2\lambda}} dx.$$

Applying (49) gives for $\lambda < 2D^2/(n + d)$,

$$\begin{aligned} \mathbb{E}_{X \sim \mu_\theta^\lambda} [\|X\|^n \cdot \mathbf{1}[X \notin \mathbb{B}_d(0; 2D)]] &\leq \\ &\frac{1}{Z_\lambda} \cdot 2\pi^{d+n-1} \cdot \left(\frac{2\lambda}{\mu_{\text{qg}}}\right) \cdot \max\{(d+n)/2, 1\} \cdot D^{d+n-2} e^{-\frac{D^2}{\lambda}}. \end{aligned} \quad (51)$$

For a lower bound on Z_λ , we use the estimate (see [38, Remark A.21]): for a compact set $U \subset \mathbb{R}^d$ and $x_0 \in \mathcal{S}$,

$$\int_U e^{-g(x)/\lambda} dx \geq \lambda^{\frac{d}{2}} \left[(2\pi)^{d/2} \det \left(\frac{\partial^2 g(x_0)}{\partial x^2} \right)^{-\frac{1}{2}} - c\lambda \right].$$

Since $\det \left(\frac{\partial^2 g(x_0)}{\partial x^2} \right) \leq M_g^d$ (by Proposition 3.7), it follows that

$$Z_\lambda \geq \lambda^{\frac{d}{2}} \left[(2\pi)^{d/2} M_g^{-\frac{d}{2}} - c\lambda \right].$$

Thus, if

$$\lambda \leq \min \left\{ \frac{(2\pi)^{d/2} M_g^{-\frac{d}{2}}}{2c}, \frac{2D^2}{n+d} \right\},$$

we have

$$Z_\lambda \geq \lambda^{\frac{d}{2}} \cdot (2\pi)^{d/2} M_g^{-\frac{d}{2}} / 2.$$

Substituting this into (51) completes the proof. \square

We then prove Lemma 5.1 which states that every global minimizer of $\phi_{\lambda, \delta}(\theta, \cdot)$ lies in a bounded interval.

Proof. Upper bound on $\beta^(\theta)$:* Pick a $\beta^*(\theta) \in \arg \min_\beta \phi_{\lambda, \delta}(\theta, \beta)$. It follows that

$$\begin{aligned} \beta^*(\theta) &\leq \beta^*(\theta) + \delta^{-1} \mathbb{E}[\max\{0, f(\theta, X) - \beta^*(\theta)\}] \\ &= \min_\beta \phi_{\lambda, \delta}(\theta, \beta) \end{aligned} \quad (52)$$

In the following, we give an upper bound on $\min_\beta \phi_{\lambda, \delta}(\theta, \beta)$. First, note that similar to the proof of Lemma 4.4, we have

$$\left| \min_\beta \phi_{0, \delta}(\theta, \beta) - \min_\beta \phi_{\lambda, \delta}(\theta, \beta) \right| \leq \frac{L_{f,1}}{\delta} \cdot \mathbb{W}_1(\mu_\theta^\lambda, \mu_\theta^0).$$

Using this bound along with the result of Proposition 2.11, we obtain

$$\begin{aligned}\beta^*(\theta) &\leq \min_{\beta} \phi_{\lambda,\delta}(\theta, \beta) \leq \min_{\beta} \phi_{0,\delta}(\theta, \beta) + |\min_{\beta} \phi_{0,\delta}(\theta, \beta) - \min_{\beta} \phi_{\lambda,\delta}(\theta, \beta)| \\ &\leq \min_{\beta} \phi_{0,\delta}(\theta, \beta) + \frac{L_{f,1}}{\delta} \cdot K_0 \lambda^{\frac{1}{2}}.\end{aligned}\tag{53}$$

Then we have for $Y \sim \mu_{\theta}^0$,

$$\min_{\beta} \phi_{0,\delta}(\theta, \beta) = \text{SQ}_{1-\delta}(f(\theta, Y)) \leq \max_{x \in \mathcal{S}(\theta)} f(\theta, x),$$

where the last inequality comes from the definition of superquantile and the fact that $\text{supp}(\mu_{\theta}^0) = \mathcal{S}(\theta)$. By Equation (5), $\max_{x \in \mathcal{S}(\theta)} f(\theta, x) \leq L_{f,0}(D)$. Hence, we have $\min_{\beta} \phi_{0,\delta}(\theta, \beta) \leq L_{f,0}(D)$ and then from (53), we obtain

$$\beta^*(\theta) \leq L_{f,0}(D) + \frac{L_{f,1}}{\delta} \cdot K_0 \lambda^{1/2}\tag{54}$$

Lower bound on $\beta^*(\theta)$: By the definition of the $(1 - \delta)$ -quantile of the random variable $f(\theta, X)$ under $X \sim \mu_{\theta}^{\lambda}$, it holds that

$$\mathbb{P}_{X \sim \mu_{\theta}^{\lambda}}[f(\theta, X) < \beta^*(\theta)] > 1 - \delta.$$

Because $\delta \leq 1/2$, we in particular have

$$\mathbb{P}_{X \sim \mu_{\theta}^{\lambda}}[f(\theta, X) < \beta^*(\theta)] > \frac{1}{2}.$$

W.L.O.G., we assume that $\mathcal{S}(\theta) \subseteq \mathbb{B}_d(0; D)$ with sufficiently large D . Then

$$\begin{aligned}\frac{1}{2} &< \mathbb{P}_{X \sim \mu_{\theta}^{\lambda}}[f(\theta, X) < \beta^*(\theta)] \leq \\ &\mathbb{P}[f(\theta, X) < \beta^*(\theta), X \in \mathbb{B}_d(0; 2D)] + \mathbb{P}[f(\theta, X) < \beta^*(\theta), X \notin \mathbb{B}_d(0; 2D)] \\ &\leq \mathbb{P}[f(\theta, X) < \beta^*(\theta), X \in \mathbb{B}_d(0; 2D)] + \mathbb{P}[X \notin \mathbb{B}_d(0; 2D)],\end{aligned}$$

Next, we use the result in Lemma D.1 for $n = 0$, to give the following bound:

$$\mathbb{P}_{X \sim \mu_{\theta}^{\lambda}}[X \notin \mathbb{B}_d(0; 2D)] \leq W_0 \cdot \lambda^{-\frac{d}{2}+1} e^{-\frac{D^2}{\lambda}}.$$

Then

$$\begin{aligned}\mathbb{P}[f(\theta, X) < \beta^*(\theta), X \in \mathbb{B}_d(0; 2D)] &\geq \\ &\frac{1}{2} - W_0 \cdot \lambda^{-\frac{d}{2}+1} e^{-\frac{D^2}{\lambda}}.\end{aligned}\tag{55}$$

For the case $d \leq 2$, when $\lambda \leq \frac{D^2}{\log(4W_0)}$, we have $\mathbb{P}[f(\theta, X) < \beta^*(\theta), X \in \mathbb{B}_d(0; 2D)] \geq \frac{1}{4}$. For the case $d > 2$, when

$$\lambda \leq \frac{2D^2}{(d-2) \cdot W_{\text{Lam}} \left(\frac{2}{d-2} \left(\frac{4W_0}{D} \right)^{\frac{2}{d-2}} \right)},$$

where W_{Lam} is the Lambert function, we have

$$\mathbb{P}[f(\theta, X) < \beta^*(\theta), X \in \mathbb{B}_d(0; 2D)] \geq \frac{1}{4}.$$

Thus, there exists some $x_0 \in \mathbb{B}_d(0; 2D)$ such that $f(\theta, x_0) \leq \beta^*(\theta)$. We conclude from Equation (5), $-L_{f,0}(2D) \leq \min_{x \in \mathbb{B}_d(0; D)} f(\theta, x) \leq \beta^*(\theta)$. This completes the proof. \square

D.2 Proof of Lemma 5.2

This subsection proves the mean-square accuracy bound for the PSGD estimator of $\tilde{F}_{\text{SQ-G}}(\theta)$. This estimate is the key input in the zeroth-order convergence proof.

For completeness, we state the following bounds, which are used in the convergence analysis of PSGD (see Algorithm 1). The function $\phi_{\lambda,\delta}(\theta, \beta)$ is $(1 + \delta^{-1})$ -Lipschitz on β since, given $\theta \in \Theta$, for every $\beta_1, \beta_2 \in \mathbb{R}$,

$$\begin{aligned} |\phi_{\lambda,\delta}(\theta, \beta_1) - \phi_{\lambda,\delta}(\theta, \beta_2)| &\leq |\beta_1 - \beta_2| + \frac{1}{\delta} \cdot \mathbb{E}[|h(f(\theta, X) - \beta_1) - h(f(\theta, X) - \beta_2)|] \\ &\leq \left[1 + \frac{1}{\delta}\right] \cdot |\beta_1 - \beta_2|. \end{aligned} \quad (56)$$

Here the last inequality comes from $h(t) := \max\{t, 0\}$ is 1-Lipschitz. Moreover,

$$|\tilde{\partial}_\beta \phi_{\lambda,\delta}(\theta, \beta; X)| = \left|1 + \frac{1}{\delta} \hat{\partial}_\beta [\max\{f(\theta, X) - \beta, 0\}]\right|^2 \leq |1 + \delta^{-1}| := \sigma.$$

Here $\hat{\partial}_\beta [\max\{f(\theta, X) - \beta, 0\}]$ is the sub-gradient of $\max\{f(\theta, X) - \beta, 0\}$ and is bounded uniformly by 1. We then provide the proof of Lemma 5.2 in the following:

Proof. To give an upper bound on $\mathbb{E}[|\tilde{\psi}(\theta) - \tilde{F}_{\text{SQ-G}}(\theta)|^2 | \theta]$, by the triangle inequality, we have

$$\begin{aligned} \mathbb{E}[|\phi_{\lambda,\delta}(\theta, \hat{\beta}; \tilde{X}_I) - \tilde{F}_{\text{SQ-G}}(\theta)|^2 | \theta] &\leq \\ &2\mathbb{E}[|\phi_{\lambda,\delta}(\theta, \hat{\beta}; \tilde{X}_I) - \phi_{\lambda,\delta}(\theta, \hat{\beta})|^2 | \theta] + 2\mathbb{E}[|\phi_{\lambda,\delta}(\theta, \hat{\beta}) - \tilde{F}_{\text{SQ-G}}(\theta)|^2 | \theta] \\ &= 2\underbrace{\mathbb{E}[|\phi_{\lambda,\delta}(\theta, \hat{\beta}; \tilde{X}_I) - \phi_{\lambda,\delta}(\theta, \hat{\beta})|^2 | \theta]}_{(i)} + 2\underbrace{\mathbb{E}[|\phi_{\lambda,\delta}(\theta, \hat{\beta}) - \min_{\beta} \phi_{\lambda,\delta}(\theta, \beta)|^2 | \theta]}_{(ii)}, \end{aligned} \quad (57)$$

where the last equation follows from $\tilde{F}_{\text{SQ-G}}(\theta) = \min_{\beta} \phi_{\lambda,\delta}(\theta, \beta)$. We will give the upper bounds on the terms (i) and (ii) in the following.

Upper bound on (i) in (57): We use the following chain of inequalities:

$$\begin{aligned} \mathbb{E}[|\phi_{\lambda,\delta}(\theta, \hat{\beta}; \tilde{X}_I) - \phi_{\lambda,\delta}(\theta, \hat{\beta})|^2 | \theta] &= \mathbb{E} \left[\mathbb{E} \left[|\phi_{\lambda,\delta}(\theta, \hat{\beta}; \tilde{X}_I) - \phi_{\lambda,\delta}(\theta, \hat{\beta})|^2 | \theta, \hat{\beta} \right] \right] \\ &= \frac{1}{\delta^2} \cdot \mathbb{E} \left[\mathbb{E} \left[\left(\frac{1}{|I|} \sum_{i \in I} h(f(\theta, \tilde{X}^{(i)}) - \hat{\beta}) - \mathbb{E}[h(f(\theta, X) - \hat{\beta}) | \theta, \hat{\beta}] \right)^2 | \theta, \hat{\beta} \right] \right] \\ &= \frac{1}{\delta^2} \cdot \mathbb{E} \left[\left(\frac{1}{|I|^2} \sum_{i \in I} \mathbb{E} \left[\left(h(f(\theta, \tilde{X}^{(i)}) - \hat{\beta}) - \mathbb{E}[h(f(\theta, X) - \hat{\beta}) | \theta, \hat{\beta}] \right)^2 | \theta, \hat{\beta} \right] \right) \right], \end{aligned} \quad (58)$$

where the last inequality comes from the fact that $\{h(f(\theta, \tilde{X}^{(i)}) - \hat{\beta})\}_{i \in I}$ are independent random variables given θ and $\hat{\beta}$.

Now we give a constant upper bound on (58) in the following:

$$\begin{aligned} &\mathbb{E} \left[\left(h(f(\theta, \tilde{X}^{(i)}) - \hat{\beta}) - \mathbb{E}[h(f(\theta, X) - \hat{\beta}) | \theta, \hat{\beta}] \right)^2 | \theta, \hat{\beta} \right] \\ &\leq \mathbb{E} \left[\left(h(f(\theta, \tilde{X}^{(i)}) - \hat{\beta}) - h(f(\theta, X) - \hat{\beta}) \right)^2 | \theta, \hat{\beta} \right] \end{aligned}$$

$$\begin{aligned}
&\leq \mathbb{E} \left[\left(f(\theta, \tilde{X}^{(i)}) - f(\theta, X) \right)^2 \mid \theta, \hat{\beta} \right] \\
&\leq 4\mathbb{E} \left[(f(\theta, X))^2 \mid \theta, \hat{\beta} \right] \\
&\stackrel{(a)}{\leq} 4\mathbb{E} \left[(C_f \|X\|^{n_f} + D_f)^2 \mid \theta, \hat{\beta} \right] \\
&\leq 8C_f^2 \mathbb{E}[\|X\|^{2n_f}] + 8D_f^2 \\
&\stackrel{(b)}{\leq} \tilde{C}_f := 8C_f^2 \cdot \left((2D)^{2n_f} + W_{2n_f} \cdot \lambda^{-\frac{d}{2}} e^{-\frac{D^2}{\lambda}} \right) + 8D_f^2,
\end{aligned} \tag{59}$$

where step (a) follows from Assumption 2.8, and step (b) uses Lemma D.1. Then from (58), we get

$$\mathbb{E}[|\phi_{\lambda,\delta}(\theta, \hat{\beta}; \tilde{X}_I) - \phi_{\lambda,\delta}(\theta, \hat{\beta})|^2 \mid \theta] \leq \frac{\tilde{C}_f}{\delta^2 |I|}. \tag{60}$$

Upper bound on (ii) in (57): Because $\phi_{\lambda,\delta}(\theta, \cdot)$ is σ -Lipschitz in β and the feasible interval for β is $[-B, B]$, we have the deterministic range bound

$$0 \leq \phi_{\lambda,\delta}(\theta, \hat{\beta}) - \min_{\beta} \phi_{\lambda,\delta}(\theta, \beta) \leq R := 2\sigma B.$$

Given that (i) $\phi_{\lambda,\delta}(\theta, \cdot)$ is convex and Lipschitz, (ii) the feasible set is bounded, and (iii) the stochastic sub-gradient $\tilde{\partial}_{\beta} \phi_{\lambda,\delta}(\theta, \beta; X)$ satisfies $|\tilde{\partial}_{\beta} \phi_{\lambda,\delta}(\theta, \beta; X)| \leq \sigma := 1 + \delta^{-1}$, we invoke the convergence guarantees for convex Lipschitz objectives [51, 67]. Accordingly, the output $\hat{\beta}$ of PSGD (see Algorithm 1) satisfies

$$\mathbb{P} \left(\phi_{\lambda,\delta}(\theta, \hat{\beta}) - \min_{\beta} \phi_{\lambda,\delta}(\theta, \beta) \leq \epsilon_v \mid \theta \right) \geq 1 - \Delta.$$

after at most $\mathcal{O}(B^2 \sigma^2 \epsilon_v^{-2} \log^2(\Delta^{-1}))$ iterations.

From $0 \leq \phi_{\lambda,\delta}(\theta, \hat{\beta}) - \min_{\beta} \phi_{\lambda,\delta}(\theta, \beta) \leq R$ and the tail bound we get

$$\mathbb{E} \left[\left(\phi_{\lambda,\delta}(\theta, \hat{\beta}) - \min_{\beta} \phi_{\lambda,\delta}(\theta, \beta) \right)^2 \mid \theta \right] \leq \epsilon_v^2 (1 - \Delta) + R^2 \Delta \leq \epsilon_v^2 + R^2 \Delta.$$

Choosing $\Delta := \min\{1, \epsilon_v^2/R^2\}$ yields

$$\mathbb{E} \left[\left(\phi_{\lambda,\delta}(\theta, \hat{\beta}) - \min_{\beta} \phi_{\lambda,\delta}(\theta, \beta) \right)^2 \mid \theta \right] \leq 2\epsilon_v^2, \tag{61}$$

at the cost of

$$L \geq C \cdot \frac{B^2}{\delta^2 \epsilon_v^2} \cdot \log^2 \left(\frac{1}{\epsilon_v \delta} \right).$$

Thus, by substituting (61) and (60) into (57), we obtain

$$\mathbb{E}[|\tilde{\psi}(\theta) - \tilde{F}_{\text{SQ-G}}(\theta)|^2 \mid \theta] \leq 2\epsilon_v^2 + \frac{2\tilde{C}_f}{\delta^2 |I|}. \tag{62}$$

By picking $\delta = \epsilon_v^k$ and $|I| \geq 4\tilde{C}_f \epsilon_v^{-2k-2}$ and

$$L \geq \mathcal{O} \left(k^2 \cdot \frac{B^2}{\epsilon_v^{2(k+1)}} \cdot \log^2 \left(\frac{1}{\epsilon_v} \right) \right),$$

we get $\mathbb{E}[|\tilde{\psi}(\theta) - \tilde{F}_{\text{SQ-G}}(\theta)|^2 \mid \theta] \leq \epsilon_v^2$. \square

D.3 Proof of Theorem 5.5

We now prove Theorem 5.5. The argument follows the standard projected zeroth-order analysis for the smoothed objective, and the only additional step is to bound the error introduced by replacing F_{\max} with $\tilde{\psi}$ using Equation (26) and Lemma 5.2.

Proof. The proof has two parts. We first follow the standard convergence analysis for projected zeroth-order methods applied to the smoothed objective of F_{\max} . The only nonstandard step is then to control the additional error induced by replacing F_{\max} with $\tilde{\psi}$ in the gradient estimator, where we invoke Lemma 5.2.

Step 1: Standard zeroth-order analysis for the smoothed problem. We define the smoothed objective $\psi_\rho(\theta) := \mathbb{E}_{u \sim \text{uniform}(\mathbb{S}^{m-1})}[F_{\max}(\theta + \rho u)]$, where u is uniformly distributed on the unit sphere \mathbb{S}^{m-1} . As shown in [68, Theorem 1 and Lemma 2], for any $L_{f,1}$ -Lipschitz function $f : \mathbb{R}^m \rightarrow \mathbb{R}$, the smoothed version $f_\rho(\theta) := \mathbb{E}_{u \sim \text{uniform}(\mathbb{S}^{m-1})}[f(\theta + \rho u)]$ satisfies:

- f_ρ is a $\rho\sqrt{m}L_{f,1}$ -approximation of f , f_ρ is a $L_{f,1}$ -Lipschitz function,
- f_ρ is differentiable with gradient Lipschitz constant $L_{f,2} = \sqrt{m}L_{f,1}\rho^{-1}$,
- $\nabla f_\rho(\theta) \in \partial_\rho f(\theta)$, the ρ -subdifferential of f , as shown in [57, Theorem 3.1].

In our scenario, by using Corollary 3.4, F_{\max} is Lipschitz continuous with the constant $L_{F_{\max},1} := L_{f,1}(1 + L_{g,2}/\mu)$. By applying the aforementioned findings on F_{\max} , it follows that ψ_ρ is $(L_{\psi,2} = \sqrt{m}L_{F_{\max},1}\rho^{-1})$ -smooth. Furthermore, the gradient $\nabla\psi_\rho(\theta)$ is contained in the ρ -subdifferential set of F_{\max} at the point θ . Therefore, if a point θ satisfies $\|\mathcal{G}_\Theta(\theta, \nabla\psi_\rho; \eta)\| \leq \epsilon$, then θ is an (ϵ, ρ, η) -generalized Goldstein stationary point of F_{\max} (see Definition 5.4). In what follows, we analyze the convergence of Algorithm 2 to a critical point of ψ_ρ in terms of the gradient mapping.

Given the $(L_{\psi,2} = \sqrt{m}L_{F_{\max},1}\rho^{-1})$ -smoothness of $\psi_\rho(\theta)$, we have

$$\psi_\rho(\theta_{i+1}) \leq \psi_\rho(\theta_i) + \langle \nabla\psi_\rho(\theta_i), \theta_{i+1} - \theta_i \rangle + \frac{L_{\psi,2}}{2} \|\theta_{i+1} - \theta_i\|^2 \quad (63)$$

Substituting $\theta_{i+1} - \theta_i = -\tilde{\eta}_i \mathcal{G}_\Theta(\theta_i, \tilde{\mathbf{g}}_\rho(\theta_i); \tilde{\eta}_i)$, we have

$$\psi_\rho(\theta_{i+1}) \leq \psi_\rho(\theta_i) - \tilde{\eta}_i \langle \nabla\psi_\rho(\theta_i), \mathcal{G}_\Theta(\theta_i, \tilde{\mathbf{g}}_\rho(\theta_i); \tilde{\eta}_i) \rangle + \frac{L_{\psi,2}}{2} \tilde{\eta}_i^2 \|\mathcal{G}_\Theta(\theta_i, \tilde{\mathbf{g}}_\rho(\theta_i); \tilde{\eta}_i)\|^2 \quad (64)$$

Expanding the inner product and rearranging terms

$$\begin{aligned} \psi_\rho(\theta_{i+1}) &\leq \psi_\rho(\theta_i) - \tilde{\eta}_i \langle \tilde{\mathbf{g}}_\rho(\theta_i), \mathcal{G}_\Theta(\theta_i, \tilde{\mathbf{g}}_\rho(\theta_i); \tilde{\eta}_i) \rangle + \frac{L_{\psi,2}}{2} \tilde{\eta}_i^2 \|\mathcal{G}_\Theta(\theta_i, \tilde{\mathbf{g}}_\rho(\theta_i); \tilde{\eta}_i)\|^2 \\ &\quad - \tilde{\eta}_i \langle \nabla\psi_\rho(\theta_i) - \tilde{\mathbf{g}}_\rho(\theta_i), \mathcal{G}_\Theta(\theta_i, \tilde{\mathbf{g}}_\rho(\theta_i); \tilde{\eta}_i) \rangle \end{aligned} \quad (65)$$

Further simplifying and using the fact that $\|\mathcal{G}_\Theta(\theta, v; \eta)\|^2 \leq \langle \mathcal{G}_\Theta(\theta, v; \eta), v \rangle$ for every $v \in \Theta$, we have

$$\begin{aligned} \psi_\rho(\theta_{i+1}) &\leq \psi_\rho(\theta_i) - \left[\tilde{\eta}_i - \frac{L_{\psi,2}}{2} \tilde{\eta}_i^2 \right] \cdot \|\mathcal{G}_\Theta(\theta_i, \tilde{\mathbf{g}}_\rho(\theta_i); \tilde{\eta}_i)\|^2 \\ &\quad - \tilde{\eta}_i \langle \nabla\psi_\rho(\theta_i) - \tilde{\mathbf{g}}_\rho(\theta_i), \mathcal{G}_\Theta(\theta_i, \nabla\psi_\rho(\theta_i); \tilde{\eta}_i) \rangle \\ &\quad - \tilde{\eta}_i \langle \nabla\psi_\rho(\theta_i) - \tilde{\mathbf{g}}_\rho(\theta_i), \mathcal{G}_\Theta(\theta_i, \nabla\psi_\rho(\theta_i); \tilde{\eta}_i) - \mathcal{G}_\Theta(\theta_i, \tilde{\mathbf{g}}_\rho(\theta_i); \tilde{\eta}_i) \rangle \\ &\leq \psi_\rho(\theta_i) - \left[\tilde{\eta}_i - \frac{L_{\psi,2}}{2} \tilde{\eta}_i^2 \right] \cdot \|\mathcal{G}_\Theta(\theta_i, \tilde{\mathbf{g}}_\rho(\theta_i); \tilde{\eta}_i)\|^2 \\ &\quad - \tilde{\eta}_i \langle \nabla\psi_\rho(\theta_i) - \tilde{\mathbf{g}}_\rho(\theta_i), \mathcal{G}_\Theta(\theta_i, \nabla\psi_\rho(\theta_i); \tilde{\eta}_i) \rangle + \tilde{\eta}_i \|\nabla\psi_\rho(\theta_i) - \tilde{\mathbf{g}}_\rho(\theta_i)\|^2, \end{aligned} \quad (66)$$

where the last inequality comes from the Cauchy-Schwartz inequality and $\|\mathcal{G}_\Theta(\theta, v_1; \eta) - \mathcal{G}_\Theta(\theta, v_2; \eta)\| \leq \|v_1 - v_2\|$. Let us define $\mathbf{g}_\rho(\theta) := \frac{1}{b_u} \sum_{t=1}^{b_u} \mathbf{g}_\rho(\theta, u_t)$ where $\mathbf{g}_\rho(\theta, u_t) := \frac{m}{2\rho} \cdot [F_{\max}(\theta + \rho u_t) - F_{\max}(\theta - \rho u_t)]u_t$. Then

$$\begin{aligned} \psi_\rho(\theta_{i+1}) &\leq \psi_\rho(\theta_i) - \left[\tilde{\eta}_i - \frac{L_{\psi,2} \tilde{\eta}_i^2}{2} \right] \cdot \|\mathcal{G}_\Theta(\theta_i, \tilde{\mathbf{g}}_\rho(\theta_i); \tilde{\eta}_i)\|^2 \\ &\quad - \tilde{\eta}_i \langle \nabla \psi_\rho(\theta_i) - \mathbf{g}_\rho(\theta_i), \mathcal{G}_\Theta(\theta_i, \nabla \psi_\rho(\theta_i); \tilde{\eta}_i) \rangle \\ &\quad - \tilde{\eta}_i \langle \mathbf{g}_\rho(\theta_i) - \tilde{\mathbf{g}}_\rho(\theta_i), \mathcal{G}_\Theta(\theta_i, \nabla \psi_\rho(\theta_i); \tilde{\eta}_i) \rangle + \tilde{\eta}_i \|\nabla \psi_\rho(\theta_i) - \tilde{\mathbf{g}}_\rho(\theta_i)\|^2, \end{aligned} \quad (67)$$

By picking $\tilde{\eta}_i \leq 1/L_{\psi,2}$, we have

$$\begin{aligned} \|\mathcal{G}_\Theta(\theta_i, \tilde{\mathbf{g}}_\rho(\theta_i); \tilde{\eta}_i)\|^2 &\leq \frac{2[\psi_\rho(\theta_i) - \psi_\rho(\theta_{i+1})]}{\tilde{\eta}_i} \\ &\quad - 2 \langle \nabla \psi_\rho(\theta_i) - \mathbf{g}_\rho(\theta_i), \mathcal{G}_\Theta(\theta_i, \nabla \psi_\rho(\theta_i); \tilde{\eta}_i) \rangle \\ &\quad - 2 \langle \mathbf{g}_\rho(\theta_i) - \tilde{\mathbf{g}}_\rho(\theta_i), \mathcal{G}_\Theta(\theta_i, \nabla \psi_\rho(\theta_i); \tilde{\eta}_i) \rangle + 2 \|\nabla \psi_\rho(\theta_i) - \tilde{\mathbf{g}}_\rho(\theta_i)\|^2. \end{aligned} \quad (68)$$

Then by using Young's inequality ($\langle \mathbf{a}, \mathbf{b} \rangle \leq c\|\mathbf{a}\|^2/2 + \|\mathbf{b}\|^2/(2c)$) for the vectors \mathbf{a}, \mathbf{b} and positive constant c , we have

$$\begin{aligned} \|\mathcal{G}_\Theta(\theta_i, \tilde{\mathbf{g}}_\rho(\theta_i); \tilde{\eta}_i)\|^2 &\leq \frac{2[\psi_\rho(\theta_i) - \psi_\rho(\theta_{i+1})]}{\tilde{\eta}_i} \\ &\quad - 2 \langle \nabla \psi_\rho(\theta_i) - \mathbf{g}_\rho(\theta_i), \mathcal{G}_\Theta(\theta_i, \nabla \psi_\rho(\theta_i); \tilde{\eta}_i) \rangle + 4 \|\mathbf{g}_\rho(\theta_i) - \tilde{\mathbf{g}}_\rho(\theta_i)\|^2 \\ &\quad + 4^{-1} \|\mathcal{G}_\Theta(\theta_i, \nabla \psi_\rho(\theta_i); \tilde{\eta}_i)\|^2 + 2 \|\nabla \psi_\rho(\theta_i) - \tilde{\mathbf{g}}_\rho(\theta_i)\|^2. \end{aligned} \quad (69)$$

Using [54, Lemma D1], $\mathbb{E}_{u_t}[\mathbf{g}_\rho(\theta_i) \mid \theta_i] = \nabla \psi_\rho(\theta_i)$. Taking expectation given θ_i

$$\begin{aligned} \mathbb{E}[\|\mathcal{G}_\Theta(\theta_i, \tilde{\mathbf{g}}_\rho(\theta_i); \tilde{\eta}_i)\|^2 \mid \theta_i] &\leq \\ &\quad \frac{2[\psi_\rho(\theta_i) - \mathbb{E}[\psi_\rho(\theta_{i+1}) \mid \theta_i]]}{\tilde{\eta}_i} + 4 \mathbb{E}[\|\mathbf{g}_\rho(\theta_i) - \tilde{\mathbf{g}}_\rho(\theta_i)\|^2 \mid \theta_i] + \\ &\quad + 4^{-1} \mathbb{E}[\|\mathcal{G}_\Theta(\theta_i, \nabla \psi_\rho(\theta_i); \tilde{\eta}_i)\|^2 \mid \theta_i] + 2 \mathbb{E}[\|\nabla \psi_\rho(\theta_i) - \tilde{\mathbf{g}}_\rho(\theta_i)\|^2 \mid \theta_i]. \end{aligned} \quad (70)$$

The term involving $\nabla \psi_\rho(\theta_i) - \mathbf{g}_\rho(\theta_i)$ vanishes because $\mathbb{E}_{u_t}[\mathbf{g}_\rho(\theta_i) \mid \theta_i] = \nabla \psi_\rho(\theta_i)$ and $\mathcal{G}_\Theta(\theta_i, \nabla \psi_\rho(\theta_i); \tilde{\eta}_i)$ is deterministic given θ_i . Moreover, by $(a+b)^2 \leq 2(a^2 + b^2)$,

$$\mathbb{E}[\|\nabla \psi_\rho(\theta_i) - \tilde{\mathbf{g}}_\rho(\theta_i)\|^2 \mid \theta_i] \leq 2 \mathbb{E}[\|\nabla \psi_\rho(\theta_i) - \mathbf{g}_\rho(\theta_i)\|^2 \mid \theta_i] + 2 \mathbb{E}[\|\mathbf{g}_\rho(\theta_i) - \tilde{\mathbf{g}}_\rho(\theta_i)\|^2 \mid \theta_i].$$

Substituting this into (70), we obtain

$$\begin{aligned} \mathbb{E}[\|\mathcal{G}_\Theta(\theta_i, \tilde{\mathbf{g}}_\rho(\theta_i); \tilde{\eta}_i)\|^2 \mid \theta_i] &\leq \\ &\quad \frac{2[\psi_\rho(\theta_i) - \mathbb{E}[\psi_\rho(\theta_{i+1}) \mid \theta_i]]}{\tilde{\eta}_i} + 4 \mathbb{E}[\|\nabla \psi_\rho(\theta_i) - \mathbf{g}_\rho(\theta_i)\|^2 \mid \theta_i] \\ &\quad + 8 \mathbb{E}[\|\mathbf{g}_\rho(\theta_i) - \tilde{\mathbf{g}}_\rho(\theta_i)\|^2 \mid \theta_i] + 4^{-1} \mathbb{E}[\|\mathcal{G}_\Theta(\theta_i, \nabla \psi_\rho(\theta_i); \tilde{\eta}_i)\|^2 \mid \theta_i]. \end{aligned} \quad (71)$$

In order to give a bound on $\mathbb{E}[\|\mathcal{G}_\Theta(\theta_i, \nabla \psi_\rho(\theta_i); \tilde{\eta}_i)\|^2 \mid \theta_i]$, we have

$$\begin{aligned} \mathbb{E}[\|\mathcal{G}_\Theta(\theta_i, \nabla \psi_\rho(\theta_i); \tilde{\eta}_i)\|^2 \mid \theta_i] &\leq 2 \mathbb{E}[\|\mathcal{G}_\Theta(\theta_i, \tilde{\mathbf{g}}_\rho(\theta_i); \tilde{\eta}_i)\|^2 \mid \theta_i] \\ &\quad + 2 \mathbb{E}[\|\mathcal{G}_\Theta(\theta_i, \tilde{\mathbf{g}}_\rho(\theta_i); \tilde{\eta}_i) - \mathcal{G}_\Theta(\theta_i, \nabla \psi_\rho(\theta_i); \tilde{\eta}_i)\|^2 \mid \theta_i] \\ &\stackrel{(a)}{\leq} 2 \mathbb{E}[\|\mathcal{G}_\Theta(\theta_i, \tilde{\mathbf{g}}_\rho(\theta_i); \tilde{\eta}_i)\|^2 \mid \theta_i] + 2 \mathbb{E}[\|\tilde{\mathbf{g}}_\rho(\theta_i) - \nabla \psi_\rho(\theta_i)\|^2 \mid \theta_i] \end{aligned}$$

$$\begin{aligned} &\leq 2\mathbb{E}[\|\mathcal{G}_\Theta(\theta_i, \tilde{\mathbf{g}}_\rho(\theta_i); \tilde{\eta}_i)\|^2 | \theta_i] \\ &\quad + 4\mathbb{E}[\|\nabla\psi_\rho(\theta_i) - \mathbf{g}_\rho(\theta_i)\|^2 | \theta_i] + 4\mathbb{E}[\|\tilde{\mathbf{g}}_\rho(\theta_i) - \mathbf{g}_\rho(\theta_i)\|^2 | \theta_i]. \end{aligned} \quad (72)$$

where (a) follows by $\|\mathcal{G}_\Theta(\theta, v_1; \eta) - \mathcal{G}_\Theta(\theta, v_2; \eta)\| \leq \|v_1 - v_2\|$. Incorporating (71) in (72), we get

$$\begin{aligned} \mathbb{E}[\|\mathcal{G}_\Theta(\theta_i, \nabla\psi_\rho(\theta_i); \tilde{\eta}_i)\|^2 | \theta_i] &\leq \frac{4[\psi_\rho(\theta_i) - \mathbb{E}[\psi_\rho(\theta_{i+1}) | \theta_i]]}{\tilde{\eta}_i} \\ &\quad + 12\mathbb{E}[\|\nabla\psi_\rho(\theta_i) - \mathbf{g}_\rho(\theta_i)\|^2 | \theta_i] + 20\mathbb{E}[\|\mathbf{g}_\rho(\theta_i) - \tilde{\mathbf{g}}_\rho(\theta_i)\|^2 | \theta_i] \\ &\quad + 2^{-1}\mathbb{E}[\|\mathcal{G}_\Theta(\theta_i, \nabla\psi_\rho(\theta_i); \tilde{\eta}_i)\|^2 | \theta_i]. \end{aligned} \quad (73)$$

Finally, we get

$$\begin{aligned} \mathbb{E}[\|\mathcal{G}_\Theta(\theta_i, \nabla\psi_\rho(\theta_i); \tilde{\eta}_i)\|^2 | \theta_i] &\leq \\ &\quad \frac{8[\psi_\rho(\theta_i) - \mathbb{E}[\psi_\rho(\theta_{i+1}) | \theta_i]]}{\tilde{\eta}_i} + 24\mathbb{E}[\|\nabla\psi_\rho(\theta_i) - \mathbf{g}_\rho(\theta_i)\|^2 | \theta_i] \\ &\quad + 40\mathbb{E}[\|\mathbf{g}_\rho(\theta_i) - \tilde{\mathbf{g}}_\rho(\theta_i)\|^2 | \theta_i]. \end{aligned} \quad (74)$$

Up to this point, the analysis is standard for constrained zeroth-order methods and does not use the specific structure of F_{\max} .

Step 2: Controlling the directional and oracle errors. We first bound the variance coming from the random directions. Since the variables $\{\mathbf{g}_\rho(\theta_i, u_{i,t})\}_{t=1}^{b_u}$ are i.i.d. and satisfy $\mathbb{E}_{u_t}[\mathbf{g}_\rho(\theta_i, u_{i,t}) | \theta_i] = \nabla\psi_\rho(\theta_i)$, we have

$$\begin{aligned} &\mathbb{E}[\|\nabla\psi_\rho(\theta_i) - \mathbf{g}_\rho(\theta_i)\|^2 | \theta_i] \\ &= \frac{1}{b_u^2} \sum_{t=1}^{b_u} \mathbb{E}[\|\mathbf{g}_\rho(\theta_i, u_{i,t}) - \nabla\psi_\rho(\theta_i)\|^2 | \theta_i] \\ &\leq \frac{1}{b_u} \mathbb{E}[\|\mathbf{g}_\rho(\theta_i, u)\|^2 | \theta_i] \\ &\leq \frac{m^2 L_{F_{\max},1}^2}{b_u}, \end{aligned} \quad (75)$$

where we used

$$\|\mathbf{g}_\rho(\theta_i, u)\| = \frac{m}{2\rho} |F_{\max}(\theta_i + \rho u) - F_{\max}(\theta_i - \rho u)| \leq mL_{F_{\max},1}.$$

We now invoke Lemma 5.2 to bound the oracle term in (74):

$$\begin{aligned} &\mathbb{E}[\|\tilde{\mathbf{g}}_\rho(\theta_i) - \mathbf{g}_\rho(\theta_i)\|^2 | \theta_i] \\ &\leq \frac{m^2}{\rho^2 b_u} \sum_{t=1}^{b_u} \mathbb{E}[|\tilde{\psi}(\theta_i + \rho u_{i,t}) - F_{\max}(\theta_i + \rho u_{i,t})|^2 \\ &\quad + |\tilde{\psi}(\theta_i - \rho u_{i,t}) - F_{\max}(\theta_i - \rho u_{i,t})|^2] \\ &\leq \frac{m^2}{\rho^2} \cdot \mathcal{O}(\epsilon_v^2), \end{aligned} \quad (76)$$

where the last inequality comes from Lemma 5.2 with $|I| \geq 4\tilde{C}_f \epsilon_v^{-2-2k}$, and

$$L = \mathcal{O}\left(\frac{k^2 B^2}{\epsilon_v^{2+2k}} \cdot \log^2(\epsilon_v^{-1})\right).$$

By choosing $\tilde{\eta}_i = \eta \leq 1/L_{\psi,2} = m^{-1/2}\rho L_{F_{\max,1}}^{-1}$ and integrating (75) and (76) into (74), followed by averaging over θ_i , we obtain

$$\begin{aligned} \frac{1}{N} \sum_{t=1}^N \mathbb{E}[\|\mathcal{G}_{\Theta}(\theta_i, \nabla\psi_{\rho}; \eta)\|^2] &\leq \frac{8\psi_{\rho}(\theta_0) - 8\mathbb{E}[\psi_{\rho}(\theta_N)]}{N\eta} + \mathcal{O}\left(\frac{m^2}{b_u}\right) \\ &\quad + \frac{40m^2}{\rho^2} \cdot \mathcal{O}(\epsilon_v^2) \\ &\leq \mathcal{O}\left(\frac{m^{\frac{1}{2}} \cdot (\psi_{\rho}(\theta_0) - \mathbb{E}[\psi_{\rho}(\theta_N)])}{N\rho} + \frac{m^2}{b_u} + \frac{m^2}{\rho^2} \cdot \epsilon_v^2\right) \\ &\leq \mathcal{O}\left(\frac{m \cdot \text{diam}(\Theta)}{N\rho^2} + \frac{m^2}{b_u} + \frac{m^2}{\rho^2} \cdot \epsilon_v^2\right), \end{aligned} \quad (77)$$

where the final inequality results from the Lipschitz continuity of F_{\max} with constant $(\sqrt{m}\rho^{-1}L_{F_{\max,1}})$ and the boundedness of domain Θ .

Let us define $\hat{\theta} = \arg \min_{i \in [1:N]} \mathbb{E}[\|\mathcal{G}_{\Theta}(\theta_i, \nabla\psi_{\rho}; \eta)\|^2]$. Then by Jensen's inequality, we have

$$\mathbb{E}[\|\mathcal{G}_{\Theta}(\hat{\theta}, \nabla\psi_{\rho}; \eta)\|] = \mathcal{O}\left(\frac{m^{\frac{1}{2}}(\text{diam}(\Theta))^{\frac{1}{2}}}{\sqrt{N}\rho} + \frac{m}{\sqrt{b_u}} + \frac{m}{\rho} \cdot \epsilon_v\right). \quad (78)$$

Let us pick $\epsilon_v = \rho\epsilon m^{-1}$, $N \geq m \cdot \text{diam}(\Theta) \cdot \epsilon^{-2}\rho^{-2}$, and $b_u \geq m^2\epsilon^{-2}$. Then $\mathbb{E}[\|\mathcal{G}_{\Theta}(\hat{\theta}, \nabla\psi_{\rho}; \eta)\|] = \mathcal{O}(\epsilon)$. We also pick $b_u = \mathcal{O}(m^2\epsilon^{-2})$. Then the total number of samples from Gibbs measure is

$$N \times (b_u L + b_u |I|) = \mathcal{O}\left(\frac{m^{5+2k} \cdot \text{diam}(\Theta) \cdot (k^2 B^2 + \tilde{C}_f) \cdot \log^2(m\epsilon^{-1}\rho^{-1})}{\epsilon^{2k+6}\rho^{2k+4}}\right). \quad (79)$$

□

E Computational Complexity of Gibbs Oracle

In this section, we modify the result of Section 5 for the setting where the Gibbs samples are generated approximately by LMC rather than drawn exactly from the Gibbs distribution.

E.1 Runtime Complexity of Algorithm 1 by Using LMC

We first replace Algorithm 1 by Algorithm 3, where the only change is that the exact samples $\{\tilde{X}^l\}_{l=0}^{L-1}$ from the Gibbs distribution $\mu_{\hat{\theta}}^{\lambda}$ are replaced by approximate samples $\{\tilde{X}_l^n\}_{l=0}^{L-1}$, each \tilde{X}_l^n being produced by running an n -step Langevin Monte Carlo (LMC) algorithm (see Equation (30)). Our goal is to establish an updated version of Lemma 5.2 tailored to Algorithm 3.

We pick $\lambda > 0$ and define the following approximate objective:

$$\tilde{\phi}_{\lambda,\delta}(\theta, \beta) := \beta + \frac{1}{\delta} \mathbb{E}_{X \sim \hat{\mu}_n} [\max\{f(\theta, X) - \beta, 0\}], \quad (80)$$

where $\hat{\mu}_n$ denotes the empirical distribution induced by n -step LMC output. Since

$$|\tilde{\phi}_{\lambda,\delta}(\theta, \beta) - \phi_{\lambda,\delta}(\theta, \beta)| \leq \frac{L_{f,1}}{\delta} \mathbb{W}_1(\hat{\mu}_n, \mu_{\hat{\theta}}^{\lambda}),$$

Algorithm 3 PSGD-LMC(θ, β_0)

Input: θ, β_0

- 1: **for** $l = 0$ to $L - 1$ **do**
 - 2: $\beta^{l+1} = \text{Proj}_{[-B, B]}(\beta^l - \eta_l \tilde{\partial}_\beta \phi_{\lambda, \delta}(\theta, \beta^l; \tilde{X}_i^n))$
 $[\{\tilde{X}_i^n\}_{l=0}^{L-1}$ are i.i.d samples of L parallel LMC methods.]
 - 3: **end for**
 - 4: $\tilde{\beta} = \frac{1}{L} \sum_{i=1}^L \beta^i$
-

we can invoke the LMC Wasserstein bound from Section 5.3 to obtain

$$|\tilde{\phi}_{\lambda, \delta}(\theta, \beta) - \phi_{\lambda, \delta}(\theta, \beta)| \leq \frac{L_{f,1}}{\delta} \cdot 2C_{PI}^{1/2} C^{1/2} \varepsilon. \quad (81)$$

Setting $\epsilon_v := \varepsilon/\delta$ with $\delta = \epsilon_v^k$ and running LMC for $n = \tilde{O}(d \epsilon_v^{-6-6k})$ iterations yields

$$|\tilde{\phi}_{\lambda, \delta}(\theta, \beta) - \phi_{\lambda, \delta}(\theta, \beta)| = \mathcal{O}(\epsilon_v).$$

Since (81) holds for every β , the same argument as in Lemma 4.4 implies

$$|\min_{\beta} \tilde{\phi}_{\lambda, \delta}(\theta, \beta) - \min_{\beta} \phi_{\lambda, \delta}(\theta, \beta)| = \mathcal{O}(\epsilon_v).$$

We then define the LMC-based estimator of $\tilde{F}_{\text{SQ-G}}(\theta)$ by

$$\hat{\psi}(\theta) := \phi_{\lambda, \delta}(\theta, \tilde{\beta}; \hat{X}_I^n) = \tilde{\beta} + \frac{1}{\delta|I|} \sum_{i \in I} \max\{f(\theta, \hat{X}_i^n) - \tilde{\beta}, 0\}, \quad (82)$$

where $\hat{X}_I^n := \{\hat{X}_i^n\}_{i \in I}$ are i.i.d. n -step LMC samples from $\hat{\mu}_n$.

We then restate lemma 5.2 by using the updates of algorithm 3 as follows:

Lemma E.1. *Given $\theta \in \Theta$, by using Algorithm 3 (PSGD-LMC(θ, β_0)), we obtain*

$$\mathbb{E}[|\hat{\psi}(\theta) - \tilde{F}_{\text{SQ-G}}(\theta)|^2 \mid \theta] = \mathcal{O}(\epsilon_v^2), \quad (83)$$

with $|I| \geq \tilde{C}_f \epsilon_v^{-2k-2}$ and the number of iterations of PSGD as follows

$$L \times n \geq \tilde{O}\left(\frac{dk^2 B^2 \log^2(\epsilon_v^{-1})}{\epsilon_v^{8+8k}}\right).$$

Here \tilde{C}_f is a constant, and B is defined in Lemma 5.1.

Proof. The proof mirrors that of Lemma 5.2; we highlight only the modifications due to the use of LMC samples and the function $\tilde{\phi}_{\lambda, \delta}$.

Step 1: PSGD error for $\tilde{\phi}_{\lambda, \delta}$. Fix $\theta \in \Theta$, and let $\tilde{\beta}$ denote the output of PSGD-LMC(θ, β_0). As in the proof of Lemma 5.2, $\tilde{\phi}_{\lambda, \delta}(\theta, \cdot)$ is convex, σ -Lipschitz with $\sigma = 1 + \delta^{-1}$, and optimized over the interval $[-B, B]$. Therefore, the high-probability PSGD guarantee (18) applies to $\tilde{\phi}_{\lambda, \delta}$ verbatim: for any $\epsilon_v > 0$ and $\Delta \in (0, 1)$,

$$\mathbb{P}\left(\tilde{\phi}_{\lambda, \delta}(\theta, \tilde{\beta}) - \min_{\beta \in [-B, B]} \tilde{\phi}_{\lambda, \delta}(\theta, \beta) \leq \epsilon_v \mid \theta\right) \geq 1 - \Delta,$$

after at most

$$L = \mathcal{O}(B^2 \sigma^2 \epsilon_v^{-2} \log^2(\Delta^{-1})).$$

Choosing $\delta = \epsilon_v^k$ so that $\sigma = \mathcal{O}(\epsilon_v^{-k})$ and taking $\Delta := \min\{1, \epsilon_v^2/R^2\}$ as in the proof of Lemma 5.2, we obtain

$$\mathbb{E}\left[\left(\tilde{\phi}_{\lambda,\delta}(\theta, \tilde{\beta}) - \min_{\beta} \tilde{\phi}_{\lambda,\delta}(\theta, \beta)\right)^2 \mid \theta\right] \leq C \epsilon_v^2, \quad (84)$$

for some constant $C > 0$, using

$$L = \mathcal{O}(k^2 B^2 \epsilon_v^{-2-2k} \log^2(\epsilon_v^{-1})). \quad (85)$$

Step 2: From $\tilde{\phi}_{\lambda,\delta}$ to $\phi_{\lambda,\delta}$ and $\tilde{F}_{\text{SQ-G}}$. Recall that $\tilde{F}_{\text{SQ-G}}(\theta) = \min_{\beta} \phi_{\lambda,\delta}(\theta, \beta)$. For the same $\tilde{\beta}$ as above,

$$\begin{aligned} \phi_{\lambda,\delta}(\theta, \tilde{\beta}) - \tilde{F}_{\text{SQ-G}}(\theta) &= \phi_{\lambda,\delta}(\theta, \tilde{\beta}) - \min_{\beta} \phi_{\lambda,\delta}(\theta, \beta) \\ &\leq |\phi_{\lambda,\delta}(\theta, \tilde{\beta}) - \tilde{\phi}_{\lambda,\delta}(\theta, \tilde{\beta})| + \left(\tilde{\phi}_{\lambda,\delta}(\theta, \tilde{\beta}) - \min_{\beta} \tilde{\phi}_{\lambda,\delta}(\theta, \beta)\right) \\ &\quad + \left|\min_{\beta} \tilde{\phi}_{\lambda,\delta}(\theta, \beta) - \min_{\beta} \phi_{\lambda,\delta}(\theta, \beta)\right|. \end{aligned}$$

By the uniform approximation bound (81) and its consequence for minimizers (see the discussion after (81)), both $|\phi_{\lambda,\delta}(\theta, \beta) - \tilde{\phi}_{\lambda,\delta}(\theta, \beta)|$ and $|\min_{\beta} \tilde{\phi}_{\lambda,\delta}(\theta, \beta) - \min_{\beta} \phi_{\lambda,\delta}(\theta, \beta)|$ are $\mathcal{O}(\epsilon_v)$, uniformly in β , provided n is chosen as below. Combining these with (84) and using $(a + b + c)^2 \leq 3(a^2 + b^2 + c^2)$ gives

$$\mathbb{E}\left[\left(\phi_{\lambda,\delta}(\theta, \tilde{\beta}) - \tilde{F}_{\text{SQ-G}}(\theta)\right)^2 \mid \theta\right] \leq C_2 \epsilon_v^2, \quad (86)$$

for some constant $C_2 > 0$, provided the LMC chain length satisfies

$$n = \tilde{\mathcal{O}}(d \epsilon_v^{-6-6k}),$$

as in the Wasserstein–convergence bound used in Section 5.3.

Step 3: Bounding the MSE of $\hat{\psi}(\theta)$. By Jensen's inequality and the triangle inequality,

$$\begin{aligned} \mathbb{E}\left[|\hat{\psi}(\theta) - \tilde{F}_{\text{SQ-G}}(\theta)|^2 \mid \theta\right] &\leq 3 \underbrace{\mathbb{E}\left[|\hat{\psi}(\theta) - \tilde{\psi}(\theta)|^2 \mid \theta\right]}_{(1)} \\ &\quad + 3 \underbrace{\mathbb{E}\left[|\tilde{\psi}(\theta) - \phi_{\lambda,\delta}(\theta, \tilde{\beta})|^2 \mid \theta\right]}_{(2)} + 3 \underbrace{\mathbb{E}\left[|\phi_{\lambda,\delta}(\theta, \tilde{\beta}) - \tilde{F}_{\text{SQ-G}}(\theta)|^2 \mid \theta\right]}_{(3)}. \end{aligned} \quad (87)$$

We bound the three terms as follows.

1. Conditioning on θ and $\tilde{\beta}$, using independence across $i \in I$,

$$\mathbb{E}\left[|\hat{\psi}(\theta) - \tilde{\psi}(\theta)|^2 \mid \theta\right] = \mathbb{E}\left[\left|\frac{1}{\delta|I|} \sum_{i \in I} (h(f(\theta, \hat{X}_i^n) - \tilde{\beta}) - h(f(\theta, \tilde{X}^i) - \tilde{\beta}))\right|^2 \mid \theta\right] \quad (88)$$

$$\leq \frac{1}{\delta^2|I|} \sum_{i \in I} \mathbb{E}\left[\left(h(f(\theta, \hat{X}_i^n) - \tilde{\beta}) - h(f(\theta, \tilde{X}^i) - \tilde{\beta})\right)^2 \mid \theta\right] \quad (89)$$

$$\leq \frac{L_{f,1}^2}{\delta^2} \mathbb{W}_2^2(\hat{\mu}_n, \mu_{\tilde{\theta}}^{\lambda}), \quad (90)$$

since $h(f(\theta, \cdot) - \tilde{\beta})$ is $L_{f,1}$ -Lipschitz. By the LMC convergence bound used in Section 5.3, choosing $n = \tilde{\mathcal{O}}(d \epsilon_v^{-6-6k})$ ensures $\mathbb{W}_2^2(\hat{\mu}_n, \mu_{\tilde{\theta}}^{\lambda}) = \mathcal{O}(\epsilon_v^{2+2k})$, and hence

$$\mathbb{E}\left[|\hat{\psi}(\theta) - \tilde{\psi}(\theta)|^2 \mid \theta\right] \leq C_3 \epsilon_v^2 \quad (91)$$

for some constant $C_3 > 0$.

Algorithm 4 Projected Stochastic Zeroth-order with LMC (PSZO-LMC)

Initialization: $\beta_0, \theta_0, \lambda, \delta < 1/2$, and integers N, n .

- 1: **for** $k = 0$ to $N - 1$ **do**
 - 2: Query i.i.d. samples of $|I|$ parallel LMC methods, denoted by $\hat{X}_I^n = \{\hat{X}_i^n\}_{i \in I}$.
 - 3: Sample $\{u_{k,t}\}_{t=1}^{b_u}$ independently and uniformly from a unit sphere.
 - 4: $\beta_{k,t}^+ = \text{PSGD-LMC}(\theta_k + \rho u_{k,t}, \beta_0), \forall t \in [1 : b_u]$.
 - 5: $\beta_{k,t}^- = \text{PSGD-LMC}(\theta_k - \rho u_{k,t}, \beta_0), \forall t \in [1 : b_u]$.
 - 6: $\hat{\psi}(\theta_k + \rho u_{k,t}) = \phi_{\lambda, \delta}(\theta_k + \rho u_{k,t}, \beta_{k,t}^+; \hat{X}_I^N)$.
 - 7: $\hat{\psi}(\theta_k - \rho u_{k,t}) = \phi_{\lambda, \delta}(\theta_k - \rho u_{k,t}, \beta_{k,t}^-; \hat{X}_I^N)$.
 - 8: $\hat{\mathbf{g}}_\rho(\theta_k) = \frac{m}{2\rho} \cdot \frac{1}{b_u} \sum_{t=1}^{b_u} [\hat{\psi}(\theta_k + \rho u_{k,t}) - \hat{\psi}(\theta_k - \rho u_{k,t})] u_{k,t}$
 - 9: $\theta_{k+1} = \text{Proj}_\Theta(\theta_k - \tilde{\eta}_k \hat{\mathbf{g}}_\rho(\theta_k))$
 - 10: **end for**
-

2. Exactly as in (59)–(60), we have

$$\mathbb{E}[|\tilde{\psi}(\theta) - \phi_{\lambda, \delta}(\theta, \tilde{\beta})|^2 | \theta] \leq \frac{\tilde{C}_f}{\delta^2 |I|}, \quad (92)$$

for some constant $\tilde{C}_f > 0$. With $\delta = \epsilon_v^k$ and $|I| \geq \tilde{C}_f \epsilon_v^{-2k-2}$, this is $\mathcal{O}(\epsilon_v^2)$.

3. This is exactly (86):

$$\mathbb{E}[|\phi_{\lambda, \delta}(\theta, \tilde{\beta}) - \tilde{F}_{\text{SQ-G}}(\theta)|^2 | \theta] \leq C_2 \epsilon_v^2. \quad (93)$$

Substituting (91)–(93) into (87), we obtain

$$\mathbb{E}[|\hat{\psi}(\theta) - \tilde{F}_{\text{SQ-G}}(\theta)|^2 | \theta] \leq C \epsilon_v^2,$$

for some constant $C > 0$ independent of θ and ϵ_v . Finally, combining (85) with $n = \tilde{\mathcal{O}}(d \epsilon_v^{-6-6k})$ yields

$$L \times n = \tilde{\mathcal{O}}\left(\frac{d k^2 B^2 \log^2(\epsilon_v^{-1})}{\epsilon_v^{8+8k}}\right),$$

which completes the proof. \square

E.2 Proof of Theorem 5.7

First, we change Algorithm 2 to Algorithm 4 by replacing the samples of Gibbs measure with samples of the output of parallel LMCs and changing PSGD to PSGD-LMC (see Algorithm 3) in lines 4 and 5. Relative to the proof of Theorem 5.5, the directional-variance term in (74) is unchanged; the only new ingredient is the bound on the oracle term $\mathbb{E}[\|\mathbf{g}_\rho(\theta_i) - \hat{\mathbf{g}}_\rho(\theta_i)\|^2 | \theta_i]$. We provide the proof of Theorem 5.7 in the following:

Proof. The argument mirrors the proof of Theorem 5.5. We briefly recall the zeroth-order part and then highlight the only new ingredient, namely the control of the LMC-induced error via Lemma E.1.

Step 1: Zeroth-order analysis (same as Theorem 5.5). As in the proof of Theorem 5.5, we work with the smoothed objective $\psi_\rho(\theta) := \mathbb{E}_{u \sim \text{Unif}(\mathbb{S}^{m-1})}[F_{\max}(\theta + \rho u)]$. Using the smoothness of ψ_ρ and the projected gradient-mapping update, the standard analysis of constrained zeroth-order methods yields (see eq. (74) in Section D.3)

$$\mathbb{E}[\|\mathcal{G}_\Theta(\theta_i, \nabla \psi_\rho(\theta_i); \tilde{\eta}_i)\|^2 | \theta_i] \leq \frac{8(\psi_\rho(\theta_i) - \mathbb{E}[\psi_\rho(\theta_{i+1}) | \theta_i])}{\tilde{\eta}_i}$$

$$\begin{aligned}
& + 24 \mathbb{E}[\|\nabla\psi_\rho(\theta_i) - \mathbf{g}_\rho(\theta_i)\|^2 \mid \theta_i] \\
& + 40 \mathbb{E}[\|\mathbf{g}_\rho(\theta_i) - \hat{\mathbf{g}}_\rho(\theta_i)\|^2 \mid \theta_i], \tag{94}
\end{aligned}$$

where

$$\mathbf{g}_\rho(\theta_i) := \frac{1}{b_u} \sum_{t=1}^{b_u} \mathbf{g}_\rho(\theta_i, u_{i,t}), \quad \mathbf{g}_\rho(\theta, u) := \frac{m}{2\rho} [F_{\max}(\theta + \rho u) - F_{\max}(\theta - \rho u)]u,$$

and $\hat{\mathbf{g}}_\rho(\theta_i)$ is the stochastic gradient estimator used in Algorithm 4. Up to (94), the analysis is identical to Theorem 5.5; in particular,

$$\mathbb{E}[\|\nabla\psi_\rho(\theta_i) - \mathbf{g}_\rho(\theta_i)\|^2 \mid \theta_i] \leq \frac{m^2 L_{F_{\max},1}^2}{b_u}.$$

The only new task is to control $\mathbb{E}[\|\hat{\mathbf{g}}_\rho(\theta) - \mathbf{g}_\rho(\theta)\|^2 \mid \theta]$ when $\hat{\mathbf{g}}_\rho$ is built from the LMC-based oracle $\hat{\psi}$.

Step 2: Bounding the LMC-induced error via lemma E.1. In Algorithm 4, the proxy gradient in line 8 is

$$\hat{\mathbf{g}}_\rho(\theta) = \frac{m}{2\rho} \cdot \frac{1}{b_u} \sum_{t=1}^{b_u} [\hat{\psi}(\theta + \rho u_t) - \hat{\psi}(\theta - \rho u_t)]u_t, \tag{95}$$

where $\hat{\psi}(\cdot)$ is the LMC-based estimator of $\tilde{F}_{\text{SQ-G}}$ returned by PSGD-LMC (Algorithm 3). We need to bound $\mathbb{E}[\|\hat{\mathbf{g}}_\rho(\theta) - \mathbf{g}_\rho(\theta)\|^2 \mid \theta]$ in (94) with $\mathbf{g}_\rho(\theta) := \frac{1}{b_u} \sum_{t=1}^{b_u} \mathbf{g}_\rho(\theta, u_t)$ where $\mathbf{g}_\rho(\theta, u_t) := \frac{m}{2\rho} \cdot [F_{\max}(\theta + \rho u_t) - F_{\max}(\theta - \rho u_t)]u_t$. Then

$$\begin{aligned}
& \mathbb{E}[\|\hat{\mathbf{g}}_\rho(\theta) - \mathbf{g}_\rho(\theta)\|^2 \mid \theta] \leq \\
& \frac{m^2}{\rho^2} \mathbb{E} \left[\left| \hat{\psi}(\theta + \rho u_t) - F_{\max}(\theta + \rho u_t) \right|^2 + \left| \hat{\psi}(\theta - \rho u_t) - F_{\max}(\theta - \rho u_t) \right|^2 \mid \theta \right]. \tag{96}
\end{aligned}$$

Thus it suffices to bound $\mathbb{E}[|\hat{\psi}(\theta) - F_{\max}(\theta)|^2 \mid \theta]$.

By Lemma E.1, for any $\theta \in \Theta$ we have

$$\mathbb{E}[|\hat{\psi}(\theta) - \tilde{F}_{\text{SQ-G}}(\theta)|^2 \mid \theta] = \mathcal{O}(\epsilon_v^2), \tag{97}$$

provided that

$$|I| \geq \tilde{C}_f \epsilon_v^{-2k-2}, \quad L \times n \geq \tilde{\mathcal{O}} \left(\frac{d k^2 B^2 \log^2(\epsilon_v^{-1})}{\epsilon_v^{8+8k}} \right),$$

with \tilde{C}_f a constant and B as in Lemma 5.1. Moreover, by the uniform approximation result for the superquantile–Gibbs relaxation (see Theorem 4.2), we have

$$\left| \tilde{F}_{\text{SQ-G}}(\theta) - F_{\max}(\theta) \right| = \mathcal{O}(\epsilon_v) \quad \text{for all } \theta \in \Theta. \tag{98}$$

Combining (97) and (98) and using $(a + b)^2 \leq 2(a^2 + b^2)$, we obtain

$$\begin{aligned}
\mathbb{E}[|\hat{\psi}(\theta) - F_{\max}(\theta)|^2 \mid \theta] & \leq 2 \mathbb{E}[|\hat{\psi}(\theta) - \tilde{F}_{\text{SQ-G}}(\theta)|^2 \mid \theta] + 2 |\tilde{F}_{\text{SQ-G}}(\theta) - F_{\max}(\theta)|^2 \\
& = \mathcal{O}(\epsilon_v^2). \tag{99}
\end{aligned}$$

Substituting (99) into (96) yields

$$\mathbb{E}[\|\hat{\mathbf{g}}_\rho(\theta) - \mathbf{g}_\rho(\theta)\|^2 \mid \theta] = \mathcal{O} \left(\frac{m^2}{\rho^2} \epsilon_v^2 \right). \tag{100}$$

Step 3: Convergence rate and choice of parameters. Plugging (100) into (94), choosing a constant stepsize $\tilde{\eta}_i = \eta \leq m^{-1/2} \rho L_{F_{\max,1}}^{-1}$, and summing $i = 0, \dots, N - 1$ exactly as in the proof of Theorem 5.5 gives

$$\frac{1}{N} \sum_{i=0}^{N-1} \mathbb{E}[\|\mathcal{G}_{\Theta}(\theta_i, \nabla \psi_{\rho}(\theta_i); \eta)\|^2] = \mathcal{O}\left(\frac{m \operatorname{diam}(\Theta)}{N \rho^2} + \frac{m^2}{b_u} + \frac{m^2}{\rho^2} \epsilon_v^2\right).$$

Let $\hat{\theta}$ be the best iterate in terms of the gradient-mapping norm. By Jensen's inequality,

$$\mathbb{E}[\|\mathcal{G}_{\Theta}(\hat{\theta}, \nabla \psi_{\rho}(\hat{\theta}); \eta)\|] = \mathcal{O}\left(\sqrt{\frac{m \operatorname{diam}(\Theta)}{N \rho^2}} + \frac{m}{\sqrt{b_u}} + \frac{m}{\rho} \epsilon_v\right).$$

Setting $\epsilon_v := \rho \epsilon m^{-1}$ and taking $N \gtrsim m \operatorname{diam}(\Theta) \rho^{-2} \epsilon^{-2}$ and $b_u \gtrsim m^2 \epsilon^{-2}$ yields

$$\mathbb{E}[\|\mathcal{G}_{\Theta}(\hat{\theta}, \nabla \psi_{\rho}(\hat{\theta}); \eta)\|] = \mathcal{O}(\epsilon),$$

so $\hat{\theta}$ is an (ϵ, ρ, η) -generalized Goldstein stationary point of F_{\max} .

Each outer iteration of Algorithm 4 uses b_u two-point evaluations of the oracle $\hat{\psi}$. Each call to $\hat{\psi}$ in turn runs PSGD-LMC with $|I|$ parallel LMC chains of length n . Consequently, the total number of lower-level gradient evaluations is $N \times n \times (b_u L + b_u |I|)$, and the total number of upper-level function evaluations is $N \times b_u \times |I|$. Substituting the choices of N , n , L , and $|I|$ from Lemma E.1 and the LMC mixing bound (Proposition 5.6), with the choice $\epsilon_v = \rho \epsilon m^{-1}$, gives

$$N \times n \times (b_u L + b_u |I|) = \mathcal{O}\left(\frac{d m^{11+8k} [k^2 B^2 + \tilde{C}_f] \log^2(\epsilon^{-1})}{\epsilon^{8k+12} \rho^{8k+10}}\right),$$

$$N \times b_u \times |I| = \mathcal{O}\left(\frac{m^{2k+5}}{\rho^{2k+4} \epsilon^{2k+6}}\right),$$

which is the claimed complexity bounds. \square

F Compute-matched Comparisons under a Fixed Wall-clock Budget

This appendix complements the iteration-based results in Section 6 by comparing methods under a fixed wall-clock time budget. As emphasized in Section 6, PSZO-MinSel invokes a Gibbs-superquantile oracle implemented via PSGD and parallel-chain Langevin Monte Carlo, so the cost per outer iteration can differ substantially from gradient-based baselines.

Timing protocol and selection. Toy-example methods are implemented in JAX, while data hyper-cleaning methods are implemented in PyTorch; all experiments are executed on the same machine described in Section 6. To obtain reliable timings, we exclude one-time compilation by running a short warm-up pass before timing and synchronize the device when recording timestamps. Runtimes are measured as wall-clock seconds elapsed from the start of the timed run; for JAX experiments we time a JIT-compiled step function and record timestamps with device synchronization to avoid asynchronous timing artifacts. As in Section 6, for each method we select the best-so-far iterate within a budget T , $\hat{\theta}(T) \in \arg \min\{\mathcal{E}_n : t_n \leq T\}$, where \mathcal{E}_n is $F(\theta_n)$ for the toy example and the validation loss in (34) for data hyper-cleaning. All tables below report performance evaluated at $\hat{\theta}(T)$.

F.1 Toy example: fixed-runtime results

Per-iteration timing. Table 5 reports the mean wall-clock time per outer iteration (post warm-up) for the toy example. This highlights the substantial per-iteration cost gap between PSZO-MinSel and gradient-based baselines.

d	V-PBGD	G-PBGD	RHG	IAPTT-GM	PSZO-MinSel
2	0.022	0.018	0.026	0.027	6.74
5	0.021	0.018	0.027	0.032	7.90
10	0.022	0.018	0.036	0.045	8.10
20	0.021	0.017	0.045	0.046	9.70

Table 5: Mean wall-clock time per outer iteration (ms) on the toy example with $k = d - 1$.

d	V-PBGD	G-PBGD	RHG	IAPTT-GM	PSZO-MinSel
2	0.510	0.264	0.313	0.094	0.016±0.014
5	0.203	0.213	0.235	0.113	0.034±0.017
10	0.245	0.278	0.260	0.180	0.053±0.013
20	0.333	0.201	0.322	0.190	0.083±0.006

Table 6: Compute-matched analogue of Table 1: best-so-far absolute error $|\hat{\theta}(T_{\text{toy}}) - \theta^*|$ under a fixed wall-clock budget $T_{\text{toy}} = 10$ s.

F.1.1 Optimistic formulation: dimension sweep under fixed time

Table 6 replicates Table 1 under a fixed wall-clock budget $T_{\text{toy}} = 10$ seconds and reports the best-so-far absolute error $|\hat{\theta}(T_{\text{toy}}) - \theta^*|$.

Under equal time, PSZO-MinSel retains a clear advantage across dimensions, consistent with the iteration-based conclusions in Section 6.

F.1.2 Optimistic formulation: constant manifold dimension under fixed time

Table 7 replicates Table 2 under the same budget $T_{\text{toy}} = 10$ seconds, with fixed manifold dimension $k = 1$. With fixed intrinsic dimension, PSZO-MinSel remains stable as d increases, reinforcing that performance is governed primarily by the manifold dimension rather than the ambient dimension.

F.2 Data hyper-cleaning: fixed-runtime results

Per-iteration timing. Table 8 reports the mean wall-clock time per outer iteration (post warm-up) on MNIST for representative models.

RHG and PSZO-MinSel have much higher per-outer costs in this task, making fixed-runtime evaluation particularly important.

Fixed-runtime performance. Table 9 replicates Table 4 under a fixed budget $T_{\text{hc}} = 1800$ seconds. For each method, we select the iterate achieving the lowest validation loss within T_{hc} and report the corresponding test accuracy and F1-score.

At low noise ($p = 40\%$), PSZO-MinSel is slightly below the strongest baselines but remains comparable under the same runtime budget; as the pollute rate increases ($p = 60\%, 80\%$), PSZO-MinSel achieves the best performance, consistent with the benefits of trajectory-based selection under heavier corruption.

d	V-PBGD	G-PBGD	RHG	IAPTT-GM	PSZO-MinSel
5	0.105	0.235	0.202	0.137	0.029±0.038
10	0.105	0.235	0.237	0.170	0.0208±0.022
20	0.104	0.238	0.237	0.170	0.021±0.014
30	0.104	0.254	0.237	0.155	0.018±0.011

Table 7: Compute-matched analogue of Table 2: best-so-far absolute error $|\hat{\theta}(T_{\text{toy}}) - \theta^*|$ under $T_{\text{toy}} = 10$ s, with fixed $k = 1$.

Model	V-PBGD	G-PBGD	RHG	IAPTT-GM	PSZO-MinSel
Linear	0.015	0.016	15.6	0.068	13.5
2-layer MLP	0.022	0.026	18.4	0.087	17.1

Table 8: Mean wall-clock time per outer iteration (s) on MNIST data hyper-cleaning (post warm-up).

References

- [1] Pierre Ablin, Gabriel Peyré, and Thomas Moreau. Super-efficiency of automatic differentiation for functions defined as a minimum. In *International Conference on Machine Learning*, pages 32–41. PMLR, 2020.
- [2] Margarita Antoniou, Ankur Sinha, and Gregor Papa. δ -perturbation of bilevel optimization problems: An error bound analysis. *Operations Research Perspectives*, 13:100315, 2024.
- [3] Michael Arbel and Julien Mairal. Amortized implicit differentiation for stochastic bilevel optimization. *arXiv preprint arXiv:2111.14580*, 2021.
- [4] Michael Arbel and Julien Mairal. Non-convex bilevel games with critical point selection maps. *Advances in Neural Information Processing Systems*, 35:8013–8026, 2022.
- [5] Kuang Bai, Jane J Ye, and Shangzhi Zeng. Optimality conditions for bilevel programmes via moreau envelope reformulation. *Optimization*, 74(12):2685–2719, 2025.
- [6] Yasmine Beck, Ivana Ljubić, and Martin Schmidt. A survey on bilevel optimization under uncertainty. *European Journal of Operational Research*, 311(2):401–426, 2023.
- [7] Imane Benchouk, Lateef Jolaoso, Khadra Nachi, and Alain Zemkoho. Scholtes relaxation method for pessimistic bilevel optimization. *Set-Valued and Variational Analysis*, 33(2):10, 2025.
- [8] Luca Bertinetto, Joao F Henriques, Philip HS Torr, and Andrea Vedaldi. Meta-learning with differentiable closed-form solvers. *arXiv preprint arXiv:1805.08136*, 2018.
- [9] Richard L Bishop and Richard J Crittenden. *Geometry of manifolds: Geometry of Manifolds*, volume 15. Academic press, 2011.
- [10] Mathieu Blondel, Quentin Berthet, Marco Cuturi, Roy Frostig, Stephan Hoyer, Felipe Llinares-López, Fabian Pedregosa, and Jean-Philippe Vert. Efficient and modular implicit differentiation. *Advances in neural information processing systems*, 35:5230–5242, 2022.
- [11] Jérôme Bolte, Quoc-Tung Le, Edouard Pauwels, and Samuel Vaiter. Bilevel gradient methods and morse parametric qualification. *arXiv preprint arXiv:2502.09074*, 2025.

Table 9: Compute-matched analogue of Table 4 under a fixed wall-clock budget $T_{\text{hc}} = 1800$ seconds (pollute rate $p \in \{40, 60, 80\}\%$): test accuracy (%) and F1 score (%), evaluated at the best-so-far iterate within the time budget (mean \pm 95% CI over 10 runs).

p	Method	Linear model		2-layer MLP	
		Test acc.	F1	Test acc.	F1
40	RHG	60.50 \pm 0.32	45.5 \pm 0.4	60.54 \pm 0.29	42.3 \pm 0.4
	IAPTT-GM	90.4 \pm 0.45	80.5 \pm 0.5	93.76 \pm 0.33	76.9 \pm 0.3
	G-PBGD	83.55 \pm 0.57	71.3 \pm 0.4	82.64 \pm 0.62	72.3 \pm 0.4
	V-PBGD	89.43 \pm 0.23	83.2 \pm 0.3	86.56 \pm 0.10	80.2 \pm 0.2
	PSZO-MinSel	88.5 \pm 0.51	78.2 \pm 0.4	90.3 \pm 0.44	79.2 \pm 0.2
60	RHG	62.74 \pm 0.69	33.8 \pm 0.4	63.34 \pm 0.42	35.5 \pm 0.3
	IAPTT-GM	79.42 \pm 0.38	45.4 \pm 0.3	78.82 \pm 0.45	50.5 \pm 0.4
	G-PBGD	69.48 \pm 0.42	40.2 \pm 0.2	66.65 \pm 0.42	46.5 \pm 0.6
	V-PBGD	73.14 \pm 0.25	48.7 \pm 0.3	72.63 \pm 0.28	52.4 \pm 0.3
	PSZO-MinSel	80.50 \pm 0.30	57.3 \pm 0.4	82.50 \pm 0.40	56.5 \pm 0.4
80	RHG	50.2 \pm 0.4	24.5 \pm 0.4	54.5 \pm 0.5	20.9 \pm 0.3
	IAPTT-GM	65.4 \pm 0.54	30.1 \pm 0.4	64.54 \pm 0.42	32.9 \pm 0.2
	G-PBGD	67.5 \pm 0.33	30.9 \pm 0.8	62.60 \pm 0.34	30.4 \pm 0.4
	V-PBGD	64.23 \pm 0.22	32.5 \pm 0.2	61.22 \pm 0.23	30.9 \pm 0.4
	PSZO-MinSel	70.34 \pm 0.45	36.7 \pm 0.5	68.43 \pm 0.38	39.1 \pm 0.4

- [12] Jérôme Bolte, Quoc-Tung Le, Edouard Pauwels, and Samuel Vaiter. Geometric and computational hardness of bilevel programming. *Mathematical Programming*, pages 1–36, 2025.
- [13] He Chen, Jiajin Li, and Anthony Man-Cho So. Set smoothness unlocks clarke hyper-stationarity in bilevel optimization. *arXiv preprint arXiv:2506.04587*, 2025.
- [14] Lesi Chen, Jing Xu, and Jingzhao Zhang. On finding small hyper-gradients in bilevel optimization: Hardness results and improved analysis. In *The Thirty Seventh Annual Conference on Learning Theory*, pages 947–980. PMLR, 2024.
- [15] Xuxing Chen, Tesi Xiao, and Krishnakumar Balasubramanian. Optimal algorithms for stochastic bilevel optimization under relaxed smoothness conditions. *Journal of Machine Learning Research*, 25(151):1–51, 2024.
- [16] Sinho Chewi. *Log-concave Sampling*. 2024. Draft available at <https://chewisinho.github.io/>.
- [17] Tzuu-Shuh Chiang, Chii-Ruey Hwang, and Shuenn Jyi Sheu. Diffusion for global optimization in \mathbb{R}^n . *SIAM Journal on Control and Optimization*, 25(3):737–753, 1987.
- [18] Frank H Clarke. *Optimization and nonsmooth analysis*. SIAM, 1990.
- [19] Benoît Colson, Patrice Marcotte, and Gilles Savard. An overview of bilevel optimization. *Annals of Operations Research*, 153(1):235–256, 2007.
- [20] Chris Criscitiello, Quentin Rejock, and Nicolas Boumal. If a smooth function is globally PL and coercive, then it has a unique minimizer, 2025. URL: www.racetothetbottom.xyz/posts/PL-smooth-unique/.

- [21] Mathieu Dagréou, Thomas Moreau, Samuel Vaiter, and Pierre Ablin. A lower bound and a near-optimal algorithm for bilevel empirical risk minimization. In *International Conference on Artificial Intelligence and Statistics*, pages 82–90. PMLR, 2024.
- [22] Stephan Dempe. *Foundations of bilevel programming*. Springer, 2002.
- [23] Stephan Dempe, Joydeep Dutta, and BS Mordukhovich. New necessary optimality conditions in optimistic bilevel programming. *Optimization*, 56(5-6):577–604, 2007.
- [24] Stephan Dempe, Boris S Mordukhovich, and Alain B Zemkoho. Necessary optimality conditions in pessimistic bilevel programming. *Optimization*, 63(4):505–533, 2014.
- [25] Stephan Dempe and Alain Zemkoho. Bilevel optimization. In *Springer optimization and its applications*, volume 161. Springer, 2020.
- [26] Stephan Dempe and Alain B Zemkoho. On the karush–kuhn–tucker reformulation of the bilevel optimization problem. *Nonlinear Analysis: Theory, Methods & Applications*, 75(3):1202–1218, 2012.
- [27] Felix Draxler, Kambis Veschgini, Manfred Salmhofer, and Fred Hamprecht. Essentially no barriers in neural network energy landscape. In *International conference on machine learning*, pages 1309–1318. PMLR, 2018.
- [28] Matthias Feurer and Frank Hutter. Hyperparameter optimization. *Automated machine learning: Methods, systems, challenges*, pages 3–33, 2019.
- [29] Luca Franceschi, Michele Donini, Paolo Frasconi, and Massimiliano Pontil. Forward and reverse gradient-based hyperparameter optimization. In *International conference on machine learning*, pages 1165–1173. PMLR, 2017.
- [30] Lucy L Gao, Jane J Ye, Haian Yin, Shangzhi Zeng, and Jin Zhang. Moreau envelope based difference-of-weakly-convex reformulation and algorithm for bilevel programs. *arXiv preprint arXiv:2306.16761*, 2023.
- [31] Timur Garipov, Pavel Izmailov, Dmitrii Podoprikin, Dmitry P Vetrov, and Andrew G Wilson. Loss surfaces, mode connectivity, and fast ensembling of dnns. *Advances in neural information processing systems*, 31, 2018.
- [32] Saeed Ghadimi and Mengdi Wang. Approximation methods for bilevel programming. *arXiv preprint arXiv:1802.02246*, 2018.
- [33] Tommaso Giovannelli, Griffin Dean Kent, and Luis Nunes Vicente. Inexact bilevel stochastic gradient methods for constrained and unconstrained lower-level problems. *Journal of Global Optimization*, pages 1–46, 2025.
- [34] Allen A Goldstein. Optimization of lipschitz continuous functions. *Mathematical Programming*, 13:14–22, 1977.
- [35] Yun Gong, Niao He, and Zebang Shen. Poincare inequality for local log-polyak-lojasiewicz measures: Non-asymptotic analysis in low-temperature regime. *arXiv preprint arXiv:2501.00429*, 2024.
- [36] Alfred Gray. The volume of a small geodesic ball of a riemannian manifold. *Michigan Mathematical Journal*, 20(4):329–344, 1974.

- [37] Riccardo Grazi, Luca Franceschi, Massimiliano Pontil, and Saverio Salzo. On the iteration complexity of hypergradient computation. In *International Conference on Machine Learning*, pages 3748–3758. PMLR, 2020.
- [38] Mareike Hasenpflug, Daniel Rudolf, and Björn Sprungk. Wasserstein convergence rates of increasingly concentrating probability measures. *The Annals of Applied Probability*, 34(3):3320–3347, 2024.
- [39] Mingyi Hong, Hoi-To Wai, Zhaoran Wang, and Zhuoran Yang. A two-timescale stochastic algorithm framework for bilevel optimization: Complexity analysis and application to actor-critic. *SIAM Journal on Optimization*, 33(1):147–180, 2023.
- [40] Feihu Huang. Optimal hessian/jacobian-free nonconvex-pl bilevel optimization. *arXiv preprint arXiv:2407.17823*, 2024.
- [41] Chii-Ruey Hwang. Laplace’s method revisited: weak convergence of probability measures. *The Annals of Probability*, pages 1177–1182, 1980.
- [42] Haoming Jiang, Zhehui Chen, Yuyang Shi, Bo Dai, and Tuo Zhao. Learning to defend by learning to attack. In *International Conference on Artificial Intelligence and Statistics*, pages 577–585. PMLR, 2021.
- [43] Xiaotian Jiang, Jiayang Li, Mingyi Hong, and Shuzhong Zhang. A correspondence-driven approach for bilevel decision-making with nonconvex lower-level problems. *arXiv preprint arXiv:2509.01148*, 2025.
- [44] Michael Jordan, Guy Kornowski, Tianyi Lin, Ohad Shamir, and Manolis Zampetakis. Deterministic nonsmooth nonconvex optimization. In *The Thirty Sixth Annual Conference on Learning Theory*, pages 4570–4597. PMLR, 2023.
- [45] Thomas Kleinert, Martine Labbé, Fränk Plein, and Martin Schmidt. There’s no free lunch: on the hardness of choosing a correct big-m in bilevel optimization. *Operations research*, 68(6):1716–1721, 2020.
- [46] Guy Kornowski, Swati Padmanabhan, and Ohad Shamir. On the hardness of meaningful local guarantees in nonsmooth nonconvex optimization. *arXiv preprint arXiv:2409.10323*, 2024.
- [47] Guy Kornowski and Ohad Shamir. Oracle complexity in nonsmooth nonconvex optimization. *Advances in Neural Information Processing Systems*, 34:324–334, 2021.
- [48] Rohith Kudithipudi, Xiang Wang, Holden Lee, Yi Zhang, Zhiyuan Li, Wei Hu, Rong Ge, and Sanjeev Arora. Explaining landscape connectivity of low-cost solutions for multilayer nets. *Advances in neural information processing systems*, 32, 2019.
- [49] Jeongyeol Kwon, Dohyun Kwon, Stephen Wright, and Robert D Nowak. A fully first-order method for stochastic bilevel optimization. In *International Conference on Machine Learning*, pages 18083–18113. PMLR, 2023.
- [50] Jeongyeol Kwon, Dohyun Kwon, Steve Wright, and Robert Nowak. On penalty methods for nonconvex bilevel optimization and first-order stochastic approximation. *arXiv preprint arXiv:2309.01753*, 2023.
- [51] Guanghui Lan, Arkadi Nemirovski, and Alexander Shapiro. Validation analysis of mirror descent stochastic approximation method. *Mathematical programming*, 134(2):425–458, 2012.
- [52] John M Lee. Smooth manifolds. In *Introduction to smooth manifolds*, pages 1–29. Springer, 2003.

- [53] John M Lee. *Riemannian manifolds: an introduction to curvature*, volume 176. Springer Science & Business Media, 2006.
- [54] Jiajin Li, Linglingzhi Zhu, and Anthony Man-Cho So. Nonsmooth composite nonconvex-concave minimax optimization. In *OPT 2022: Optimization for Machine Learning (NeurIPS 2022 Workshop)*, 2022.
- [55] Shiyu Liang, Ruoyu Sun, Yixuan Li, and Rayadurgam Srikant. Understanding the loss surface of neural networks for binary classification. In *International Conference on Machine Learning*, pages 2835–2843. PMLR, 2018.
- [56] Gui-Hua Lin, Mengwei Xu, and Jane J Ye. On solving simple bilevel programs with a nonconvex lower level program. *Mathematical Programming*, 144(1):277–305, 2014.
- [57] Tianyi Lin, Zeyu Zheng, and Michael Jordan. Gradient-free methods for deterministic and stochastic nonsmooth nonconvex optimization. *Advances in Neural Information Processing Systems*, 35:26160–26175, 2022.
- [58] Zhanran Lin, Puheng Li, and Lei Wu. Exploring neural network landscapes: Star-shaped and geodesic connectivity. *arXiv preprint arXiv:2404.06391*, 2024.
- [59] Bo Liu, Mao Ye, Stephen Wright, Peter Stone, and Qiang Liu. Bome! bilevel optimization made easy: A simple first-order approach. *Advances in neural information processing systems*, 35:17248–17262, 2022.
- [60] June Liu, Yuxin Fan, Zhong Chen, and Yue Zheng. Pessimistic bilevel optimization: a survey. *International Journal of Computational Intelligence Systems*, 11(1):725–736, 2018.
- [61] Risheng Liu, Jiabin Gao, Jin Zhang, Deyu Meng, and Zhouchen Lin. Investigating bi-level optimization for learning and vision from a unified perspective: A survey and beyond. *IEEE Transactions on Pattern Analysis and Machine Intelligence*, 44(12):10045–10067, 2021.
- [62] Risheng Liu, Yaohua Liu, Shangzhi Zeng, and Jin Zhang. Towards gradient-based bilevel optimization with non-convex followers and beyond. *Advances in Neural Information Processing Systems*, 34:8662–8675, 2021.
- [63] Yuan Liu. The poincaré inequality and quadratic transportation-variance inequalities. *Electron. J. Probab*, 25(1):1–16, 2020.
- [64] Zhuanghua Liu, Cheng Chen, Luo Luo, and Bryan Kian Hsiang Low. Zeroth-order methods for constrained nonconvex nonsmooth stochastic optimization. In *International Conference on Machine Learning*, pages 30842–30872. PMLR, 2024.
- [65] Songtao Lu. TSP: A two-sided smoothed primal-dual method for nonconvex bilevel optimization. In *Proceedings of the 42nd International Conference on Machine Learning*, volume 267, pages 40665–40708. PMLR, 2025.
- [66] Zhi-Quan Luo, Jong-Shi Pang, and Daniel Ralph. *Mathematical programs with equilibrium constraints*. Cambridge University Press, 1996.
- [67] Arkadij Semenovič Nemirovskij and David Borisovich Yudin. Problem complexity and method efficiency in optimization. 1983.

- [68] Yurii Nesterov and Vladimir Spokoiny. Random gradient-free minimization of convex functions. *Foundations of Computational Mathematics*, 17(2):527–566, 2017.
- [69] Quynh Nguyen. On connected sublevel sets in deep learning. In *International conference on machine learning*, pages 4790–4799. PMLR, 2019.
- [70] Fabian Pedregosa. Hyperparameter optimization with approximate gradient. In *International conference on machine learning*, pages 737–746. PMLR, 2016.
- [71] P Petersen. Riemannian geometry. *Graduate Texts in Mathematics/Springer-Verlag*, 2006.
- [72] Ieva Petrulionytė, Julien Mairal, and Michael Arbel. Functional bilevel optimization for machine learning. *Advances in Neural Information Processing Systems*, 37:14016–14065, 2024.
- [73] Quentin Rebjock and Nicolas Boumal. Fast convergence to non-isolated minima: four equivalent conditions for c^2 functions. *Mathematical Programming*, pages 1–49, 2024.
- [74] R Tyrrell Rockafellar, Stanislav Uryasev, et al. Optimization of conditional value-at-risk. *Journal of risk*, 2:21–42, 2000.
- [75] Levent Sagun, Utku Evci, V Ugur Guney, Yann Dauphin, and Leon Bottou. Empirical analysis of the hessian of over-parametrized neural networks. *arXiv preprint arXiv:1706.04454*, 2017.
- [76] Amirreza Shaban, Ching-An Cheng, Nathan Hatch, and Byron Boots. Truncated back-propagation for bilevel optimization. In *The 22nd international conference on artificial intelligence and statistics*, pages 1723–1732. PMLR, 2019.
- [77] Han Shen, Quan Xiao, and Tianyi Chen. On penalty-based bilevel gradient descent method. *Mathematical Programming*, pages 1–51, 2025.
- [78] Lai Tian, Kaiwen Zhou, and Anthony Man-Cho So. On the finite-time complexity and practical computation of approximate stationarity concepts of lipschitz functions. In *International Conference on Machine Learning*, pages 21360–21379. PMLR, 2022.
- [79] Meltem Apaydin Ustun, Liang Xu, Bo Zeng, and Xiaoning Qian. Hyperparameter tuning through pessimistic bilevel optimization. *arXiv preprint arXiv:2412.03666*, 2024.
- [80] Luca Venturi, Afonso S Bandeira, and Joan Bruna. Spurious valleys in two-layer neural network optimization landscapes. *arXiv preprint arXiv:1802.06384*, 2018.
- [81] Luis N Vicente and Paul H Calamai. Bilevel and multilevel programming: A bibliography review. *Journal of Global optimization*, 5(3):291–306, 1994.
- [82] Wolfram Wiesemann, Angelos Tsoukalas, Polyxeni-Margarita Kleniati, and Berç Rustem. Pessimistic bilevel optimization. *SIAM Journal on Optimization*, 23(1):353–380, 2013.
- [83] Quan Xiao, Songtao Lu, and Tianyi Chen. A generalized alternating method for bilevel optimization under the polyak-łojasiewicz condition. *arXiv preprint arXiv:2306.02422*, 2023.
- [84] Mengwei Xu and Jane J Ye. A smoothing augmented lagrangian method for solving simple bilevel programs. *Computational Optimization and Applications*, 59:353–377, 2014.
- [85] Junjie Yang, Kaiyi Ji, and Yingbin Liang. Provably faster algorithms for bilevel optimization. *Advances in Neural Information Processing Systems*, 34:13670–13682, 2021.

- [86] Yifan Yang, Peiyao Xiao, and Kaiyi Ji. Achieving $\mathcal{O}(\varepsilon^{-1.5})$ complexity in hessian/jacobian-free stochastic bilevel optimization. *Advances in Neural Information Processing Systems*, 36:39491–39503, 2023.
- [87] Jane J Ye and XY Ye. Necessary optimality conditions for optimization problems with variational inequality constraints. *Mathematics of Operations Research*, 22(4):977–997, 1997.
- [88] Jane J Ye and Daoli Zhu. New necessary optimality conditions for bilevel programs by combining the mpec and value function approaches. *SIAM Journal on Optimization*, 20(4):1885–1905, 2010.
- [89] Jane J Ye and DL Zhu. Optimality conditions for bilevel programming problems. *Optimization*, 33(1):9–27, 1995.
- [90] JJ Ye, DL Zhu, and Qiji Jim Zhu. Exact penalization and necessary optimality conditions for generalized bilevel programming problems. *SIAM Journal on optimization*, 7(2):481–507, 1997.
- [91] Alain B Zemkoho and Shenglong Zhou. Theoretical and numerical comparison of the karush–kuhn–tucker and value function reformulations in bilevel optimization. *Computational Optimization and Applications*, 78(2):625–674, 2021.
- [92] Bo Zeng. A practical scheme to compute the pessimistic bilevel optimization problem. *INFORMS Journal on Computing*, 32(4):1128–1142, 2020.
- [93] Jingzhao Zhang, Hongzhou Lin, Stefanie Jegelka, Suvrit Sra, and Ali Jadbabaie. Complexity of finding stationary points of nonconvex nonsmooth functions. In *International Conference on Machine Learning*, pages 11173–11182. PMLR, 2020.